



UNIVERSITÀ DEGLI STUDI DI PALERMO

Dottorato di ricerca in Oncologia e Chirurgia Sperimentali

Dipartimento di Discipline Chirurgiche Oncologiche e Stomatologiche (Di.Chir.On.S.)

International joint PhD program - University of Palermo (Italy) and Universiteit Antwerpen (Belgium)

ROLE OF EXOSOMES RELEASED BY CHRONIC MYELOGENOUS LEUKEMIA CELLS IN THE CROSS-TALK WITH ENDOTHELIAL CELLS

Doctoral Dissertation of:
Dr. Marco Giallombardo

Supervisors:

Prof. Paolo Vigneri

Prof. Juan Iovanna

Tutor Unipa:

Prof. Riccardo Alessandro

Tutors UAntwerpen:

Prof. Christian Rolfo

Prof. Patrick Pauwels

The Chair of the Doctoral Program:

Prof. Giuseppina Campisi

Years 2014/2016 – Cycle XXIX

International joint PhD program - University of Palermo (Italy) and Universiteit Antwerpen (Belgium)

Title of the thesis:

Role of exosomes released by chronic myelogenous leukemia cells in the cross-talk with endothelial cells

Doctoral Dissertation of:
Dr. Marco Giallombardo

Supervisors:

Prof. Paolo Vigneri

Prof. Juan Iovanna

Tutor Unipa:

Prof. Riccardo Alessandro

Tutors UAntwerpen:

Prof. Christian Rolfo

Prof. Patrick Pauwels

The Chair of the Doctoral Program:

Prof. Giuseppina Campisi

Thesis for the Degree of Doctor in Medical Sciences (In de medische wetenschappen) at the Universiteit Antwerpen to be defended by Marco Giallombardo.

Thesis for the Degree of Doctor in Experimental Oncology and Surgery – (University of Palermo)

Years 2014/2016 – Cycle XXIX

INDEX

Abstract	Pag. 5
Summary – Informative Abstract	Pag. 5
CHAPTER 1. Background, Rationale and Objectives:	Pag. 9
- 1.1 Chronic Myelogenous Leukemia: from the molecular biology of the disease to targeted therapy	Pag. 9
- 1.2 Role of bone marrow microenvironment in CML	Pag. 10
- 1.3 Exosomes: biogenesis, structure and functions	Pag. 11
- 1.3.1 Exosomes in cancer	Pag. 13
- 1.4 Curcumin: a small antioxidant molecule with potent anticancer effects	Pag. 14
- 1.5 Rationale and Objectives	Pag. 14
- 1.5.1 Exosomal shuttling of miR-126 in endothelial cells modulates adhesive and migratory abilities of chronic myelogenous leukemia cells	Pag. 15
- 1.5.2 Curcumin inhibits <i>in vitro</i> and <i>in vivo</i> chronic myelogenous leukemia cells growth: a possible role for exosomal disposal of miR-21	Pag. 16
- 1.5.3 Curcumin modulates chronic myelogenous leukemia exosomes composition and affects angiogenic phenotype, <i>via</i> exosomal miR-21	Pag. 17
CHAPTER 2 - Materials and Methods	Pag. 19
CHAPTER 3 - Results	
- 3.1 Exosomal shuttling of miR-126 in endothelial cells modulates adhesive and migratory abilities of	

chronic myelogenous leukemia cells	Pag. 33
- 3.2 Curcumin inhibits <i>in vitro</i> and <i>in vivo</i> chronic myelogenous leukemia cells growth: a possible role for exosomal disposal of miR-21	Pag. 38
- 3.3 Curcumin modulates chronic myelogenous leukemia exosomes composition and affects angiogenic phenotype, <i>via</i> exosomal miR-21	Pag. 44
CHAPTER 4 - Discussion	
- 4.1 Exosomal shuttling of miR-126 in endothelial cells modulates adhesive and migratory abilities of chronic myelogenous leukemia cells	Pag. 53
- 4.2 Curcumin inhibits <i>in vitro</i> and <i>in vivo</i> chronic myelogenous leukemia cells growth: a possible role for exosomal disposal of miR-21	Pag. 56
- 4.3 Curcumin modulates chronic myelogenous leukemia exosomes composition and affects angiogenic phenotype, <i>via</i> exosomal miR-21	Pag. 59
CHAPTER 5 - Tables and Figures	
- 5.1 Exosomal shuttling of miR-126 in endothelial cells modulates adhesive and migratory abilities of chronic myelogenous leukemia cells	Pag. 63
- 5.2 Curcumin inhibits <i>in vitro</i> and <i>in vivo</i> chronic myelogenous leukemia cells growth: a possible role for exosomal disposal of miR-21	Pag. 70
- 5.3 Curcumin modulates chronic myelogenous leukemia exosomes composition and affects angiogenic phenotype, <i>via</i> exosomal miR-21	Pag. 81
CHAPTER 6 - Bibliography	Pag. 93
CHAPTER 7 - Scientific Products	Pag. 104
CHAPTER 8 - Acknowledgements	Pag. 108

Abstract

Exosomes released by Chronic myelogenous leukemia cells (CML-derived exosomes) contain high amount of miR-126. CML-derived exosomes, internalized by endothelial cells, modulate adhesive and migratory abilities of CML cells. Curcumin treatment of CML cells cause a selective packaging of OncomiR-21 into the released exosomes (Curcu-exosomes), that may contribute to the antileukemic effect of Curcumin. Curcu-exosomes attenuate also the promotion of the angiogenic phenotype mediated by CML-derived exosomes. These data indicate that CML-derived exosomes are involved in CML progression and that Curcumin could be a potential adjuvant agent for CML treatment with a double effect, on cancer cells and on tumour microenvironment.

Abstract

Exosomen die vrijgegeven worden door Chronische Myelogene Leukemie cellen (CML-afgeleide exosomen) bevatten een grote hoeveelheid miR-126. CML-afgeleide exosomen, die geïnternaliseerd worden door endotheliale cellen, moduleren de adhesieve en migratoire eigenschappen van CML-cellen. De behandeling van CML-cellen met Curcumin leidt tot de selectieve verpakking van OncomiR-21 in the vrijgegeven exosomen (Curcu-exosomen), dit kan bijdragen tot het anti-leukemische effect van Curcumin. Curcu-exosomen vertragen ook de bevordering van het angiogene fenotype door CML-afgeleide exosomen. Deze data geven een indicatie dat CML-afgeleide exosomen betrokken zijn bij CML progressie en dat Curcumin een mogelijk adjuvant agens kan zijn voor de behandeling van CML met een dubbel effect, zowel op de kankercellen als op de tumor micro-omgeving.

Summary - Informative abstract

Introduction: Chronic myeloid leukemia (CML) is a myeloproliferative disorder in which leukemic cells harbor a reciprocal t(9:22) chromosomal translocation that leads to the formation of Bcr-Abl, a chimeric oncoprotein with a constitutive tyrosine kinase activity. In turn, Bcr-Abl modulates several biological mechanisms, among which induced proliferation, inhibition of apoptosis and alteration of leukemic blasts adhesion to the bone marrow (BM) microenvironment. Well described resistance mechanisms limit the use of selective tyrosine kinase inhibitors (TKIs), such as Imatinib mesylate. It has become clear that leukemic cancer cells are able to produce their own signals in BM in order to support their growth and survival, also through the release of extracellular vesicles, such as exosomes. Tumor derived exosomes are nanovesicles which contain proteins and microRNAs that mediate cell-cell communication and are involved in angiogenesis and tumor progression. It has been described that exosomal content sorting change in response to cell stimuli, such as under a specific treatment. Curcumin derived from the plant *Curcuma longa* has been shown to exhibit antitumor activities in a wide spectrum of human cancer. **Results:** To elucidate whether miRNAs secreted from chronic myelogenous leukemia cells (CML) are shuttled into endothelial cells affecting their phenotype, we first analysed miRNAs content in exosomes derived from LAMA84 CML cells. Among the 124 miRNAs identified in LAMA84 exosomes, we focused our attention on miR-126 which was found to be over-expressed in exosomes compared with producing parental cells. Transfection of LAMA84 with Cy3-labelled miR-126 and co-culture of leukemia cells with endothelial cells (ECs) confirmed that miR-126 is

shuttled into HUVECs. The treatment of HUVECs with LAMA84 exosomes for 24 hours reduced CXCL12 and VCAM1 expression, both at the mRNA and protein level, and negatively modulated LAMA84 motility and cells adhesion. Transfection in HUVECs of miR-126 inhibitor reversed the decrease of CXCL12 and restored the motility and adhesion of LAMA84 cells while the over-expression of miR-126, showed opposite effects.

Moreover, the addition of Curcumin to CML cells caused a dose-dependent increase of PTEN, target of miR-21. Curcumin treatment also decreased AKT phosphorylation and VEGF expression and release. Colony formation assays indicated that Curcumin affects the survival of CML cells. Some observation suggest a possible cellular disposal of miRNAs by exosomes. To elucidate if Curcumin caused a decrease of miR-21 in CML cells and its packaging in exosomes, we analyzed miR-21 content in K562 and LAMA84 cells and exosomes, after treatment with Curcumin. Furthermore, we showed that addition of Curcumin to CML cells caused a downregulation of Bcr-Abl expression through the cellular increase of miR-196b.

The effect of Curcumin was then investigated on a CML xenograft in SCID mice. We observed that animals treated with Curcumin, developed smaller tumors compared to mice control. Real time PCR analysis showed that exosomes, released in the plasma of the Curcumin-treated mice, were enriched in miR-21 with respect the control.

Finally, we discovered that the treatment of HUVECs with exosomes released by CML cells after Curcumin treatment (Curcu-exosomes) reduced RhoB expression and negatively modulated endothelial cells motility. We showed that the addition of CML control exosomes to HUVECs caused an increase in IL8 and VCAM1 levels, but Curcu-exosomes reversed these effects thus attenuating their angiogenic properties. This antiangiogenic effect was confirmed with *in vitro* and *in vivo* vascular network formation assays. SWATH analysis of the proteomic profile of Curcu-exosomes revealed that Curcumin treatment deeply changes their molecular properties, in particular, Curcumin induces a release of exosomes depleted in pro-angiogenic proteins and enriched in proteins endowed with anti-angiogenic activity. Among the proteins differential expressed we focused on MARCKS, since it was the most modulated protein and a target of miR-21. **Conclusion:** Our results show that the miR-126 shuttled by exosomes is biologically active in the target cells, and support the hypothesis that exosomal miRNAs have an important role in tumor-endothelial crosstalk occurring in the bone marrow microenvironment, potentially affecting disease progression. Moreover, our results suggested that a selective packaging of miR-21 in exosomes may contribute to the antileukemic effect of Curcumin in CML. Curcumin treatment of CML cells attenuates the promotion of the angiogenic phenotype of ECs mediated by CML-derived exosomes, modulating also the endothelial barrier organization. These data indicate that Curcumin could be a potential adjuvant agent for CML treatment with a double effect, on cancer cells and on tumour microenvironment.

Samenvatting – Informatief abstract

Introductie: Chronische myeloïde leukemie (CML) is te wijten aan een verstoring in de proliferatie van myeloïde progenitor cellen, waarbij de leukemische cellen een reciproke t(9/22) chromosomale translocatie bevatten die leidt tot de vorming van Bcr-Abl, een chimeer onco-eiwit met een constitutieve tyrosine kinase activiteit. Op zijn beurt moduleert Bcr-Abl verschillende biologische mechanismen: het induceert proliferatie, inhibeert apoptose en verandert de adhesie van leukemische blasten in de beenmerg (BM) micro-omgeving. Goed beschreven resistentiemechanismen limiteren het gebruik van selectieve tyrosine kinase inhibitoren (TKIs) zoals imatinib mesylaat. Het is duidelijk geworden dat

leukemische kankercellen in staat zijn om hun eigen signalen in het BM te produceren, en zo hun eigen groei en overleving te ondersteunen, mede door de vrijstelling van extracellulaire vesikels, zoals exosomen. Tumor-afgeleide exosomen zijn nanovesikels die eiwitten en microRNAs bevatten en die cel-cel communicatie bewerkstelligen en betrokken zijn bij angiogenese en tumor progressie. Het is beschreven dat de inhoud van deze exosomen verandert in respons op cel stimuli, zoals een specifieke behandeling. Het is aangetoond dat Curcumin, een afgeleide van de plant *Curcuma longa*, anti-kanker eigenschappen bezit in een breed spectrum van humane kankers. **Resultaten:** Om na te gaan of miRNAs, gesecreteerd door chronische myelogene leukemie cellen, worden opgenomen in endotheliale cellen en hun fenotype beïnvloeden, hebben we eerst de miRNA inhoud van exosomen geanalyseerd die afgescheiden werden door LAMA84 CML cellen. Onder de 124 geïdentificeerde miRNAs in de LAMA84 exosomen, focusten we onze aandacht op miR-126 dat overgeëxprimeerd was in de exosomen in verhouding met de productie in parentale cellen. Transfectie van LAMA84 met Cy3 gelabeld miR-126 en cocultuur van leukemiecellen met endotheliale cellen (ECs) bevestigde dat miR-126 overgebracht werd naar HUVECs. De behandeling van HUVECs met LAMA84-exosomen gedurende 24 uur reduceerde CXCL12 en VCAM1 expressie, zowel op mRNA als op eiwitniveau, en reduceerde de motiliteit en celadhesie van LAMA84. Transfectie van miR-126 in HUVECs deed de reductie van CXCL12 teniet en herstelde de motiliteit en adhesie van LAMA84 cellen, terwijl overexpressie van miR-126 de omgekeerde effecten toonde. Bovendien, de toevoeging van Curcumin aan CML cellen veroorzaakte een dosisafhankelijke stijging van PTEN, een target van miR-21. Curcumin behandeling verlaagde ook AKT-fosforylatie en VEGF-expressie en -secretie. Een kolonievormende assay toonde aan dat Curcumin de overleving van CML cellen beïnvloedde. Sommige observaties suggereren een mogelijke cellulaire afgifte van miRNAs door exosomen. Om na te gaan of Curcumin een verlaging in miR-21 in CML cellen en de verpakking in exosomen beïnvloed, hebben we de hoeveelheid van miR-21 na Curcumin behandeling bepaald in K562 en LAMA84 cellen en exosomen. Verder hebben we aangetoond dat de toevoeging van Curcumin aan CML cellen een neerregulatie van Bcr-Abl expressie veroorzaakte via een cellulaire toename van miR-196b. Het effect van Curcumin is vervolgens onderzocht in een xenograft van CML in SCID muizen. We observeerden dat de dieren die behandeld werden met Curcumin kleinere tumoren ontwikkelden in vergelijking met de controlemuizen. Real-time PCR analyse toonde aan dat de exosomen, die vrijgegeven werden in het plasma van met Curcumin behandelde muizen, aangerijkt waren met miR-21 ten opzichte van de controle. Tenslotte ontdekten we dat de behandeling van HUVECs met exosomen, afgegeven door de CML cellen na behandeling met Curcumin (Curcu-exosomen), de RhoB expressie reduceerde en de motiliteit van endotheelcellen negatief beïnvloedde. We toonden aan dat de toevoeging van exosomen uit CML controlecellen aan HUVECs een verhoging veroorzaakte van IL8 en VCAM1 levels, maar dat Curcu-exosomen deze effecten omkeerden en daarbij de angiogene eigenschappen onderdrukte. Dit anti-angiogeen effect werd bevestigd door *in vitro* en *in vivo* vasculaire netwerkformatie assays. SWATH analyse van het proteomisch profiel van Curcu-exosomen toonde dat Curcumin behandeling de moleculaire eigenschappen grondig veranderde. In het bijzonder induceerde Curcumin de afgifte van exosomen met verminderde pro-angiogene eiwitten en aangerijkt in eiwitten met anti-angiogene activiteit. Van deze differentieel geëxprimeerde eiwitten focusten we ons op MARCKS, aangezien dit zowel het sterkst gewijzigde eiwit was, als een target voor miR-21. **Conclusie:** Onze resultaten tonen aan dat miR-126, dat getransfereerd wordt door exosomen, biologisch actief is in de doelcellen. Dit ondersteunt de hypothese dat exosomale miRNAs een belangrijke rol spelen in de tumor-endotheliale crosstalk die plaatsvindt in de beenmergmicro-omgeving en die potentieel bijdraagt tot ziekte progressie. Bovendien

suggereren onze resultaten dat de selectieve verpakking van miR-21 in exosomen kan bijdragen tot het antileukemisch effect van Curcumin in CML. Curcuminbehandeling van CML cellen vertraagd de bevordering van het angiogene fenotype van ECs, gemedieerd door CML-afgeleide exosomen, en moduleert de organisatie van de endotheliale barrière. Deze data duiden erop dat Curcumin tot potentieel adjuvant agens kan dienen voor de behandeling van CML met een dubbel effect, zowel op de kankercellen als op de tumor micro-omgeving.

CHAPTER 1

Background

1.1 Chronic Myelogenous Leukemia: from the molecular biology of the disease to targeted therapy

Chronic myelogenous leukemia (CML) is a myeloproliferative disorder originated from a hematopoietic stem cell or multipotent progenitor cell¹. Clinically, this disease can be subdivided into three phases: chronic, accelerated and acute². The chronic phase can progress to an accelerated phase, characterized by a further increase of myeloid progenitor cells respect to differentiated cells in the blood and bone marrow (BM), leading to a subsequent blast crisis, typical feature of acute phase².

Cytogenetically, the well-known marker of this disease is the Philadelphia (Ph) chromosome, originated from a reciprocal t(9:22) (q34;q11) translocation, though not all CML patients harbor Ph chromosome. This aberration generates the fusion of the breakpoint cluster region (BCR) and the abelson tyrosine kinase (ABL) genes, located on chromosome 22 and 9, respectively, leading to BCR-ABL fusion gene¹. This fusion gene encodes for Bcr-Abl chimeric protein, an oncoprotein with constitutive tyrosine kinase activity that characterizes the molecular biology of CML¹.

In most cases, it has been documented that different breaking points in BCR gene (called major or “M”, minor or “m” and micro or “μ”), generate three main Bcr-Abl fusion proteins of 210, 190 and 230 kDa³. Despite the presence of different isoforms, the most common Bcr-Abl protein described in CML patients is the 210 kDa (called p210)³.

The ABL tyrosine kinase constitutively active in Bcr-Abl chimeric protein is able to modulate several signalling transduction pathways that include Phosphoinositide-3-Kinase/AKT, Ras/MAP-Kinases and factors such as Stat5⁴. Recently, it was described an interaction

between Bcr-Abl and Interferon regulatory factor 5 (IRF5) showing, interestingly, that the inactivation of IRF5 contributes to leukemic transformation⁵.

The constitutive kinase activity of Bcr-Abl and, in turn, the alteration of several signalling transduction pathways, leads this chimeric oncoprotein to play a crucial role and drives several disease progression mechanisms^{3,4}. In CML, Bcr-Abl is involved in increased proliferation, altered cell adhesion, inhibition of apoptosis and enhanced bone marrow angiogenesis resulting, thus, an excellent candidate for targeted therapy^{3,6,7}.

This aberrant oncoprotein has contributed to the development of new target therapies like tyrosine kinase inhibitors (TKIs), such as Imatinib mesylate (IM)⁸. IM has revolutionized the therapy of CML patients, decreasing drastically the number of patients that need hematopoietic stem cell transplantation⁸. IM is an ATP-competitive inhibitor that binds the ATP binding pocket of Bcr-Abl oncoprotein, leading to the inactivation of their constitutive kinase activity⁸. The inhibition of Bcr-Abl activity causes the inactivation of the related downstream signalling pathways and, in turn, the decrease of cell proliferation and induction of apoptosis, restoring the physiological hematopoiesis⁸. Recently, other more selective and potent TKIs against BCR-ABL, such as Dasatinib and Nilotinib, were introduced as new therapeutic options².

Although TKIs have truly revolutionized the treatment of CML, mechanisms of resistance to these drugs have been documented⁹⁻¹¹. These mechanisms are subdivided in innate and acquired resistances, which limit the use of these drugs⁹⁻¹¹. The research of novel targeted therapeutic options are needed in order to overcome the drug resistance, perhaps supported by natural adjuvant therapies.

1.2 Role of bone marrow microenvironment in CML

Bone marrow (BM) microenvironment is a dynamic and interactive set of stromal cells, that include endothelial cells, reticular cells, macrophages, adipocytes, chondroblasts, mesenchymal stromal cells (MSCs) among others¹²⁻¹⁵. Stromal cells secrete extracellular matrix components, such as laminin, collagen I and IV, glycosaminoglycans, fibronectin, hyaluronic acid proteoglycans, building a live scaffold that becomes a stromal niche into the bone marrow¹²⁻¹⁵.

Stromal microenvironment is strongly involved also in cancer progression¹⁶. Close interest is focused on the complex interaction between cancer cells and host cells in the pathological

tumour microenvironment¹⁶. It has been described that in the BM microenvironment, MSCs are able to attract tumour cells and promote tumour growth, survival, metastasis, osteolysis, and drug resistance¹⁶. Leukaemia cells are stimulated to produce several molecules that include adhesive proteins, cytokines, growth factors, chemokines and their receptors such as CXCL8, CXCL12 and CXCR4, involved in CML progression^{17,18}. CXCL12 is a chemokine that binds specifically to CXCR4, a G-protein coupled receptor. *In vitro* and *in vivo* studies have described a key role of CXCR4/CXCL12 axis in the migration of cells within tissues and in the homing of immune cells in the bone marrow¹⁷. In the CML progression, a modulation of CXCR4/CXCL12 interaction has a role in the mobilization of leukemic cells in the bloodstream^{18,19}. CXCL8, known also as IL-8, is a pro-inflammatory chemokine frequently over-expressed in endothelial cells, stromal cells and in several tumours where, in synergy with VEGF, contributes to modulate tumour growth and angiogenesis^{20,21}.

It has been documented that the cross-talk between endothelial cells and tumour cells contributes to tumour angiogenesis²². VCAM1 is a cell-cell adhesion molecule constitutively expressed on the endothelial cells in the bone marrow, where it has a key role in the homing of Ph positive leukemic cells²³.

The complex cell-cell and cell-ECM interactions that occur between tumour cells and tumour microenvironment components could be subdivided in: I) dependent interactions, mediated by adhesion molecules; II) independent interactions, mediated by soluble molecules such as chemokines and growth factors^{24,25}. During the last decade, it was described a novel way of independent intercellular communication mediated by extracellular vesicles (EVs)^{26,27}. EVs is an “umbrella” term that indicates an heterogeneous group of membranous vesicles released by different cell types²⁸. EVs can be subdivided into 2 main classes: exosomes and microvesicles, distinguished according to their different biogenesis, dimension and molecular composition^{26,27}. We focused our attention on exosomes, that play a crucial role in the cross-talk between tumour cells and tumour microenvironment, modulating tumour progression²⁹⁻³¹.

1.3 Exosomes: biogenesis, structure and functions.

Exosomes are cup-shaped membranous nanovesicles with a diameter of around 30-100 nm³². Their biogenesis is mediated by an endosomal mechanism: part of the extracellular membrane is incorporated in a cytoplasmic early endosome (EE), which will

contain the proteins present in the extracellular side of the cellular membrane to the inner side of the EE, leading to the generation of mature endosome³³⁻³⁵. The inward budding of the mature endosome membranes leads to the formation of intraluminal nanovesicles (ILVs), creating multivesicular bodies (MVBs) into the cytoplasm. At this step, MVBs can fuse to the lysosomes, leading to degradation of their content, or fuse to the extracellular membrane, leading to the release of their ILVs (now called exosomes) in extracellular space and, then, in body fluids^{34,35}.

The molecular mechanisms involved in exosomes biogenesis are still unclear^{33,34}. Nowadays, two theories are the main accepted: one mediated by the endosomal sorting complex required for transport (ESCRT) molecules (called ESCRT-dependent) and another mediated by neurospingomyelinase activity and ceramide biosynthesis (called ESCRT-independent)^{36,37}.

It has been demonstrated that exosomes contains a complex milieu of proteins, lipids and nucleic acids, that are reported, in a continuous updating process, in database as ExoCarta and Vesiclepedia^{38,39}. Up to date, 9769 different proteins exosomal were identified, such as enzymes, GTPases, tetraspanins like CD9, CD63 and CD81, proteins involved in exosomes biogenesis as Alix and TSG101, heat-shock proteins, among others³⁸. In several exosomal analysis, proteins such as CD9, CD63, CD81, Alix and TSG101, are considered potential markers for exosome characterization^{33,34}. Moreover, it has been demonstrated that exosomes contain DNA and several coding and non-coding RNA molecules^{40,41}. MicroRNAs (miRNAs) are small (19–22 nucleotides) non-coding RNA molecules that, binding to partially complementary 3' UTR of mRNA target, lead it to degradation or translation inhibition⁴². MicroRNAs analysis has described the presence of 2838 different miRNAs found in exosomes. The lipid bilayer membrane of exosomes is enriched in phospholipids, diglycerides, ceramide, eicosenoic acid, cholesterol, sphingolipids, sphingomyelin and biologically active lipids such as leukotrienes and prostaglandins^{27,43}. Exosomal lipid membranes confer an high-degree of stability and protection to the content against several enzymes such as proteases and nucleases⁴⁴.

Exosomes will target recipient cells through unclear uptake mechanisms; however, four mechanisms are mainly accepted: I) interaction with target cell through specific receptor-ligand interaction in a juxtacrine fashion; II) binding as a ligand for cell membrane receptors; III) aspecific fusion with target cell membrane; IV) internalization through a phagocytosis mechanism⁴⁵⁻⁴⁸. Exosomes are described in several body fluids such as blood, saliva, breast

milk, sperm, urine, synovial liquid, among others⁴⁴. The presence of exosomes in several body fluids suggest the idea of their key role in paracrine and distant cell-cell communication needed in physiological and pathological processes⁴⁴. Exosomes modulate the biological functions of target cells acting as an horizontal transmitter of protein and miRNAs. Valadi et al, described, for the first time, miRNAs and mRNAs contained into exosomes and that exosomal mRNAs could be transferred and translated in target cells⁴⁹. Exosomal miRNAs can be shuttled to target cells keeping their biological functions, modulating then the expression of target cell mRNAs in a post-transcriptional manner⁵⁰⁻⁵². Interestingly, MVBs are jointed to miRNA effector complexes, indicating the existence of a selective packaging mechanism of miRNA into exosomes⁵³.

1.3.1 Exosomes in cancer

Several studies have described even more clearly a pleiotropic role of Tumour Derived Exosomes (TDEs) in the tumour microenvironment, leading to the promotion of tumour progression⁴⁸. The tumour microenvironment modulation is dependent on the exosomes-mediated cell-cell communication between cancer and host cells⁵⁴.

TDEs promote primary tumour growth, inducing extracellular matrix remodeling through the expression of activators of metalloproteinase proteins (MMPs) and angiogenesis⁴⁸. Moreover, TDEs are involved in drug-resistance mechanisms. Safei et al described, for the first time, that cisplatin-resistant ovarian cancer cells are able to eliminate hydrophilic anticancer drugs by loading the compound into the exosomes that highly express multidrug resistance-associated protein 2 (MRP2)⁵⁵. It was recently demonstrated that exosomes released by breast cancer cell lines following Trastuzumab (antibody-based drug against HER2) treatment, contain high amount of HER2 membrane receptor. Exosomes, containing HER2 receptor, once released in the conditioned media can bind selectively Trastuzumab, decreasing the drug amount available to target parental cancer cells⁵⁶; in this way, cancer cells maintain their oncogenic potential.

TDEs are also involved in the selection and promotion of pre-metastatic niche, preparing the future metastases sites. Exosomes are considered one of the most casual agents for the “seed and soil” theory⁵⁷, according to which the “education” of the pre-metastatic site is necessary for the acceptance of circulating cancer cells^{48,58-60}. Recently, in melanoma patients, it was demonstrated that TDEs are involved in the pre-metastatic niche formation

activating bone marrow progenitor cells⁵⁸. Moreover, Costa-Silva et al demonstrated that pancreatic ductal adenocarcinoma derived exosomes induce liver pre-metastatic niche formation in naive mice, increasing liver metastases³¹.

Overall, these data suggest a crucial role of exosomes in the tumour microenvironment, inducing biological effects on targeted cells and leading to cancer progression. TDEs, with their content and their presence in several body fluids, could be one of the most attractive sources of potential non-invasive liquid biopsy biomarkers⁴⁴.

1.4 Curcumin: a small antioxidant molecule with potent anticancer effects

Curcumin (diferuloylmethane) is a polyphenol, first isolated in 1815 and identified as (1E,6E)-1,7-bis (4-hydroxy-3-methoxyphenyl) -1,6- heptadiene-3,5-dione (IUPAC ID)⁶¹. This powder is extracted from *Curcuma longa*, a spice used frequently in southeast Asia, a continent with low incidence of some cancers⁶¹. It has been clearly documented that diet is strongly involved on the differences in cancer epidemiology⁶².

Curcumin is described to modulate several molecular targets that include transcription factors, growth factors and their receptors, cytokines, enzymes, and genes regulating cell proliferation and apoptosis⁶³. The anticancer properties of Curcumin have been demonstrated by its inhibition of tumour initiation, migration, invasion and angiogenesis⁶⁴. Moreover, in leukemic cancer cells, Curcumin is able to induce apoptotic-mediated cell death and inhibits cancer cell proliferation through the upregulation of miR-15a and miR-16 that, in turn, decrease the expression of the anti-apoptotic Bcl-2 and the leukemic oncogene WT1. Curcumin suppresses tumour growth and metastasis in colorectal cancer through downregulation of miR-21, a well known oncomiRNA^{65,66}. Difluorinated Curcumin (CDF), a nontoxic analog of the dietary ingredient Curcumin has been shown to modulate also the expression of miR-21 and PTEN in pancreatic cancer⁶⁷.

In this work, we focused our attention on the idea to explore the potential anticancer effects of Curcumin in CML cells mediated by their released exosomes, in order to investigate also its potential role as adjuvant therapy in CML.

1.5 Rationals and Objectives

The main objective of my research project was to further understand the role played by CML-derived exosomes in the paracrine cross-talk between leukaemia cells and endothelial

cells. The pattern of miRNA and protein expression of CML-derived exosomes was evaluated in order to select specific molecules involved in tumour angiogenesis. Two CML cell lines (LAMA84 and K562) and the endothelial cells HUVECs were used as experimental models. The experimental strategy was to isolate LAMA84 and K562-derived exosomes and to treat HUVECs with exosomes in order to study the cross-talk between tumour and host cells. Moreover, I evaluated if Curcumin treatment of CML cells could induce exosomes-mediated anticancer effects, studying also the modulation of the cross-talk with ECs.

The aims of this thesis can be subdivided into three subsequent steps:

1. To investigate the pattern of miRNA expression in exosomes released by CML cells, in order to evaluate the expression of miRNAs involved in CML progression that could be shuttled to endothelial cells. (Paragraphs: **“Exosomal shuttling of miR-126 in endothelial cells modulates adhesive and migratory abilities of chronic myelogenous leukemia cells”**⁶⁸);
2. To investigate if Curcumin treatment of CML cells is able to induce anticancer effect modulating the expression of selected miRNAs and proteins in cells and in the released exosomes, both *in vitro* and *in vivo*. (Paragraphs: **“Curcumin inhibits in vitro and in vivo chronic myelogenous leukemia cells growth: a possible role for exosomal disposal of miR-21”**⁶⁹);
3. To investigate the effects of exosomes released by CML cells treated with Curcumin in the cross-talk with endothelial cells. I studied also their protein profile, in order to evaluate if Curcumin treatment reduces the effects of CML-derived exosomes on CML progression (Paragraphs: **“Curcumin modulates chronic myelogenous leukemia exosomes composition and affects angiogenic phenotype, via exosomal miR-21”**⁷⁰)

1.5.1 Exosomal shuttling of miR-126 in endothelial cells modulates adhesive and migratory abilities of chronic myelogenous leukemia cells

Our research group recently showed that CML cell lines, LAMA84 and K562 cells and patient's leukemic blasts, release exosomes that are involved in the neovascularization by targeting directly endothelial cells. The treatment of HUVECs with LAMA84 exosomes activates the release of IL-8 and the induction, both *in vitro* and *in vivo*, of an angiogenic

phenotype^{71,72}. It was demonstrated that exosomes contain miRNAs that can be shuttled to target cells; miR-210 and miR-92a, contained into exosomes released by K562 cells, can enhance endothelial cell migration and tube formation^{73,74}.

During the first year of my PhD program I focused my attention on the miRNAs profiling of exosomes released by CML cells. In preliminary experiments, we found that miR-126 was expressed 6 fold greater in LAMA84 exosomes compared with parental cells. Target prediction algorithms have shown that miR-126 targets both vascular cell adhesion molecule 1 (VCAM1) and CXCL12 mRNAs; their modulation, is described to have a role in adhesion to endothelial cells and in leukocyte homing in bone marrow, respectively^{75,76}. In this context, it has been also demonstrated that CXCL12 up-regulates VCAM1 in myeloma cells and chronic lymphocytic leukaemia B cells and this modulation can play a crucial role in the localization of cancer cells to the bone marrow^{23,77}.

In this first study, we investigated the exosomes-mediated cross-talk between CML and endothelial cells, evaluating if exosomes released by LAMA84 cells, containing high amount of miR-126, could transfer this miRNA into HUVECs, thus leading to a potential modulation of CML progression.

1.5.2 Curcumin inhibits *in vitro* and *in vivo* chronic myelogenous leukemia cells growth: a possible role for exosomal disposal of miR-21

Several natural polyphenols, such as Curcuminoids, can modulate, both *in vitro* and *in vivo*, the expression of several miRNAs⁷⁸. Curcumin is the main active natural polyphenol extracted from rhizomes (*Curcuma longa*). Interestingly, it has been shown that Curcumin is able to inhibit several biological process involved in cancer progression, as cell proliferation, inflammation, invasion, angiogenesis, and apoptosis in several cancers^{79,80}. Curcumin downregulates, in human colon-rectal carcinoma cell lines, the expression of several miRNAs (miR-17-5p, miR-20a, mir-21 and miR-27a) associated with increased apoptosis, decreased cell proliferation, and tumour invasion⁸¹. Curcumin is able to downregulate also miR-21, a miRNA with oncogenic properties found overexpressed in several cancer types. Curcumin leads to a decrease of tumour growth and progression in colorectal cancer⁶⁶. Bioinformatics analysis, confirmed experimentally, shows that mir-21 targets the 3'-UTR of PTEN, one of the most frequently mutated or silenced tumour suppressors in several cancers. PTEN is involved in the inhibition of PI3K-AKT pathway and in the modulation of VEGF expression in

many solid tumors⁸²⁻⁸⁴. Several studies have shown that the antagonistic effect of PTEN on PI3K/AKT signalling pathway is deregulated in numerous leukaemia, both *in vitro* and *in vivo*, due to a decrease in the expression of PTEN at gene and/or protein level⁸⁵. PTEN is also involved in the biological processes of BCR-ABL-mediated leukemogenesis⁸⁶.

MiR-196b is another microRNA associated with leukaemia: it has been described a miR-196b downregulation in EB-3 cells and in patients with B-cell acute lymphocytic leukaemia (ALL) and, in contrast, an over-expression in patients with acute myeloid leukaemia (AML)⁸⁷. The role of miR-196b in CML is still unclear. The expression of miR-196b is lower in CML patients than in healthy individuals. Bioinformatics analysis indicated Bcr-Abl as predictive target of miR-196b, and low expression levels of miR-196b were correlated with up-regulation of the oncogene Bcr-Abl⁸⁸.

Curcumin could be a promising natural compound that, in a strategy of adjuvant therapy coupled with classical tyrosine kinase inhibitor, may improve the treatment of CML patients resistant to TKIs⁸⁹.

Our preliminary results showed that Curcumin treatment of LAMA84 and K562 CML cells, caused a downregulation of miR-21 in cells and an upregulation in the released exosomes. In this study, we investigated if the treatment of CML cells with Curcumin caused an inhibition of PTEN/AKT pathway, via exosomal miR-21. We observed that Curcumin enhances a disposal of the oncomiR-21 in exosomes and this biological mechanism may contribute to the antileukemic effect.

1.5.3 Curcumin modulates chronic myelogenous leukemia exosomes composition and affects angiogenic phenotype, *via* exosomal miR-21

Angiogenesis is a complex process that depends on the interaction between growth factors, cytokines and a number of components of the extracellular matrix^{90,91}. Sabatel et al. demonstrated that miR-21 over-expression reduced the angiogenic capacity of HUVECs by directly targeting RhoB, a Rho GTPase involved in the regulation of cell growth, cellular signaling and cytoskeleton reorganization^{91,92}. Endothelial cell-cell junctions maintain a restrictive barrier that is tightly regulated to allow dynamic responses to permeability-inducing angiogenic factors. These angiogenic stimuli lead to a transient remodeling of adherens junctions (AJs), such as VE-Cadherin, depending on Rho GTPase-controlled cytoskeletal rearrangements⁹³.

As reported in this thesis, LAMA84 exosomes were enriched in miR-126, an angiomiR that was biologically active in endothelial cells, leading to an exosome-mediated cross-talk in the bone marrow microenvironment. We assessed if exosomes released by CML cell treated with Curcumin could revert the pro-angiogenic effects of CML-derived exosomes. We demonstrated that exosomes released by CML cells treated with Curcumin (Curcu-exosomes), are enriched in miR-21 and are internalized by HUVECs. Curcu-exosomes were able to downregulate the expression of RhoB, a predictive target of miR-21, thus leading to affect the endothelium monolayer integrity. In order to achieve a wider comprehension on the molecular mechanisms mediated by CML exosomes, underlying the modulation of angiogenesis, we performed a proteomic profile of exosomes released by CML cells treated or not with Curcumin using a SWATH-MS approach. We focused our attention on the different expression of proteins with pro or anti-angiogenic properties.

CHAPTER 2

Materials and Methods

Cell culture and reagents

Chronic myelogenous leukemia cells K562 and LAMA84 were obtained from (DMSZ, Braunschweig, Germany), and cultured in RPMI 1640 medium (Euroclone, UK) supplemented with 10% fetal bovine serum (Euroclone, UK), 100 U/ml penicillin, 100 mg/ml streptomycin and 2 mM L-glutamine (Euroclone, UK). HUVECs were purchased from Lonza (Clonetics, Verviers, Belgium) and grown in endothelial growth medium (EGM) according to supplier's information. In some experiments K562 and LAMA84 cells were treated with 1 μ M GW4869, a neutral sphingomyelinase 2 inhibitor, also a well-known inhibitor of exosomes release. All other reagents were purchased from Sigma (St. Louis, MO, USA), if not otherwise cited.

Exosomes isolation

Exosomes released by K562 and LAMA84 cells treated or not with Curcumin (20 and 40 μ M) during a 24 h culture period, were isolated from conditioned culture medium (CM) supplemented with 10% FBS (previously ultracentrifuged) by different centrifugation steps: 5 minutes at 300g in order to eliminate cells and debris; 15 minutes at 3000g in order to eliminate apoptotic bodies and 30 minutes at 10.000g in order to eliminate microvesicles. The cleaned CM were ultracentrifuged for 90 minutes at 100.000g at 4°C on a density gradient ultracentrifugation on a 30% sucrose/D2O cushion. Vesicles contained in the sucrose cushion were recovered, washed, ultracentrifuged for 90 minutes in PBS and collected for downstream analysis. Exosome protein content was determined by the Bradford method.

Dynamic light scattering (DLS) analysis

Exosome size distribution was determined by DLS experiments. Exosome samples were diluted 30 times to avoid inter-particle interaction and placed at 20°C in a thermostated cell compartment of a Brookhaven Instruments BI200-SM goniometer with a solid-state laser tuned at 532 nm. Scattered intensity autocorrelation functions $g_2(t)$ were measured by using a Brookhaven BI-9000 correlator and analyzed in order to determine the distribution $P(D)$ of the diffusion coefficient D by using a constrained regularization method or alternatively a gamma distribution. The size distribution, namely the distribution of hydrodynamic diameter D_h , was derived by using the Stokes-Einstein relation: $D = (k_B T) / (3\pi\eta D_h)$, where D is the diffusion coefficient, k_B is the Boltzman constant, η is the medium viscosity and T is the temperature. The mean hydrodynamic diameter of exosomes was calculated by fitting a Gaussian function to the measured size distribution.

Curcumin quantification in exosomes by HPLC assay

HPLC analyses were performed with a Shimadzu LC-10ADVP instrument with a binary pump LC-10ADVP, a UV SPD-M20A Diode Array detector, a 20 μ L injector and a computer integrating apparatus (EZ Start 7.3 software). HPLC solvents (HiPerSolvChromanorm) were obtained from VWR International (Milan, Italy). Chromatographic separation was performed on a reversed-phase column Chromolith® Performance (RP-18e, Merck, 100 \times 4.6 mm) and a mobile phase of methanol [Mobile phase A] and TFA 0.01% (v/v) aqueous solution [Mobile phase B]. The developed gradient method consisted of % change in mobile phase B with respect to time (0.01→3.00 min: 99.5% B; 3.01→15.00 min: 12% B; 15.01→16.99 min 12% B; 17.00→25.00 min 0% B; 25.01→30.00 min 99.5% B). The mobile phase was filtered through Whatman filter 0.45 μ m and degassed before use. The flow rate was set at 1 mL/min and the UV wavelength at 257, 280, 400 and 420 nm. In these conditions, the retention time for Curcumin was 17.1 minutes. Stock and working standard solutions were prepared as follow: 50 mg of Curcumin working standard dissolved in 50 mL of acetone. This stock standard solution was diluted to prepare six sets of calibration standards of Curcumin at concentrations range of 0.02–1.00 μ g/mL in acetone. (LOQ = 0.01 μ g/ ml). The standard calibration curve was constructed using peak area versus known concentrations of Curcumin. HPLC reports were highly reproducible and linearly related to concentration

(regression equation $y = 54144x - 84.22$; $R = 0.9944$; $R^2 = 0.9888$). The linear regression line was used to determine the linearity and concentration of the samples.

200 μl of exosomes sample (2 $\mu\text{g}/\mu\text{l}$ in protein content determined by Bradford method), isolated by both K562 and LAMA84 cells treated with Curcumin (10, 20 and 40 μM) (Curcu-exosomes) or not (control exosomes), were added to 200 μl of methanol and centrifuged at 14.000 rpm for 10 min; after that, the supernatant (20 μl) was analyzed by HPLC as described above. Each sample was analyzed in triplicate in order to have significative results.

Proliferation assay

In order to evaluate cell proliferation a Methyl-thiazol-tetrazolium (MTT) assay was done. K562 and LAMA84 cells were plated in triplicate at 2×10^5 per well and treated with different concentrations of Curcumin (5–40 μM) for 24 hours. HUVECs were plated in triplicate at 5×10^4 per well and treated with exosomes derived from K562 and LAMA84 cells treated or not with Curcumin (20 and 50 $\mu\text{g}/\text{ml}$) for 24 hours. Means and standard deviations (SD) generated from three independent experiments are reported as the percentage of viable cells.

Uptake of LAMA84 and K562 exosomes by HUVECs

K562 and LAMA84 exosomes were labeled with PKH26 according to supplier's information. Briefly, exosomes were incubated with PKH26 for 10 minutes at room temperature. Labeled exosomes were washed in PBS by ultracentrifugation and pellets were resuspended in low serum medium and incubated with HUVECs for 1- 4 hours at 4°C or 37°C. HUVECs, grown on coverslips coated with type I collagen (Calbiochem, Darmstadt, Germany), were treated with different doses of K562 or LAMA84 exosomes, K562 and LAMA84 Curcu-exosomes or low serum medium. In some experiment, HUVECs were also pretreated with 50 μM 5-ethyl-N-isopropyl amiloride (EIPA), well known inhibitor of exosomes uptake, for 1 hour. After incubation, cells were stained with Alexa Fluor 633[®] phalloidin or Actin Green (Molecular Probes, Life Technologies, Carlsbad, California, U.S) that binds F-actin with high affinity; nuclei were stained with Hoechst (Molecular Probes, Life Technologies, Carlsbad, California, U.S) and analysed by confocal microscopy. Each picture was acquired with laser intensities and amplifier gains adjusted to avoid pixel saturation. Each fluorophore used was excited independently and sequential detection was performed. Each picture consisted of a z-series

of images of 1024–1024 pixel resolution. IMAGE-J software (<http://imagej.nih.gov/ij/>) was used in order to perform a semi-quantitative analysis of fluorescence intensity; we selected the perinuclear area in a section at 5 μm and measured the fluorescence intensity. Values are the mean \pm SD of 15 measurements from three independent experiments.

TaqMan Human MicroRNA Array for Profiling of miRNAs

The RNAspin Mini (GE Healthcare Science, Uppsala, Sweden) kit was exploited to isolated total cellular RNA and miRNAs from LAMA84 cells and their exosomes; the RNA quality was confirmed through 2100 Bioanalyzer (Agilent Technologies, Santa Clara, CA, USA). Then was performed the reverse transcription of 600 ng of total RNA using Megaplex™ RT Primers Human Pool A (Life Technologies, Carlsbad, California, U.S.), according to manufacturer's instructions. Reverse transcription reaction conditions were optimized as follow: 16°C for 2 minutes, 42°C for 1 minute, 50°C for 1 second for 40 cycles, 85°C for 5 minutes then hold at 4°C. The product cDNA was diluted, mixed with TaqMan® Gene Expression Master Mix and loaded into each of the eight fill ports on the TaqMan® Human MicroRNA Array A (Life Technologies, Carlsbad, California, U.S.). The array was centrifuged at 1200 rpm twice for 1 minute each and then run on ABI-PRISM 7900 HT Sequence Detection System (Applied Biosystems, Foster City, CA, USA) using the manufacturer's recommended program. SDS 2.1 software was used in order to quantify data; miR-18b or RNU6-2 were selected as endogenous control in order to exploit them for data normalization. The cycle threshold (Ct) value, which was calculated relatively to the endogenous control, was used for our analysis (ΔCt). The $2^{-\Delta\Delta\text{CT}}$ (delta-delta-Ct algorithm) method was used to calculate the relative changes in gene expression.

Quantitative polymerase chain reaction (qPCR) for miRNAs and pre-miRNAs

The expression of miR-126 and miR-21 was evaluated through miScript PCR assay (QIAGEN, Hilden, Germany). RNAspin Mini kit (GE Healthcare Science, Uppsala, Sweden) was exploited in order to extract total cellular RNA and miRNAs from K562, LAMA84 cells (and their released exosomes) and HUVECs. MiScript II RT Kit (QIAGEN, Hilden, Germany) was used to performe the reverse transcription reaction, described by the manufacturer's instructions; reaction buffers were selected for downstream analysis: specifically, was used miScript *HiSpec* Buffer for cDNA synthesis to detect mature miRNA and miScript *HiFlex* Buffer for

cDNA synthesis of precursor miRNAs. qPCR was performed using miScript SYBR Green PCR Kit (QIAGEN, Hilden, Germany). Mature miR-126, miR-21 and miR-196b were detected through miScript Primer Assay and pre-miR-126 and pre-miR-21 by miScript Precursor Assay, according to manufacturer's instructions. RNU6-2 was used as stable endogenous control. Expression levels of miRNAs and pre-miRNA were determined using the comparative Ct method to calculate changes in Ct and ultimately fold and percent change. An average Ct value for each RNA was obtained from triplicate reactions.

qPCR for PTEN, VEGF, BCR-ABL, RhoB, VCAM1, IL8, MARCKS, VEGFR, ZO1 and VE-Cadherin

1 µg of total RNA extracted from HUVECs using the RNASpin Mini kit (GE Healthcare Science, Uppsala, Sweden) was reverse transcribed using the High Capacity cDNA Archive kit (Life Technologies, Carlsbad, California, U.S.), according to manufacturer's instructions. RT-QPCR was performed in 48-well plates using the Step-One Real-Time PCR system (Applied Biosystem). For quantitative SYBER® Green Real Time PCR, reactions were carried out in a total volume of 20 µl containing 2× SYBR® Green I Master Mix (Applied Biosystems), 2 µl cDNA and 300 nM forward and reverse primers. Primers sequence were: GAPDH (5'ATGGGGAAGGTGAAGTTCG3', 5'GGGTCATTGATGGCAACAATAT3'), MARCKS (5'TGCTCTTTGCCACCCGATAA3', 5'ACCCTAAAACCTGCACACTGCT3'), VEGFR (5'CGGTCAACAAAGTCGGGAGA3', 5'CAGT GGCACCACAAAGACACG3') ZO1 (5'TTAAGCCAGCCTCTCAACAGAAA3', 5'GGTTGATGATGCTGGGTTTGT3'), and VE-Cadherin (5'GATCAAGTCAAGCGTGAGTCG3'; 5'AGCCTCTCAATGGCGAACAC3'). RNASpin Mini kit was also used in order to extract total cellular RNA from K562 and LAMA84 cells and exosomes. 1 µg of total RNA was reverse transcribed through High Capacity cDNA Archive kit (Life Technologies, Carlsbad, California, U.S.), according to manufacturer's instructions. PTEN, VEGF and BCR-ABL transcript levels were measured by TaqMan Real Time PCR, using TaqMan gene expression assay for PTEN (Hs00262123 m1), VEGF (Hs0090005.m1) (Life Technologies, Carlsbad, California, USA). TaqMan gene expression assay were also performed for CXCL12 (Hs00171022_m1), VCAM1 (Hs00174239 m1), IL8 (HS00174103 m1), RhoB (Hs03676562 m1) BCR-ABL (Hs03024541_ft) and GAPDH (Hs99999905 m1), all obtained from Invitrogen (Foster City, CA, USA). Data were analyzed as previously described.

GAPDH was chosen as a stable endogenous control and changes in the target mRNA content were determined using the comparative Ct method, as described in the previously.

Shuttling assays for Cy3-labeled-miRNA precursor

miR-126 precursor (QIAGEN, Hilden, Germany) was labelled with Label IT siRNA Tracker Cy3 Kit, according to the manufacturer's instructions (Mirus, Madison, WI, USA). LAMA84 cells (6×10^4) were transfected with 10 nM of Cy3-labeled pre-miR-126 using HiPerFect Transfection Reagent (QIAGEN, Hilden, Germany) (LAMA84/Cy3-miR-126). The day after transfection, cells were seeded on transwells, 3 μ m pore filters in coculture with HUVECs over night. LAMA84 cells did not migrate through the 3 μ m pore filters after 18 h (data not shown). HUVECs were stained with Hoechst and analysed by confocal microscopy.

Inhibition of exosome release

LAMA84 cells, transfected with Cy3-labeled pre-miR-126, were seeded in the upper wells of transwells and incubated with 1 and 5 μ M GW4869; in the bottom wells were plated also endothelial cells. After incubation for 18 hours, the cells were processed in accordance with manufacture's instruction and finally stained with Hoechst and analyzed by confocal microscopy.

Transfection of K562, LAMA84 and HUVECs cells with miR-21 mimic or inhibitor

Transfection of miScript miR-126 or miR-21 mimic and inhibitor (QIAGEN, Hilden, Germany) in K562, LAMA84 and HUVECs cells was performed according Fast-Forward Transfection protocol (QIAGEN, Hilden, Germany). 6×10^4 cells per well were seeded in a 24-well plate in 500 μ l of EGM medium. miScript miR-126 inhibitor (2'-O-Me-miR-126), miR-21 inhibitor (2'-O-Me-miR-21), miR-126 mimic (2 μ M) or miScript miR-21 mimic (2 μ M) were diluted in 100 μ l culture medium without serum to obtain a final 5 nM miRNA concentration for working solution. Transfection of K562 and LAMA84 cells was performed, for 18 hours, through HiPerFect Transfection Reagent (QIAGEN, Hilden, Germany), according to manufacturer's instructions. AllStars Negative Control siRNA (QIAGEN, Hilden, Germany) and MiScript Inhibitor Negative Control (QIAGEN, Hilden, Germany) were used as negative controls, as indicated by manufacture's technical specifications. Transfection efficiency was determined through qPCR.

Luciferase activity assay

The 3'-UTRs of CXCL12 and VCAM1 mRNAs were cloned in pEZX-MT01 vector (Genecopoeia, Rockville, MD USA), designed based on the sequence of miR-126 binding sites. 8×10^4 HUVECs per well in a 24-well plate were seeded in 500 μ l of an appropriate culture medium and cells were transfected with 300 ng of the pEZX-MT01 firefly luciferase report appropriately diluted in 60 μ l culture medium without serum. HUVECs were then cotransfected with 6 pmol of miR-126 mimic or inhibitor using Attractene Transfection Reagent (QIAGEN, Hilden, Germany) according to manufacturer's protocol. To assess whether exosomal miR-126 targets directly VCAM1 and CXCL12 mRNAs, after the transfection with pEZXMT01 vector, HUVECs, were incubated with 50 μ g/ml of LAMA84 exosomes. The PTEN 3' UTR cloned in pEZX-MT01 vector was obtained from Genecopoeia (Rockville, MD, USA), designed based on the sequence of miR-21 binding sites. K562 and LAMA84 cells (12×10^4 per well) in a 24-well plate were seeded in 500 μ l of RPMI medium and transfected with 300 ng of the pEZX-MT01 firefly luciferase report diluted in 60 μ l culture medium without serum. K562 and LAMA84 cells were also cotransfected with 6 pmol miR-21 mimic or miR-21 inhibitor using Attractene Transfection Reagent (QIAGEN, Hilden, Germany) according to manufacturer's protocol. To investigate if Curcumin treatment induces a modulation of miR-21 expression, leading to an inhibition of expression of its target PTEN, K562 and LAMA84 cells were incubated with 20 and 40 μ M of Curcumin after the transfection of pEZX-MT01 vectors. The 3'-UTRs of RhoB was cloned in pEZX-MT01 vector (Genecopoeia, Rockville, MD USA) based on the sequence of miR-21 binding sites. 8×10^4 HUVECs per well in a 24 well plate were seeded in 500 μ l of an appropriate culture medium, the cells were transfected with 300 ng of the pEZX-MT01 firefly luciferase report diluted in 60 μ l culture medium without serum. HUVECs were cotransfected with 6 pmol of miR-21 mimic or miR-21 inhibitor using Attractene Transfection Reagent (QIAGEN, Hilden, Germany) according to manufacturer's protocol. To test if exosomal miR-21 targets RhoB mRNA, HUVECs were incubated with 20 μ g/ml of exosomes released by CML cells treated or not with Curcumin, after the transfection with pEZXMT01 vector.

GloMax[®]-Multi Detection System (Promega Corp., Madison, WI, USA) was used in order to measure consecutively the Firefly and Renilla Luciferase activities 24 hours after transfection through Dual Glo[®] Luciferase Assay System kit (Promega Corp, Madison, WI, USA).

Transfections were repeated for each samples, three times in duplicate. Normalized data were calculated as the ratio of Renilla/Firefly Luciferase activities.

Adhesion assay

HUVECs grown as a monolayer were transfected or not with miR-126 mimic, miR-126 inhibitor or scramble controls and incubated for 24 hours with indicated conditions. After treatment, HUVECs were washed with PBS, LAMA84 cells were added for 2 hours at 37°C and adherent cells were stained with haematoxylin/eosin staining. Each test group was assayed in triplicate; five high power (400x) fields were counted for each condition.

Motility assay

HUVECs monolayer transfected or not with miR-126 mimic, miR-126 inhibitor or scramble controls, were incubated for 24 hours with different amount of exosomes. After treatment, conditioned media aliquots were centrifuged to remove cellular debris and used as chemoattractant. LAMA84 cells were suspended in serum-free RPMI 1640 medium supplemented with 0.1% BSA in transwells with 8 µm pore filters and exposed to chemoattractants, for 18 hours. After incubation, cells migrated in the bottom wells were counted.

ELISA for VEGF, AKT, pAKT and IL8

Conditioned medium (CM) of HUVECs, transfected or not with miR-126 mimic or inhibitor, was collected from cells stimulated for 24 hours with different amount of LAMA84 exosomes and centrifuged in order to remove cellular debris. CXCL12 protein concentrations was evaluated by an ELISA kit (R&D Systems, Minneapolis), according to the manufacturer's protocol. Conditioned medium (CM) of K562 and LAMA84 cells, treated with different concentration (10, 20, 40 µM) of Curcumin, transfected or not with miR-21 mimic or inhibitor, was collected from cells after 24 hours of incubation. Moreover, CM of K562 and LAMA84 cells, treated with 1 µM GW4869 or cotreated with Curcumin and 1 µM GW4869, were also collected from cells after 24 h of incubation. VEGF protein levels were measured in CM aliquots (purified by centrifugation in order to remove cellular debris) using an ELISA kit (Invitrogen Carlsbad, California, USA), according to the manufacturer's protocol.

K562 and LAMA84 cells, treated with (20, 40 μ M) Curcumin, transfected or not with miR-21 mimic or inhibitor, were collected and opportunely lysated. K562 and LAMA84 cells, treated with 1 μ M GW4869 and/or cotreated with Curcumin and 1 μ M GW4869, were also collected and lysated after 24 hours of incubation. An ELISA assay (Invitrogen, Carlsbad, California, USA) was performed in order to quantify pAKT levels, according to the manufacture's protocol: specifically, was used AKT1 (pS473) ultrasensitive ELISA kit, that allows to quantify the level of AKT1 protein that is phosphorylated at 473 serine residue. To normalize the sample for the total AKT1 amount, we used an AKT1 (total) ELISA kit (Invitrogen, Carlsbad, California, USA).

CM of HUVECs, transfected or not with miR-21 mimic or inhibitor, and treated with 20 and 50 μ g/ml of Curcu-exosomes and control exosomes, was collected from the cells after 6 hours of incubation in order to measure IL8 levels. CM aliquots were then centrifuged to remove cellular debris and IL8 protein levels were measured using an ELISA kit (Invitrogen Carlsbad, California, USA), according to the manufacturer's protocol.

Western blot

After protein extraction with *Laemmly lysis buffer*, equal amount of proteins (50 μ g) of every samples were subjected to SDS-PAGE electrophoresis on Bolt™ 4-12% Bis-Tris Gels / MES running buffer System (Invitrogen, Carlsbad, California, USA), according to the manufacture's protocol. Immunoblotting was performed for 1 hour at constant 50 Volt on nitrocellulose membrane (Hybond-ECL, Amersham Bioscience, Little Chalfont, UK). The membrane was probed overnight at 4°C with specific primary antibodies: Alix, TSG101, PTEN, AKT, pAKT, Bcr-Abl, MARCKS and actin (Cell Signaling Technology, Beverly, MA). Immunocomplexes with appropriate HRP-linked secondary antibody were detected by the enhanced chemiluminescence detection system (Super Signal, Pierce, Rockford, IL, USA). K562 or LAMA84 cells (5×10^6) were incubated with 20 and 40 μ M Curcumin or DMSO for 24 hours (negative control). HUVECs were incubated, for 24 hours, with 20 μ g/ml of exosomes derived from K562 treated or not with 20 μ M of Curcumin.

Motility assay

K562 and LAMA84 cells, treated or not with 20, 40 μ M Curcumin, were suspended in serum-free RPMI 1640 medium supplemented with 0.1% BSA in transwells with 8 μ m pore filters

and exposed to complete RPMI 1640 as chemoattractant, for 24 hours. Some samples were cotreated with 20, 40 μM Curcumin and 1 μM GW4869. After incubation, cells migrated in the bottom wells were counted. HUVECs treated with 20 and 50 $\mu\text{g}/\text{ml}$ of Curcu-exosomes were also suspended in serum-free RPMI 1640 medium supplemented with 0.1% BSA in transwells with 8 μm pore filters and exposed to complete RPMI 1640 as chemoattractant for 6 hours. After incubation, cells migrated in the bottom wells were counted.

Colony formation assay

K562 or LAMA84 cells were seeded in 6-well (2000/ml/well) in Iscove's methicellulose medium (Methocult H4230, Stem Cell Technologies, Vancouver, Canada) containing or not different concentration of Curcumin (10, 20, 40 μM). After 7 days of culture, K562 and LAMA84 colonies were observed by phase-contrast microscopy and photographed. The number and area of ten colonies per condition were measured with the IMAGE-J software (<http://rsbweb.nih.gov/ij/>).

Transendothelial migration assay

The transendothelial permeability of HUVECs monolayers was evaluated using Transwell polycarbonate insert filters (Corning, Little Chalfont, UK pore size 0.4 μm). HUVECs were grown as a tight monolayer and treated for 3 and 6 hours with Curcu-exosomes and exosomes released by control cells. FITC-dextran (500 kDa, Sigma) was added at cell monolayers in 200 μl of culture medium for 30'. Samples were removed from the lower chamber for fluorescence measurements using Glomax.

Moreover, HUVECs monolayer were grown in the upper well of transwells coated with type I collagen, with 8 μm pore filter and incubated with different amount of LAMA84 exosomes (10–50 $\mu\text{g}/\text{ml}$). After incubation for 18 hours, LAMA84 cells were added and transmigration of the cells was evaluated after other 18 hours by counting the LAMA84 cells in the bottom well.

HUVEC tube formation on Matrigel

Matrigel was used to test the effects of exosomes on the *in vitro* vascular tube formation. Exosomes released by K562 and LAMA84 cells treated or not with Curcumin (20 μM), were added to HUVECs plated on Matrigel in endothelial basal medium containing 0.2% of FBS as

indicated. Cells were incubated for 3 hours and then evaluated by phase-contrast microscopy and photographed.

Immunofluorescence analysis

Confluent HUVEC monolayers were grown on coverslips coated with type I collagen (Calbiochem, Darmstadt, Germany) and were treated with 50 µg/ml of LAMA84 exosomes or low serum medium for 24 hours. After incubation, cells were processed as previously described by our group [7]; briefly, cells were fixed in 3.7% paraformaldehyde followed by permeabilization with 0.1% Triton X-100 for 3 min. Incubation with anti-CXCL12 (1:100; Cell Signalling Technologies) was performed in PBS 1% BSA overnight at 4°C. After incubation, cells were stained with Texas Red-conjugated secondary anti mouse antibodies (1:100; Molecular Probe, Eugene, OR) and analysed by confocal microscopy (Leica TSC SP8).

Confluent HUVEC monolayers grown on coverslips coated with type I collagen were treated also with 20 µg/ml of CML Curcu-exosomes, control exosomes or low serum medium for 6 hours. After incubation, cells were processed as previously described⁹². Antibodies used in these experiments were anti-RhoB (1:100; Novus), anti-ZO1 (1:100; Santa Cruz technology) and anti VE-Cadherin (1:100; Santa Cruz technology). Cells were stained with Texas Red-conjugated secondary anti mouse antibodies (1:100; Molecular Probe, Eugene, OR) and analysed by confocal microscopy (Nikon A1).

FACS analyses

VCAM1 expression on HUVECs cell membrane was determined by flow cytometry analysis. HUVECs transfected or not with miR-126 mimic or inhibitor were incubated for 6 hours or overnight with 20 µg/ml of LAMA84-exosomes in a low serum medium (EGM:RPMI, 1:9). 1×10^6 of HUVECs were washed in PBS and incubated with 20 µl of anti-VCAM1-PE antibody (BD Biosciences, Mountain View, CA, USA) for 15 minutes at 4°C according to manufacturer's instructions. Isotype matched irrelevant antibodies were used as a negative control. Viable cells were gated by forward and side scatter and analysis was performed on 100,000 acquired events for each sample. Expression of HUVECs intracellular RhoB was also determined by flow cytometry analysis. HUVECs, transfected or not with miR-21 mimic and inhibitor, were treated with 20 µg/ml of K562 exosomes treated or not with Curcumin for 6 h. After treatment, the cells were centrifuged for 5 min at $300 \times g$ and washed with PBS/

BSA. 100 μ l of Fixation buffer (reagent A of Leucoperm, AbDSerotec) was added for 15 min at room temperature, then the cells were washed in PBS/BSA and centrifuged for 5 min at 300 \times g. Cells were resuspended with 100 μ l of permeabilization buffer (reagent B of Leucoperm, AbDSerotec). Soon after, a RhoB unconjugated primary antibody (Novus Biologicals) was added for 30 min at room temperature. Cells were washed with PBS/BSA and a FITC secondary antibody was added for 15 min. Stained cells were washed with PBS/BSA and analysed on a FACS Calibur (Becton Dickinson) using Cellquest software (BD Biosciences, NJ, USA).

Proteomic analyses: Sample preparation, SWATH-MS and data analysis

250 μ g of exosomes released by curcumin-treated and control K562 cells were subjected to in-solution digestion using 50% 2,2,2-trifluoroethanol (TFE) in PBS, as previously described (Principe et al), with some modifications. Briefly, after 2 minutes sonication in an ice bath, exosomes were incubated with constant shaking for 2 h at 60°C; extracted exosomal proteins were reduced with 5 mM DTT for 30' at 60°C, alkylated with 25 mM iodoacetamide (IAA) for 30' in the dark at room temperature and digested for 18 hours adding trypsin at a ratio of 1:50 (w/w). After stopping digestion, extracted peptides were desalted using C18 Macrospin columns, dried and resuspended in 5% acetonitrile (ACN)/H₂O (5:95, v/v) containing 0.1% formic acid (FA). A pool containing an equal amount of all three samples has been prepared to generate the spectral reference library for SWATH-MS analysis.

All the analyses were performed using a Triple TOF 5600 Plus System (AB Sciex, Framingham, U.S.A.) equipped with an Eksigent ekspert nano LC 425 system. After being cleaned and pre-concentrated on a C18 reverse-phase trap column, employing a mobile phase, from loading pump, containing 0.1% v/v FA in water at a flow rate of 5 μ l/min, peptides were separated on the C18 analytical column, equilibrated at 40°C with a solvent A (0,1% FA in water), at a flow rate of 300 nL/ min, using a 100 min gradient method: (10–40% solvent B over 60 min, 40–70% solvent B over 15 min; 70–95% solvent B over 1 min, hold solvent B at 95% for 5 min, 95–10% solvent B in 1 min and hold solvent B at 10% for remaining 18 min. The solvent B was 98% ACN and 0,1% FA. To generate the spectral reference library, the pooled sample was subjected to traditional Information Dependent Acquisition (IDA). The mass spectrometer was operated such that an MS scan (400–1250 m/z; accumulation time 250 ms) analyzed TOF in high resolution mode (> 30,000), followed by 50 MS/MS scans (230–

1500 m/z, accumulation time 65 ms) analyzing TOF in high sensitivity mode (resolution > 15,000) with rolling collision energy. For fragmentation, precursors, with charges from 2 to 5, were selected if exceeding a threshold of 100 counts per second (cps); former ions were excluded for 12s. The IDA file was submitted to Protein Pilot™ 4.5 software (AB SCIEX, Toronto, Canada) using Uniprot as human protein database. The search was performed with the following settings: identification as sample type, iodoacetamide cysteine alkylation, digestion by trypsin; no special factors; run of false discovery rate analysis; protein pilot score > 0.05 with a 10% confidence threshold.

For SWATH acquisition, peptides were analysed in SWATH-MS mode. At a cycle time of 2s, 50 ms TOF/MS survey scan was performed between 400– 1250Da with 34 × 25 Da swath. Each SWATH MS/MS acquisition was performed between 230–1500 Da using a 76 ms accumulation time. Data from three independent experiments were acquired for each sample. The SWATH files were processed by Peak View v2.2 and Marker View. In Peak View they were analyzed using the following parameters: 10 peptides; 7 transitions; peptide confidence threshold of 90%; FDR threshold of 5%; exclusion of modified peptides; XIC Extraction Window of 15 min; XIC width set at 75 ppm. Protein list with FDR lower than 5% was exported to Marker View for statistical data analysis. Gene ontology and pathway analyses were performed using iPathway Guide (<http://www.advaitabio.com/ipathwayguide>).

Ethics statement

All animal experiments were conducted following the University of Palermo and Italian Legislation for Animal Care.

CML mouse xenograft

Male SCID mice four-to-five week old were obtained from Charles River (Charles River Laboratories International, Inc., MA, USA) and acclimated for a week. Mice received sterilized diet and filtered water ad libitum. Animals were observed daily and clinical signs were noted. Mice were randomly assigned to six groups of five each. Each mouse was inoculated subcutaneously (sc) in the right flank with viable single cells (2×10^7) suspended in 0.2 ml of PBS. Mice were treated every day, per os, for 2 weeks, with 2 mg of Curcumin or vehicle (corn oil) as control and no adverse reaction was observed in all mice following

administration of this dose of Curcumin or corn oil. One week after the last day of treatment, mice were sacrificed, tumours were removed and measured and plasma exosomes were purified. Blood was collected by post-mortem cardiac puncture into blood collection tubes, centrifuged at $850 \times g$ for 20 min at 20°C and the supernatant (plasma) was collected. Plasma was centrifuged at $3000 g$ for 15' at 4°C , at $10.000 g$ for 30'. The tumour weights were calculated assuming that $1\text{mm}^3 = 1\text{mg}$. Tumour volume was evaluated by caliper using the formula: $L \times W^2/2 = \text{mm}^3$ where L and W are the longest and shortest perpendicular measurements in millimeters, respectively.

RNA isolation from exosomes released in mice plasma

Exosomal RNA from prefiltered plasma was isolated through exoRNeasy kit (Qiagen Hilden, Germany) according to the manufacturer's protocol. mir-21 levels were tested by miScript PCR System (QIAGEN, Hilden, Germany) following RNA extraction from $500 \mu\text{l}$ of plasma collected from mice treated with Curcumin and control mice, treated with vehicle (corn oil).

Matrigel plug assay

Four weeks old BALB/c mice (Charles River Laboratories International, Wilmington, MA) were injected subcutaneously with $200 \mu\text{l}$ Matrigel (BD Biosciences Pharmingen, San Diego, CA) containing $100 \mu\text{g}$ of K562 and LAMA84 cells-derived exosomes treated or not with Curcumin or PBS (negative control). After 4 weeks the plugs were removed and the degree of vascularization was evaluated through determination of hemoglobin content using the Drabkin method (Drabkin's reagent kit)⁵⁴.

CHAPTER 3

Results

3.1 Exosomal shuttling of miR-126 in endothelial cells modulates adhesive and migratory abilities of chronic myelogenous leukemia cells

HUVECs internalize LAMA84 exosomes

LAMA84 cells are able to release nanovesicles into the culture medium, that we isolated on a sucrose gradient and characterized as exosomes, as previously demonstrated from our group⁷². The uptake of isolated exosomes by endothelial cells was examined by labelling exosomes with PKH-26: HUVECs treated with LAMA84 exosomes, internalized exosomes in a time and dose-dependent manner (Figure 1, panel a).

As shown in Figure 1a, exosomes are rapidly internalized into HUVECs at 37°C and localized in the perinuclear compartment after 4 hours of incubation. However, it is shown that the uptake of exosomes in HUVECs was blocked by incubation at 4°C (Figure 1, panel a) or by treatment with 50 µM of EIPA (Figure 1, panel b), a well-known blocker of macropinocytosis⁹⁴, thus supporting the hypothesis that exosomes internalization could be performed by endocytosis^{45,75}.

LAMA84 exosomes transport miRNAs

It has been described that exosomes contain coding and non-coding RNA molecules, among which miRNAs⁴⁹. Interestingly, Bioanalyzer analysis of RNAs isolated from exosomes released by LAMA84 showed the abundance of short RNAs, such as miRNA population⁴⁹. Thus, we performed a TaqMan low-density miRNA array in order to determine an exosomal profile of miRNAs with known functions. This experiment helped us to identify significative differences of expression of selected miRNAs in exosomes versus parental LAMA84 cells. With this high-throughput technique we were able to identify 200 miRNAs: 76 miRNAs were

only expressed in LAMA84 parental cells (38%), 18 miRNAs were expressed only in LAMA84 exosomes (9%) and 106 miRNAs were differentially expressed between LAMA84 exosomes and LAMA84 cells (53%). All together, these data showed that LAMA84 exosomes contain 124 miRNAs and support the idea of a selective sorting of miRNAs into the exosomes. After a bioinformatic analyses we selected miR-18b as stable endogenous control for miRNAs normalization since it showed no statistical variation of expression between cells and exosomes. Moreover, comparable data were obtained using RNU6, a well-known small nuclear RNA used for miRNAs normalization in different experimental models. Comparing exosomal versus LAMA84 parental cells miRNAs, we identified 89 miRNAs with increased level ($FC > 2$) and 17 miRNAs with decreased level ($FC < 0.5$).

Our research group had previously demonstrated that LAMA84 exosomes stimulate angiogenesis, both *in vitro* and *in vivo*⁷². Now we focused our attention on miRNAs related to angiogenic pathway, specifically miR-126 which we found enriched in LAMA84 exosomes with respect to LAMA84 parental cells. This data was further validated by miRNA expression in a single qPCR assay.

Exosome-mediated shuttling of miR-126 into endothelial cells

In order to demonstrate, the uptake of miR-126 derived from LAMA84 exosomes, in ECs, we treated HUVECs with different amount (20–50 $\mu\text{g/ml}$) of LAMA84 exosomes and, after 24 hours we analysed the levels of expression of miR-126 in HUVECs. miR-126 was up-regulated in a dose-dependent manner compared with untreated cells, as reported in Figure 2a.

In order to exclude the hypotheses that LAMA84 exosomes could induce, in HUVECs, the expression of endogenous miR-126, we quantified the expression of precursor miR-126 (pre-miR-126) in ECs through qPCR. As reported in Figure 2b, we found no significant difference of pre-miR-126 expression level after treatment of ECs with 20–50 $\mu\text{g/ml}$ of LAMA84 exosomes.

In order to confirm and visualize the transfer of exosomal miR-126 into HUVECs, LAMA84 cells were before transfected with Cy3-labeled pre-miR-126 and then co-cultured with HUVECs in transwells. Cy3-miR-126 signals were detected in HUVECs cytosol after 24 hours of co-culture (Figure 2 panel c). On the contrary, we did not detect red fluorescence in HUVECs co-cultured with LAMA84 cells treated with 1–5 μM of GW4869, a neutral

sphingomyelinase (nSMase) 2 inhibitor, also well-known as exosome release inhibitor³⁷, and with untransfected LAMA84 cells (Figure 2 panel c).

Exosomal miR-126 targets CXCL12 and VCAM 3'-UTR mRNA in HUVECs

Bioinformatic analyses showed that both VCAM1 and CXCL12 could be considered predictive mRNAs target of miR-126. We confirmed that LAMA84 exosomes-derived miR-126 binds the 3' UTR of CXCL12 mRNA using a Firefly/Renilla Duo-Luciferase reporter vector (pEZX-MT01), which has the 3'UTR of CXCL12 cloned downstream of the firefly luciferase gene (Figure 3a) (CXCL12-pEZX).

Interestingly, the firefly luciferase activity was decreased around 50% when HUVECs transfected with CXCL12-pEZX were incubated with 50 µg/ml of LAMA84 exosomes, compared with untreated HUVECs transfected with this vector (Figure 3b). The transfection of miR-126 mimic into HUVECs, containing CXCL12-pEZX, reduced the activity of firefly luciferase around 45% compared with untransfected HUVECs, similarly to LAMA84 exosomes treatment. On the contrary, we assessed an increased firefly luciferase activity when HUVECs containing CXCL12-pEZX were transfected with miR-126 inhibitor. The treatment of CXCL12-pEZX transfected HUVECs with LAMA84 exosomes, after silencing of miR-126, reverted the increased luciferase activity (Figure 3b).

Similar results were obtained when HUVECs were transfected with a Firefly/ Renilla Duo-Luciferase reporter vector (pEZX-MT01) containing the VCAM1 3'UTR mRNA downstream of luciferase gene (Figure 3c-d). These data support the idea that exogenous miR-126 carried by exosomes keeps its biological functions in target HUVECs.

LAMA84 exosomes modulate CXCL12 expression in endothelial cells

We assessed the inhibitory effect of miR-126 on CXCL12 expression at both mRNA and protein level. Through qPCR analysis, we demonstrated that the treatment of HUVECs with LAMA84 exosomes, for 24 hours, caused a decrease in CXCL12 transcript in a dose-dependent manner, specifically of 60% and 75% in HUVECs treated with 20 and 50 µg/ml of exosomes respectively (Figure 4a).

These data were confirmed also at protein level with an ELISA assay: treatment of HUVECs with LAMA84 exosomes, for 24 h, caused a dose-dependent decrease of CXCL12 protein in

HUVEC conditioned medium (Figure 4b). The results were also confirmed by immunofluorescence assays (Figure 4c).

In order to confirm the function of miR-126 delivered by LAMA84 exosomes in endothelial cells, we performed an ELISA assay of conditioned medium of HUVECs transfected with miR-126 inhibitor or mimic and then treated with different amounts of LAMA84 exosomes.

We demonstrated, by ELISA assay, that the inhibition of miR-126 levels in HUVECs increased the protein level of CXCL12 in conditioned medium and reversed the effects of LAMA84 exosomes treatment (Figure 4d); in contrast, the overexpression of miR-126 in HUVECs led to a significantly decreased CXCL12 protein in conditioned media and enhanced the effect of exosomes (Figure 4e). Taken together, our data indicate that the LAMA84 exosomes treatment induce a dose and time-dependent regulation of CXCL12 expression in HUVECs, confirmed by the study of gain and loss of function for miR-126.

LAMA84 exosomes modulate VCAM1 expression in HUVECs

Bioinformatic analysis revealed VCAM1 3'-UTR mRNA as a predictive target of miR-126; thus, through qPCR analysis, we evaluated if the treatment of HUVECs with LAMA84 exosomes induce a modulation of VCAM1 mRNA expression. Interestingly, LAMA84 exosomes induce, in dose dependent manner, VCAM1 mRNA expression up to 12 hours of treatment while there was a decrease in VCAM1 mRNA levels at later time points, suggesting a time-dependent regulation of VCAM1 expression (Figure 5a).

We demonstrated that VCAM1 mRNA expression increased 3 fold in HUVECs transfected with miR-126 inhibitor (2'-OMemir-126) compared with untransfected cells (Figure 5b). VCAM1 mRNA expression was not affected by the increase of miR-126 mimic, as shown in Figure 5c. FACS analyses shown that the VCAM1 protein level expressed in HUVEC surface decreased after 24 hours of treatment with 20 µg/ml of exosomes (Figure 5d) compared with control cells. HUVECs transfected with 2-Ome-miR-126 showed an increase of VCAM1 localization on the cell surface and reversed the effect of exosomes (Figure 5d). On the contrary, the treatment with LAMA84 exosomes (20 µg/ml) of HUVECs control and transfected with miR-126 mimic did not further affect VCAM1 protein expression compared with HUVECs only transfected with miR-126 mimic (Figure 5d). This is probably due to the presence of small amount of VCAM1 in the HUVEC surface after treatment with exosomes, carrying miR-126, or in HUVECs transfected with miR-126 mimic does not allow observation

of a further VCAM1 inhibition. Altogether, our data indicate that the LAMA84 exosomes treatment induces a dose and time-dependent regulation of VCAM1 expression in HUVECs, confirmed also by the study of gain and loss of function for miR-126.

miR-126 delivered by exosomes reduces LAMA84 cells migration

Cell migration is a crucial step for several biologic events including leukemic blasts mobilization from bone marrow. In order to investigate if LAMA84 exosomes have a role also in the modulation of leukemic cell migration we analysed the effects of conditioned medium (CM) from HUVECs treated with LAMA84 exosomes (10–50 µg/ml) on LAMA84 cells motility. LAMA84 cells migration towards HUVEC conditioned medium, for 24 hours, decreased in a dose dependent manner, as shown in figure 6. LAMA84 cells were unable to migrate towards HUVEC conditioned medium in less than 18 hours.

We obtained similar results when we used conditioned medium from HUVECs transfected with mir-126 mimic, while the silencing of miR-126 in HUVECs increased LAMA84 cells migration compared with untransfected cells (Figure 6). The use of a CM, from exosome-treated and miR-126 inhibitor transfected HUVECs, enhanced the LAMA84 cells motility compared with untransfected endothelial cells (Figure 6).

On the contrary, CM from HUVECs, transfected with miR-126 mimic and treated with LAMA84 exosomes, showed a slight modulation of LAMA84 cells motility (Figure 6), likely because the overexpression of miR-126 could not be further affected by the amount of miRNA shuttled by exosomes. These results suggest that miR-126 shuttled by LAMA84-exosomes affected LAMA84 cells migration.

miR-126 shuttled by exosomes modulates LAMA84 cells adhesion on HUVECs

In order to better understand the biological consequences of VCAM1 downregulation, we performed an adhesion assay. Specifically, to evaluate if LAMA84 exosomes treatment of HUVECs induces a time-dependent modulation of LAMA84 cells adhesion on HUVECs monolayer, we performed a time-course adhesion assay. As showed in Figure 7a the adhesion of LAMA84 cells on HUVECs monolayer increased up to 12 hours compared with control HUVECs while we observed a decreased ability to adhere to endothelial monolayer after 24 hours of pre-treatment with LAMA84 exosomes.

HUVECs transfected with mir-126 mimic decreased the leukaemia cell adhesion (Figure 7b) while the silencing of miR-126 in HUVECs reversed the effect of exosomes and restored the adhesion of LAMA84 cells on HUVECs monolayer (Figure 7c).

Effect of miR-126 shuttled by exosomes on transendothelial migration of LAMA84 cells

In order to investigate, *in vitro*, whether the modulation of CXCL12 and VCAM1 expression by miR-126 contained into LAMA84 exosomes could play an important role in leukemic blasts mobilization from the bone marrow, a transendothelial migration assay was performed. HUVECs monolayer were treated with different amount (10, 20, 50 µg/ml) of LAMA84 exosomes for 6, 12 and 24 hours. Interestingly, transendothelial migration of LAMA84 cells toward a complete medium (used as chemoattractant) decreased when HUVECs were treated with exosomes for 6 hours and markedly increased when HUVECs were treated with exosomes for 24 hours, as shown in Figure 8.

3.2 Curcumin inhibits *in vitro* and *in vivo* chronic myelogenous leukemia cells growth: a possible role for exosomal disposal of miR-21

Characterization of exosomes released from K562 and LAMA84 cells after treatment with Curcumin

Chronic myelogenous leukemia cell lines (K562 and LAMA84) were treated with different concentrations (5–40 µM) of Curcumin for 24 hours. Cells viability was evaluated by MTT assay. The results showed that 40 µM Curcumin slightly inhibits cell proliferation (about 25%), compared to control cells (DMSO 0.001%) (Figure 9a-b). Nanovesicles released from K562 and LAMA84 cells treated with Curcumin were isolated on a sucrose gradient and characterized as exosomes through biochemical and dimensional analysis: nanovesicles were analysed by Western blotting (Figure 9c-d) using antibodies specific for Alix and TSG-101, well known exosomal markers; DLS (dynamic light scattering) analyses indicated that isolated exosomes had an average hydrodynamic diameter of about 100 nm, in agreement with literature data (Figure 9e).

Curcumin decreases miR-21 levels in CML cells

The treatment of K562 and LAMA84 with Curcumin causes, as demonstrated by qPCR assay, a 50% reduction of cellular miR-21, as compared to DMSO treated cells (Figure 10a-b). Interestingly, miR-21 was enriched in exosomes released by K562 and LAMA84 cells, after treatment with 20 and 40 μ M of Curcumin (Figure 10a-b).

In order to investigate if Curcumin modulated miR-21 expression or induced a selective packaging of miR-21 in exosomes, K562 and LAMA84 cells were cotreated with 20–40 μ M Curcumin and 1 μ M of GW4869, a neutral sphingomyelinase (nSMase) 2 inhibitor, also well-known inhibitor of exosomes release^{37,95}. GW4869 induced an increase of miR-21 in K562 (Figure 11a) and LAMA84 (Figure 11b) cells compared with K562 and LAMA84 cells treated with Curcumin, the cotreatment with GW4869 and Curcumin partially reversed this effect, as shown in Figure 11.

Moreover, in order to exclude the hypothesis that Curcumin treatment of K562 and LAMA84 cells could directly modulate miR-21 expression, we evaluated, through qPCR, the levels of miR-21 precursor (pre-miR-21) both in K562 and LAMA84 cells. As shown in Figure 12, we found no significant difference of pre-miR-21 expression level in K562 (Figure 12a) and LAMA84 cells (Figure 12b) in the different experimental conditions.

MiR-21 targets PTEN 3'-UTR mRNA

Bioinformatic analysis indicates PTEN as a predictive target of miR-21. In NSCLC cells it has been showed that Curcumin exerts an anticancer effect associated to an inhibition of miR-21 and concomitant upregulation of PTEN⁹⁶. In our system, we confirmed that miR-21 binds directly to PTEN 3' UTR mRNA using a Firefly/Renilla Duo-Luciferase reporter vector (pEZX-MT01), where the 3' UTR of PTEN was cloned downstream of the firefly luciferase gene (PTEN-pEZX). K562 cells incubated with 20 and 40 μ M Curcumin and transfected with this reporter vector showed an increased firefly luciferase activity compared with untreated cells (Figure 13a) transfected with PTEN-pEZX. K562 cells cotransfected with miR-21 inhibitor and PTEN-pEZX showed an increased activity of firefly luciferase respect to untransfected K562 cells, similarly to Curcumin treatment. On the contrary, luciferase activity decreased when K562 cells, containing the reporter vector, were transfected with miR-21 mimic.

In order to confirm that the effect of Curcumin on the decrease of miR-21 is related to an selective exosomal disposal, we performed a cotreatment of K562 cells with 1 μ M GW4869 and 20 and 40 μ M Curcumin. We demonstrated that GW4869 reduced the luciferase activity

in PTEN-pEZX transfected K562 cells compared with control cells, as showed in Figure 13a. The cotreatment with 1 μ M GW4869 and 20 and 40 μ M Curcumin caused an increase of luciferase activity in PTEN-pEZX transfected K562 (Figure 13a) with respect to PTEN-pEZX transfected K562 cells treated with GW4869 alone. Similar results were obtained in LAMA84 cells (Figure 13b). These data indicate that Curcumin caused a decrease of miR-21, in K562 and LAMA84 cells, and consequently an increase of PTEN, its direct target.

Curcumin induces PTEN expression in CML cells

Our data showed that also in our model, miR-21 targets the 3' UTR of PTEN mRNA. Quantitative PCR analysis demonstrated that Curcumin treatment of CML cells, for 24 hours, caused a dose-dependent increase of PTEN mRNA (Figure 14a). Specifically, PTEN mRNA levels increase of 2,5 and 4 fold in K562 and LAMA84 cells after treatment with 20 and 40 μ M of Curcumin, respectively (Figure 14a). These results were confirmed also at protein level through western blotting analysis; addition of Curcumin to CML cells, for 24 h, caused a dose-dependent increase in PTEN protein in K562 and LAMA84 cells lysate (Figure 14b).

In order to confirm the effect of Curcumin on the selective sorting of miR-21 into the exosomes, we performed a cotreatment of CML cells with 1 μ M GW4869 and 20 μ M Curcumin. As showed in Figure 15a and b, GW4869 blocks the upregulation of PTEN mediated by Curcumin in K562 and LAMA84 cells both at mRNA and protein levels.

To further evaluate the role of miR-21 in the modulation of PTEN levels we knocked down miR-21 in CML cells using the miR-21 inhibitor (2'-OMe-miR-21). After evaluation of transfection efficiency of miR-21 inhibitor or mimic in K562 and LAMA84 cells through qPCR, we observed that the inhibition of miR-21 increases PTEN mRNA expression in both cell lines (Figure 16). On the contrary, the addition of miR-21 mimic caused, as expected, a decrease of PTEN expression (Figure 16). In order to evaluate, in K562 and LAMA84 cells, if the downregulation of PTEN expression in miR-21 mimic transfected cells was reverted after the addition of Curcumin, we treated the miR-21 mimic transfected CML cells with 20 μ M of Curcumin. As shown in Figure 16 (black bars with white dots), Curcumin counteracted the effect of the transfection with miR-21 mimic, decreasing the expression of PTEN mRNA. On the contrary in K562 and LAMA84 cells transfected with miR-21 inhibitor and treated with

Curcumin, we observed a higher increase of PTEN mRNA expression than CML cells transfected with miR-21 inhibitor alone (Figure 16, white bars).

Our data suggest that Curcumin treatment in CML cells induces a decrease of miR-21 mediated by exosomes sorting that, in turn, causes the modulation of PTEN expression, confirmed by the study of gain and loss of function for miR-21.

Curcumin modulates AKT phosphorylation in CML cells

It is demonstrated that PTEN is involved in the phosphatidylinositol 3-kinase (PI3K)/AKT transduction signalling pathway, downregulating AKT phosphorylation.

To elucidate the effect of Curcumin treatment, in CML cells, on AKT pathway, we observed, through ELISA assay, that the addition of Curcumin, for 24 h, caused a dose-dependent decrease of AKT phosphorylation in CML cells, as shown in Figure 17a and b. In order to support our hypothesis that the decrease of miR-21 was related to a selective packaging of this miRNA into CML exosomes, we treated leukemia cells with GW4869 1 μ M and, as expected, this treatment caused an increase of AKT phosphorylation. Moreover, the cotreatment of CML cells with GW4869 1 μ M and Curcumin 20–40 μ M, reverted the effects of Curcumin (Figure 17a-b).

The role of miR-21 was further evaluated by performing an ELISA assay for AKT phosphorylation of CML cells lysates, after transfection with an inhibitor or mimic of miR-21 (Figure 18a-b). MiR-21 expression was knocked down in CML cells using the miR-21 inhibitor (2'-OMe-miR-21), as demonstrated with real time PCR assay. We observed that the inhibition of miR-21 in CML cells decreased the AKT phosphorylation similar to Curcumin treatment. In contrast, the overexpression of miR-21 in CML cells increased AKT phosphorylation (Figure 18a-b). Quantitative PCR analysis shows the overexpression efficiency of miR-21, in CML cells transfected with miR-21 mimic.

Our results suggest that Curcumin treatment induces in CML cells, a dose-dependent regulation of AKT phosphorylation, confirmed by the study of gain and loss of function for miR-21.

Curcumin modulates VEGF expression in CML cells

Several studies demonstrate that PTEN modulation of the PI3K/AKT signalling pathway is also related to a downregulation of expression of vascular endothelial growth factor (VEGF)⁹⁷. In our experimental model, qPCR analysis demonstrated that Curcumin treatment of CML cells, for 24 hours, caused a dose-dependent decrease in VEGF mRNA. Specifically, 50% decrease of VEGF mRNA levels was observed in both K562 and LAMA84 cells after treatment with 40 μ M of Curcumin (Figure 19a). Transfection of miR-21 inhibitor (2'-OMe-miR-21) in both CML cells, caused a decrease of VEGF mRNA expression similar to Curcumin treatment (Figure 19b). On the contrary, the transfection of miR-21 mimic increased VEGF mRNA expression, due to its effect on the induction of PTEN expression (Figure 19b).

In order to investigate, in K562 and LAMA84 cells, if the effects of the transfection with miR-21 mimic reverted after Curcumin treatment, we treated the miR-21 mimic transfected CML cells with 20 μ M Curcumin. Interestingly, Curcumin treatment counteracted the effect of the transfection with miR-21 mimic, causing a decreased expression of VEGF mRNA, as shown in Figure 19b (white bars). In contrast, in K562 and LAMA84 cells transfected with miR-21 inhibitor and treated with Curcumin, we observed a higher decrease of VEGF mRNA expression than CML cells transfected with miR-21 inhibitor alone (Figure 19b, white bars with black dots).

In order to confirm the effects of Curcumin on VEGF protein level, we performed an ELISA assay on conditioned medium of K562 and LAMA84 cells treated both with 20 and 40 μ M Curcumin, for 24 h. Curcumin treatment caused a dose-dependent decrease of VEGF released from CML cells (Figure 19c). We observed similar effects after transfection of miR-21 inhibitor in both CML cells, while the transfection of miR-21 mimic in K562 and LAMA84 cells induced an increase of secreted VEGF (Figure 19c). The effects of the transfection with miR-21 mimic reverted after the treatment with Curcumin (Figure 19c, white bars), causing a decrease of VEGF release. On the contrary in K562 and LAMA84 cells transfected with miR-21 inhibitor and treated with Curcumin, we observed a higher decrease of VEGF release than CML cells transfected with miR-21 inhibitor alone (Figure 19c, white bars with black dots).

In order to support our hypothesis that the decrease of miR-21 was determined by a selective packaging of this miRNA in CML exosomes, we performed a cotreatment in both

K562 and LAMA84 cells with GW4869 1 μ M and Curcumin 20–40 μ M. As expected, GW4869 abrogated the down regulation of VEGF by Curcumin in both CML cells (Figure 19d).

Curcumin reduces colony formation capability of CML cells

Methocult colony formation assay shows that both K562 and LAMA84 cells, treated with Curcumin (20–40 μ M), form colonies in methylcellulose with a smaller area compared to untreated cells (Figure 20a). This assay was also performed with K562 and LAMA84 cells transfected with miR-21 mimic or inhibitor. K562 and LAMA84 cells transfected with miR-21 mimic are able to form colonies greater compared to untransfected cells (Figure 20b), while transfection with miR-21 inhibitor reduces the colonies size with respect to control cells, similarly to Curcumin treatment.

Curcumin reduces CML cells migration

Cell migration is a crucial step for several biologic events including leukemic blasts mobilization from bone marrow. We evaluated the effect of Curcumin treatment (20–40 μ M) on K562 and LAMA84 cells motility. The addition of Curcumin inhibited in a dose-dependent manner, the motility of K562 and LAMA84 cells towards complete medium (Figure 21). Interestingly, the cotreatment with 20–40 μ M of Curcumin and 1 μ M GW4869 reverted the effect of Curcumin, while the treatment with GW4869 alone increases the motility of CML cells. These results suggest that Curcumin affected migration of both CML K562 and LAMA84 cells.

Curcumin inhibits Bcr-Abl expression in CML cells by increasing miR-196b levels

BCR-ABL is an aberrant tyrosine kinase with constitutive activity that triggers several downstream pathways, thus inducing the enhanced survival and proliferation of CML cells. qPCR analysis shows that Bcr-Abl transcript levels decreased of about 20% and 45% in K562 cells after treatment with 20 and 40 μ M of Curcumin, respectively (Figure 22a). Similar data were obtained in LAMA84 cells treated for 24 hours with 40 μ M of Curcumin. Western blotting analysis confirmed these results also at protein level, where the addition of Curcumin to both CML cells, for 24 hours, caused a dose-dependent decrease of Bcr-Abl protein (Figure 22b). In order to elucidate the biological mechanisms that causes Bcr-Abl decreased expression, we focused our attention on miR-196b, a microRNA that

bioinformatics algorithms shows to target Bcr-Abl. The addition of Curcumin in both K562 and LAMA84 cells caused, as demonstrated by qPCR assay, an increase of cellular miR-196b, as compared to DMSO treated cells. In contrast, miR-196b levels was decreased in exosomes released by both CML cells after treatment with 20 and 40 μ M of Curcumin (Figure 22c-d). These data suggested that Curcumin increased miR-196b cellular levels leading to a reduction of Bcr-Abl protein amount in CML cells.

Anticancer effects of Curcumin *in vivo*

In order to validate, in an *in vivo* model, our *in vitro* data, we evaluated the effects of Curcumin on a xenograft CML tumour model. K562 and LAMA84 cells were inoculated subcutaneously in SCID mice and subsequently treated every day, for 2 weeks, with 2 mg of Curcumin or vehicle control (corn oil). One week after the last day of treatment, mice were sacrificed, tumours were extracted and exosomes were isolated from mice plasma. Interestingly, mice treated with Curcumin had smaller tumours with respect to mice treated only with corn oil (Figure 23a-b). Moreover, we isolated exosomes released in the plasma of mice treated with Curcumin and control. qPCR analysis showed that exosomes released in the plasma of Curcumin treated mice were enriched in miR-21 with respect control mice (Figure 23c).

Taken together, these results confirmed our hypothesis that the anticancer effects of Curcumin may occur through the miR-21 selective packaging in exosomes.

3.3 Curcumin modulates chronic myelogenous leukemia exosomes composition and affects angiogenic phenotype, *via* exosomal miR-21

Curcumin quantification in exosomes

Exosomes released by K562 and LAMA84 cells treated (for 24 hours) or not with Curcumin (10, 20 and 40 μ M), were purified from conditioned medium and isolated, as reported in the previous work⁶⁹. Aliquots of samples were used in order to quantify Curcumin in exosomes by HPLC analysis.

Table 1 shows the amount of Curcumin extracted from exosomes released by K562 and LAMA84 cells treated with different concentrations (10, 20 and 40 μ M) of Curcumin. Values

are the mean \pm SD of 3 samples. The results indicated that the Curcumin content in exosomes increased as a function of Curcumin concentrations added to both cell lines.

Viability assay of HUVECs treated with Curcu-exosomes

We demonstrated that exosomes released by CML cells after treatment, for 24 hours, with 20 μ M of Curcumin contain small amounts of Curcumin (Table 1). For HUVECs treatment we tested two different concentrations of Curcu-exosomes (20 and 50 μ g/ml) and we selected the treatment with 20 μ M of Curcumin because we previously demonstrated that these exosomes were particularly enriched in miR-21⁶⁹. It was performed an MTT assay in order to analyse cells viability and results indicated that the addition of CML Curcu-exosomes and control exosomes did not affect the endothelial cells (ECs) viability (Figure 25).

Uptake of Curcu-exosomes by HUVECs

In order to evaluate the ability of ECs to uptake K562 Curcu-exosomes, we treated HUVECs with exosomes labeled with PKH-26, a lipophilic dye. We demonstrated that HUVECs are able to internalize K562 Curcu-exosomes but with a slower kinetic than K562 control exosomes (Figure 26). We obtained similar results after treatment of ECs with Curcu-exosomes released by LAMA84 cells after Curcumin addition (data showed in the published paper⁷⁰).

Curcu-exosomes shuttled miR-21 into HUVECs

In the previous work we demonstrated that the exosomes released by CML cells treated with Curcumin are enriched in miR-21⁶⁹. In order to demonstrate the transfer of miR-21 in ECs, we treated HUVECs with 20 and 50 μ g/ml of Curcu-exosomes released by K562 cells and, then, the expression levels of miR-21 were analyzed in HUVECs. As shown in Figure 27a, miR-21 levels increased in HUVECs treated with Curcu-exosomes compared with untreated or treated with K562 control exosomes.

Moreover, in HUVECs transfected with miR-21 inhibitor (2'-OMe-miR-21), we observed a decrease of miR-21 expression but the addition of Curcu-exosomes reverted this effect.

In contrast, we showed that the increased level of miR-21 in HUVECs transfected with miR-21 mimic was further augmented after treatment with Curcu-exosomes (Figure 27a). In order to exclude the hypothesis that the addition of CML Curcu-exosomes, in HUVECs, could

induce the expression of endogenous miR-21, we evaluated also the levels of precursor miR-21 (pre-miR-21) through qPCR assay. Interestingly, we found no statistically significant difference of pre-miR-21 expression level after treatment of ECs with 20 and 50 µg/ml of K562 Curcu-exosomes, as shown in Figure 27b. We obtained similar results after the treatment of HUVECs with exosomes released by LAMA84 cells treated or not with Curcumin (data shown in the published paper⁷⁰).

MiR-21 targets RhoB 3'-UTR mRNA

Bioinformatics analysis indicates that RhoB is a predictive target of miR-21. Moreover, it is described that miR-21 overexpression affects endothelial organization into capillary like structures and cell migration⁹¹.

We confirmed that miR-21 binds directly to RhoB 3'UTR mRNA using a Firefly/Renilla Duo-Luciferase reporter vector (pEZX-MT01), where the 3' UTR of RhoB was cloned downstream of the firefly luciferase gene (RhoB-pEZX). When HUVECs, transfected with reporter vector, were treated with Curcu-exosomes (20 µg/ml), we observed a decrease of the firefly luciferase activity compared with untreated cells or HUVECs treated with exosomes control (Figure 28). Interestingly, we demonstrated that the down regulation of miR-21 in HUVECs transfected with RhoB-pEZX and miR-21 inhibitor, increases the activity of firefly luciferase with respect to untransfected HUVECs. Moreover, treatment of HUVECs with K562 Curcu-exosomes transfected with RhoB-pEZX and miR-21 inhibitor reverted the effect of miR-21 inhibitor only. On the contrary, luciferase activity decreased when HUVECs containing the reporter vector were transfected with miR-21 mimic, similarly to the results obtained with the treatment with Curcu-exosomes. The treatment of HUVECs, transfected with RhoB-pEZX and miR-21 mimic, with Curcu-exosomes released by K562 cells, increased the effect of miR-21 mimic (Figure 28). We obtained similar effects in HUVECs, transfected with miR-21 mimic and inhibitor, treated with Curcu-exosomes released by LAMA84 cells (data shown in the published paper⁷⁰).

Treatment of HUVECs with Curcu-exosomes inhibited RhoB expression

Since our results demonstrated that, in this experimental model, miR-21 targets directly the 3' UTR of RhoB transcript, we investigated if CML exosomes treatment could induce, in HUVECs, a modulation of RhoB mRNA expression. As expected, K562 Curcu-exosomes

caused a decrease of RhoB mRNA expression, as show in Figure 29a. In HUVECs transfected with miR-21 inhibitor, we observed a 3 fold increase of RhoB mRNA expression compared with untransfected cells. The addition of Curcu-exosomes in HUVECs transfected with miR-21 inhibitor reduced the effect of miR-21 inhibitor, leading to a decrease of expression of RhoB mRNA (Figure 29a). Transfection of HUVECs with miR-21 mimic decreased the amount of RhoB mRNA of about 60% (Figure 29a). The addition of Curcu-exosomes, in HUVECs transfected with miR-21 mimic, increased the downregulation of RhoB expression (Figure 29a). We obtained similar results in HUVECs transfected with miR-21 mimic and inhibitor and treated with exosomes released by LAMA84 cells after Curcumin addition (data shown in the published paper⁷⁰).

According to these data, FACS analyses confirmed a decrease of RhoB expression also at protein level in HUVECs after Curcu-exosomes addition. Moreover, this effect was increased when HUVECs were transfected with miR-21 mimic. On the contrary, when HUVECs were transfected with miR-21 inhibitor, Curcu-exosomes addition reverted the decrease of RhoB expression (Figure 29b).

Our results, confirmed by the study of gain and loss of function for miR-21, suggested that CML Curcu-exosomes treatment induces an exosome-mediated increase of miR-21 in endothelial cells that, keeping its biological functions in target cells, causes the modulation of RhoB expression (Figure 29a-b).

Curcu-exosomes inhibited the migration of endothelial cells

Angiogenesis is dependent on cell migration. In order to investigate, in HUVECs, the biological effects of RhoB inhibition, related to miR-21 shuttled by CML Curcu-exosomes, we evaluated the effect of Curcu-exosomes addition on HUVECs motility. As described, we observed that the treatment with CML exosomes increased the motility of ECs⁶⁹.

Interestingly, Curcu-exosomes addition is able to inhibit the motility of HUVECs, towards complete medium, in a dose-dependent manner. We obtained similar results after the transfection of miR-21 mimic in HUVECs treated with K562 exosomes (Figure 30). On the contrary, the transfection of miR-21 inhibitor induces, in HUVECs, an increased cell motility. However, the effects obtained after transfection with miR-21 mimic are more significant after the treatment with Curcu-exosomes (Figure 30), because of the stronger decrease of HUVECs motility with respect to the effects Curcu-exosomes alone. In contrast, in HUVECs

transfected with miR-21 inhibitor we observed an increase of cell motility, similar to the treatment with control exosomes. Moreover, the effects of miR-21 inhibitor transfection were reverted after the treatment with K562 Curcu-exosomes (Figure 30).

Treatment of HUVECs with Curcu-exosomes modulated IL8 expression and secretion

It is demonstrated that IL-8 have a crucial role in angiogenesis and in tumour progression. As previously showed, the treatment of HUVECs with CML-exosomes is able to increase IL-8 mRNA levels and this effect was reverted after treatment of ECs with Curcu-exosomes (Figure 31a). These results were also confirmed at protein level evaluating, by an ELISA assay, the levels of IL-8 on conditioned medium of HUVECs treated with 20 and 50 µg/ml of Curcu-exosomes and control exosomes; as expected, control exosomes treatment caused a dose-dependent increase of IL8 released from HUVECs, while this effect was reverted after treatment with Curcu-exosomes (Figure 31b). We obtained similar results in HUVECs treated with Curcu-exosomes released by LAMA84 cells (data shown in the published paper⁷⁰).

Treatment of HUVECs with Curcu-exosomes modulated VCAM1 expression

As previously described by our research group, K562 and LAMA84 exosomes are able to induce VCAM1 expression after treatment of endothelial cells for 6 hours⁵⁴. Here we showed that the addition of increasing concentration of exosomes released by CML cells to HUVECs caused, as expected, a dose-dependent increase in VCAM1 mRNA expression in endothelial cells, while the treatment with Curcu-exosomes reverted this effect (Figure 32a). Then, in order to evaluate VCAM1 expression at protein level, we performed a FACS analysis. We observed an increase of VCAM1 protein in HUVECs treated with control exosomes released by K562 cells while the treatment with Curcu-exosomes reverted this effect, with VCAM1 expression levels comparable to the untreated cells (Figure 32b,c). We obtained similar results in HUVECs treated with Curcu-exosomes released by LAMA84 cells, both at mRNA and protein level (data shown in the published paper⁷⁰).

Curcu-exosomes inhibited *in vitro* and *in vivo* tube formation

In order to evaluate the potential modulation of angiogenesis mediated by Curcu-exosomes in an *in vitro* model of angiogenesis, we analyzed the ability of HUVECs to form capillary-like

structures when plated on Matrigel. HUVECs maintained in low serum medium were unable to form a tube network while the addition of CML exosomes induced, as previously described by our research group, an endothelial network formation (Figure 33a)⁵⁴. Interestingly, the treatment with Curcu-exosomes inhibited the development of capillary structures (Figure 33a, Curcu-Exo).

Furthermore, a Matrigel plugs assay was performed in order to evaluate, *in vivo*, the angiogenic modulation of CML exosomes by examining the recruitment of vasculature into subcutaneously implanted Matrigel plugs containing CML exosomes^{54,98}. The plugs containing control CML exosomes became more vascularized with respect to plugs with Curcu-exosomes (Figure 33b). This analysis was performed evaluating haemoglobin concentration in the Curcu-exosomes-containing implants in comparison with control exosomes-containing Matrigel plugs (Figure 33c). We obtained similar results with Curcu-exosomes released by LAMA84 cells (data shown in the published paper⁷⁰).

According to these results, HUVECs treated with K562 control exosomes showed an increase in VEGFR mRNA expression levels respect to the addition of exosomes released by K562 treated with Curcumin (Figure 33d) and LAMA84 cells (data shown in the published paper⁷⁰).

Effect of Curcu-exosomes on endothelial cell tight and adherent junctions

In order to elucidate the effects of Curcu-exosomes on endothelial barrier stabilization, in particular on tight junctions, we analyzed by immunofluorescence, the localization of ZO1 in control HUVECs treated or not with Curcu-exosomes. The addition of 20 µg/ml of control exosomes caused a delocalization of ZO1 with respect to HUVECs control in which ZO1 was localized in plasma membrane. In HUVECs treated with 20 µg/ml of Curcu-exosomes released by K562 (Figure 34a) and LAMA84 (data shown in the published paper⁷⁰) cells, we observed a localization of ZO1 in HUVECs plasma membrane similar to untreated cells.

Moreover, we evaluated the effects of exosomes on the expression of endothelial specific transmembrane adhesion molecules, such as VE-Cadherin. Untreated HUVECs had a continuous peripheral VE-Cadherin staining, while the staining intensity decreased in HUVECs after treatment with 20 µg/ml of exosomes released by K562 (Figure 34b) and LAMA84 (data shown in the published paper⁷⁰) cells. This destabilizing effect was reverted after treatment with Curcu-exosomes (Figure 34b), thus supporting our hypothesis that Curcu-exosomes are involved in endothelial barrier stabilization.

Permeability of HUVEC monolayers

Vascular permeability is a parameter of endothelial cell function and its alterations are involved in cancer metastasis. In order to investigate if Curcu-exosomes decreased the alteration of HUVEC monolayers we performed a permeability assay with FITC-dextran. As showed in Figure 35a, upper panel, the permeability of HUVEC monolayer increased after treatment, for 3 and 6 hours, with CML exosomes, while the treatment with Curcu-exosomes partially protected the endothelial monolayer. Moreover, fluorescence quantitative analysis showed a five fold of increase of permeability after treatment with control exosomes and that increase was reverted after treatment with Curcu-exosomes.

The confocal analyses confirmed that Curcu-exosomes protected the integrity of HUVECs monolayer with respect to control exosomes. As shown in Figure 35b, we observed an alteration of the monolayer after treatment with CML exosomes. In contrast, the treatment of endothelial monolayer with Curcu-exosomes, decreased the alteration of the EC monolayer, but caused a rearrangement of actin, according to RhoB inhibition (Figure 29). The treatment with K562 Curcu-exosomes (Curcu-Exo K562 20 µg/ml) of the endothelial monolayer caused a decrease of RhoB expression with respect to the treatment with K562 control exosomes (Exo K562 20 µg/ml), as shown in Figure 35b, lower panel. Overall, these results indicated that Curcu-exosomes could protect the EC monolayer and reduced the vascular permeability.

Proteomic analyses of exosomes released by K562 cells treated or not with Curcumin

It is demonstrated that tumour-derived exosomes are able to modulate target cells phenotype shuttling both RNAs and cargo proteins. In order to better investigate how exosomal proteins from curcumin-treated K562 cells can mediate the anti-angiogenic effect observed on HUVECs, a proteomic analysis through SWATH-MS approach was performed, on exosomes released by K562 cells treated or not with Curcumin. SWATH analysis is a quantitative label-free method that combines the high specificity of Data Independent Acquisition (DIA) method with a targeted data extraction strategy. Only proteins with a $p \leq 0.05$ and a log₁₀ fold-change > 0.2 or < -0.2 (for upregulated and downregulated proteins, respectively) were selected for further analysis. A total of 30 proteins, differentially modulated in exosomes released by K562 cells following treatment with curcumin, were

identified; with respect to exosomes released by K562 control cells, Curcu-exosomes showed 4 up-regulated and 26 down-regulated proteins.

iPathway Guide (<http://www.advaitabio.com/ipathwayguide.html>) was exploited in order to perform a GO enrichment analysis on all differentially expressed proteins suggesting a significant enrichment for those GO terms linked with biosynthetic processes and translation. In particular, the following GO terms resulted significantly enriched: intracellular transport (p -value = 0.008; BP), nitric-oxide synthase regulator activity (p -value = 0.028; MF), translation (p -value = 0.009; BP), nucleic acid binding (p -value = 0.016; MF), cellular biosynthetic process (p -value = 0.0018; BP), ribonucleoprotein complex (p -value = 0.013; CC), anion transmembrane transporter activity (p -value = 0.016; MF), structural constituent of ribosome (p -value = 0.033; MF), nucleus (p -value = 0.014; CC), ribosomal subunit (p -value = 0.015; CC.). Among them, nitric-oxide synthase regulator activity, referred to hsp90aa1 and hsp90ab1 proteins, is particularly interesting due to the fact that the nitric oxide (NO) pathway appear to be involved in tumour angiogenesis and spread. It is documented that Heat shock protein 90 (HSP90) binds directly to endothelial NO synthase (eNOS), promoting its activity and increasing NO production⁹⁹. An accurate MEDLINE search allowed us to discover that approximately 50% of modulated protein dataset was involved with the angiogenic, invasive and metastatic processes (Table 2). Among these proteins, we focused our attention on MARCKS-related protein (MARCKSL1) because it is the mainly down-regulated protein, with a 10.6 fold down-regulation. Interestingly, miR-21 has been shown to target directly also the mRNA of MARCKS. We decided to further investigate the role played by this protein in the anti-angiogenic effect of Curcumin.

Treatment of HUVECs with Curcu-exosomes modulated MARCKS expression

Recently, miR-21 has been shown to directly target MARCKS, by binding in the 3' UTR region (from the nt713–734) of its transcript. MARCKS are known to affect the architecture of the actin cytoskeleton in endothelial cells, modulating EC motility and permeability¹⁰⁰. In order to validate the high-throughput proteomic data, we evaluated MARCKS expression both at mRNA and protein level. As showed in Figure 36a, we observed, through qPCR, that Curcumin induced a decrease of MARKCS mRNA expression. Moreover, Curcu-Exosomes treatment of HUVECs induced a modulation of MARCKS mRNA expression. In HUVECs transfected with miR-21 inhibitor (2'-O Me miR-21), MARCKS mRNA expression showed a 5

fold increase with respect to untransfected cells. On the contrary, transfection of HUVECs with mir-21 mimic caused a 60% decrease of the relative amount of MARCKS mRNA (Figure 36b).

Interestingly, through Western Blotting analysis we observed an increase of MARCKS, at protein level, in HUVECs treated with control exosomes compared to untreated HUVECs, while the treatment with Curcu-exosomes reverted this effect (Figure 36c,d). We also observed, by FACS analyses, a decrease of MARCKS after treatment with Curcu-exosomes, and this effect was reinforced when HUVECs transfected with miR-21 mimic were treated with Curcu-exosomes. The treatment of HUVECs, transfected with miR-21 inhibitor, with Curcu-exosomes has proved to be able to revert the effect on MARCKS decreased expression (Figure 36e). Taken together, these results confirmed that Curcu-exosomes carry miR-21 that, keeping the biological functions, inhibits MARCKS expression in endothelial cells.

CHAPTER 4

Discussion

4.1 Exosomal shuttling of miR-126 in endothelial cells modulates adhesive and migratory abilities of chronic myelogenous leukemia cells

It is known that in chronic myelogenous leukemia the bone marrow microenvironment contributes to cancer progression through the crosstalk between BM resident cells and cancer cells. This crosstalk could be involved in drug resistance and CML stem cell survival¹⁰¹. Endothelial cells, one of the most important component of bone marrow, have a crucial role in tumour development and progression. ECs form tumour-associated vessels to provide nutritional and oxygen support to the tumour or may sustain leukemia cell growth and dissemination through the secretion of cytokines and extracellular matrix components¹⁰².

Our study increases the knowledge in the complex interaction between bone marrow microenvironment and cancer cells by investigating the role of tumour derived exosomes. Our research group previously demonstrated that LAMA84 cells release exosomes able to induce in endothelial cells an angiogenic phenotype stimulating IL-8 dependent autocrine loop, both *in vitro* and *in vivo*^{71,72,98}.

In this study we showed that CML cells may modulate, *in vitro*, gene expression in endothelial cells by the release of exosomal miRNAs that are biologically active. The analysis of the pattern of miRNA expression showed a similarity in the miRNAs detected in exosomes and parental cells. However, according with other literature data¹⁰³, we observed that miRNAs loading into exosomes seems to be not casual but regulated by a sorting

mechanism, that is still unclear. Our experiments indicate that exosomes are incorporated with an energy and ceramide-dependent pathway. In order to support this idea, we observed that the incubation of LAMA84 cells at 4°C or with GW4869 inhibited the transfer of exosomal miR-126 into HUVECs.

Of the 124 miRNAs that we identified in exosomes, we focused our attention on miR-126, considered an angiomiR overexpressed in highly vascularized tissues. It is described that miR-126 is involved in many aspects of endothelial cell biology, including cell motility and survival, vasculature integrity and cytoskeletal organization¹⁰⁴. The involvement of miR-126 in cancer biology is related not only to modulation of angiogenesis but also directly in cancer pathogenesis¹⁰⁵. In myeloid leukemia, miR-126 was found to down-regulate HOXA9, an oncogene encoding a transcription factor that regulates hematopoietic development¹⁰⁶. Cammarata and colleagues found that miR-126, upregulated in acute myeloid leukemia, induced cell proliferation via the inhibition of PLK, one member of the Polo-like kinase that regulates the cell cycle¹⁰⁷. Our study suggests that miR-126 may affect CML progression modulating the bone marrow microenvironment, due to inappropriate cancer cell retention, adhesion and motility.

We also observed that CXCL12 and VCAM1, critical components of the bone marrow niche, are in part regulated by miR-126 contained in LAMA84 exosomes. CXCL12 is a chemokine abundantly produced by the bone marrow microenvironment, and the described axis with its receptor CXCR4 is important in malignant cell trafficking^{108,109}. Sipkins and colleagues have demonstrated that disruption of the interactions between CXCL12 and its receptor CXCR4 inhibits the homing of Nalm-6 cells (an acute lymphoblastic leukaemia cell line) to the BM¹¹⁰. Our data showed that exosomal shuttling of miR-126 to endothelial cells decreases CXCL12 release from HUVECs and concomitantly reduces the motility of LAMA84 cells towards HUVEC conditioned medium. To further analyse the role of miR-126 in the modulation of CXCL12 secretion, we transfected HUVECs with the inhibitor of miR-126 that can bind and inhibit miR-126 molecules, or its negative control scramble oligomer. As expected, in HUVECs transfected with miR-126 inhibitor, we observed a decrease of about 45% of miR-126 expression and concomitantly an increase of CXCL12 protein level. Consistently with these data, the transfection of HUVECs with miR-126 mimic caused a

decrease of CXCL12 level and lower migration tendency of LAMA84 cells toward EC conditioned medium.

Another target of miR-126 that may be involved in CML disease progression is VCAM1, a cell-cell adhesion molecule. Literature data showed that miR-126 downregulated VCAM1 expression in endothelial cells through a post-transcriptional mechanism⁷⁶. Fish et al. also reported that VCAM1 mRNA levels were elevated upon miR-126 inhibition, but were not decreased in the presence of miR-126 mimic thus supporting the hypothesis of a regulative mechanism at translational level⁷⁵. Moreover, it was demonstrated that forced expression of miR-126 in Lin⁻ bone marrow cells induced minimal change in the relative levels of VCAM1 mRNA but caused a decrease in the proportion of surface VCAM1-positive Sca-1^{hi} c-Kit^{hi} cells within this population¹¹¹. Functionally, a recent report from Salvucci and colleagues reported that miR-126 contained in G-CSF-mobilized vesicles in the bone marrow induced hematopoietic stem/progenitor cell (HSPC) mobilization by reducing the expression of VCAM1 in HSPC endothelial cells and other non-hematopoietic cells¹¹¹.

We found that the treatment of HUVECs with LAMA84 exosomes, for 24 hours, downregulated VCAM1 mRNA and protein expression and caused a decrease of LAMA84 adhesion cells on the HUVECs monolayer. We provide evidences that this mechanism can be related to exosomal miR-126 and these effects were partially reduced by transfection of miR-126 inhibitor in HUVECs. As a functional consequence of the diminished amount of VCAM1 in ECs, the adhesion of LAMA84 to HUVECs was reduced after exosome treatment. In our previous study, we demonstrated that the treatment of endothelial cells with exosomes for short times (6 hours), induced VCAM1 at both the mRNA and protein level and increased adhesion of LAMA84 cells on the HUVECs monolayer⁷².

In this new study, we found that the treatment of endothelial cells with exosomes for 24 hours downregulated VCAM1 mRNA and protein expression and caused a decrease of LAMA84 adhesion cells on the HUVECs monolayer. In order to explain these apparently contrasting results, we hypothesize that in the first 6 hours, the exosome treatment of HUVECs induces the expression of VCAM1 to allow the adhesion of the cancer cells on the endothelium, as the first step of cells migration. After a longer time of HUVECs exposure to exosomes, LAMA84 cells lose the ability to adhere on the endothelial cells and increase their capacity to migrate towards a richer source of chemoattractants.

The downregulation of CXCL12 and VCAM1 by miR-126 and their upregulation when this miRNA is knocked down indicate that miR-126 is deeply involved in the regulation of these two proteins. We demonstrated with an *in vitro* transendothelial cell migration assay that the treatment of HUVECs with LAMA84 exosomes induces LAMA84 cell migration through endothelial monolayer, likely due to a decrease of VCAM1-mediated adhesion of leukemia cells to ECs and a concomitant chemotaxis toward serum.

Our data suggest a potential exosome-mediated crosstalk in the bone marrow microenvironment that could facilitate the exit of LAMA84 cells from the bone marrow and their dissemination in the bloodstream at least partly due to the delivery of exosomal miR-126.

4.2 Curcumin inhibits *in vitro* and *in vivo* chronic myelogenous leukemia cells growth: a possible role for exosomal disposal of miR-21

The understanding of the molecular basis of chronic myeloid leukemia development led to the synthesis of Imatinib mesylate (IM), a highly specific Bcr-Abl, tyrosine kinase inhibitor. Although a vast majority of patients with CML respond to IM, resistance might occur *de novo* or during treatment¹¹². Resistance to IM or to the second, third generation of TKIs has attracted the attention to find new therapies or different compounds to use as adjuvants for conventional therapy. In this work we investigated the antineoplastic effect of Curcumin in CML cells.

Curcuminoids are known to inhibit the tumour growth affecting the activity of multiple molecular targets involved in carcinogenesis. Curcumin exhibits its anticancer effects by regulating genes involved in cellular signaling pathways, including nuclear factor-kappa B, protein kinase B (AKT), mitogen-activated protein kinase (MAPK), p53, and other pathways¹¹³.

In this study, we provide evidence that Curcumin may affect *in vitro* and *in vivo* malignant properties of CML cells and we suggest that these effects are mediated by a disposal of miR-21 in exosomes released by CML cells.

In our previous paper, we demonstrated that LAMA84 cells release exosomes containing several miRNAs, differentially expressed compared to parental cells. We focused our attention on miR-126; LAMA84-exosomes were enriched in this angiomiR that was biologically active in endothelial cells. Other groups have also evidenced that miRNAs contained in the exosomes released by K562 cells, are able to modulate cell communication and influence the genetic changes within CML patients¹¹⁴. Recently, several studies have indicated that miRNAs may be considered a new class of oncogenes. These oncomiRNAs induce tumour growth negatively regulating tumour suppressor genes. The modulation of oncomiRNAs levels might represent an alternative strategy for cancer treatment.

Ostenfeld et al showed a possible advantage for cancer cells to eliminate tumor-suppressor miRNAs via exosomes; this mechanism may support the metastatic process. They demonstrated a selective pressure for disposal of miR-23b, which may contribute to the transcriptomic changes associated with a cellular metastatic state¹¹⁵.

De Candia et al demonstrated that reduction of intracellular level of miR-150, a key regulator of mRNAs critical for lymphocyte differentiation and functions, via its selective release in the external milieu, may regulate gene expression during lymphocyte activation¹¹⁶.

We hypothesized a novel role for exosome release as a route to cellular disposal of selected oncogenic miRNAs, such as miR-21, as a consequence of Curcumin treatment. MicroRNA-21 has been indicated as a miRNA overexpressed in several solid tumors; miR-21 is involved in a number of steps of tumor progression, such as proliferation, angiogenesis, antiapoptotic and response to chemotherapy. A number of miR-21 target genes have been identified, including PTEN, PDCD4, and BTG2, which play important roles in the oncogenic process¹¹⁷. It was demonstrated that decreased expression of miR-21 in human lung cancer cells by inhibition of NOX (NADPH oxidase) reduces metastasis¹¹⁸. Moreover the downregulation of miR-21 expression restrains non-small cell lung cancer cell proliferation and migration through upregulation of PDCD4¹¹⁹.

Few studies have focused on the role of miR-21 in CML progression. Li et al demonstrated that anti-miR-21 oligonucleotides (AMO-miR-21) sensitized K562 cells, to arsenic trioxide by inducing apoptosis. AMO-miR-21 down-regulated mature miR-21 expression level and partially induced up-regulation of PDCD4 level¹²⁰. Other groups demonstrated that antisense

oligonucleotide against miR-21 inhibits migration and induces apoptosis in leukemic K562 cells¹²¹.

Our data indicate that Curcumin might exert anticancer effects through elimination of oncomiR-21, via exosomes. We showed that Curcumin caused a decrease of miR-21, but not pre-miR-21, in CML cells after Curcumin treatment. On the contrary, we observed an increase of miR-21 in the exosomes released by CML cells after addition of Curcumin.

Our results are in line with other studies that demonstrated the effects of Curcumin on cancer cell survival through down-regulation of miR-21 and increase of PTEN. PTEN up regulation, caused by non-genomic mechanisms, such as post transcriptional regulation by non-coding RNA, antagonizes the PI3K-AKT pathway¹²². This inhibitory effect acts on the PI-3K-AKT pathway, which controls cell proliferation and survival.

Focusing our attention on mRNA targets of miR-21 that could be involved in cancer progression, we found that the decrease of cellular miR-21, significantly up-regulated the expression of PTEN modulating the phosphorylation of AKT. Several studies also showed that Curcumin inhibited the phosphorylation of AKT, mTOR, and their downstream substrates. It was demonstrated that Difluorinated Curcumin (CDF), a nontoxic analog of Curcumin modulated the expression of miR-21 and PTEN in pancreatic cancer and inhibited the growth of colon cancer cells⁶⁷. Functionally, an increase of PTEN and the consequent decrease of AKT phosphorylation caused an inhibition of cell survival, as we demonstrated by an *in vitro* colony formation assay. Our current data show a negative correlation between miR-21 and PTEN and support the role of Curcumin on modulation of PTEN expression, via a selective packaging of miR-21 in CML exosomes. PTEN also modulates VEGF expression, down-regulating PI3K/AKT pathway; forced expression of PI3K or AKT alone directly increased VEGF mRNA expression, suggesting that PI3K and AKT are sufficient to regulate VEGF expression. We demonstrated that Curcumin treatment caused a decrease of VEGF, both at mRNA and protein levels, in K562 and LAMA84 cells and that this effect is also mediated by PTEN, downregulating PI3K/AKT pathway.

Angiogenesis in haematological malignancies is similar to that seen in solid tumors; secreted VEGF contributes to haematological disease progression by an autocrine or paracrine mechanism. VEGF signaling inhibition results in significant tumour growth delay in a wide

range of animal models¹²³. As shown by our results, Curcumin treatment caused a decrease of VEGF at mRNA and protein levels, in K562 and LAMA84 cells (Figure 19). Masuelli et al demonstrated *in vivo* the anticancer effects of Curcumin alone or in combination with resveratrol. The authors observed that the administration of Curcumin in Balb/c mice reduced the growth of the transplanted salivary gland cancer cells and this effect is potentiated by the combination of Curcumin and resveratrol¹²⁴.

Interestingly, we observed an opposite effects of Curcumin on the cellular level of miR-196b, a microRNA that was recently associated to CML development. Recent studies have indicated that miR-196b inhibits cell proliferation and promotes apoptosis in ALL cells. The expression levels of miR-196b were significantly lower in patients with CML than in healthy controls⁸⁸. Bioinformatic analysis suggest that Bcr-Abl is a predictive target of miR-196b. We observed that Curcumin caused an increase of miR-196b in CML cells and the decrease of its levels in the released exosomes, leading to a down regulation of the chimeric oncoprotein Bcr-Abl both at mRNA and protein levels in leukaemia cells.

Our *in vivo* experiments demonstrated that Curcumin treatment of animals lead to a significant reduction in tumour growth, as measured by the decrease in size of the subcutaneous xenografts compared to untreated animals. Moreover, the exosomes amount in plasma of treated mice was higher than control mice and we discovered that these exosomes are enriched in miR-21 compared to control exosomes.

Overall, these results suggested an antineoplastic role of Curcumin in CML cells, suggesting that Curcumin could be a potential adjuvant agent against CML. Curcumin induced selective packaging of oncomiR-21 in exosomes, an increase of miR-196b in CML cells and the previous described modulations of PTEN, pAKT, VEGF and Bcr-Abl expression in CML cells, as represented in figure 24.

4.3 Curcumin modulates chronic myelogenous leukemia exosomes composition and affects angiogenic phenotype, *via* exosomal miR-21

Exosomes play a key role in cell-to-cell communication. Several studies have demonstrated that exosomes modulate angiogenic process^{68,72,90}. Our research group

discovered that CML cells affect vascular remodeling in *in vitro* and *in vivo* models through the IL8 modulation in endothelial cells. We also demonstrated that exosomes released from CML cells stimulate bone marrow stromal cells to produce IL8 that, in turn, is able to affect both *in vitro* and *in vivo* leukemia cell malignant phenotype⁵⁴.

Recently, the critical role played by miRNAs delivered by exosomes in cell-to-endothelial cell communication in leukemia has been investigated. In our previous paper, we demonstrated that miR-126 shuttled by CML exosomes is biologically active in targeting endothelial cells and affects CML cell motility and adhesion⁶⁸. Umezu et al. observed that exosomes, collected from miR-92a-overexpressing leukemia cells, are internalized by endothelial cells, resulting in an enhanced migration and tube formation⁷³. These data indicated that exosomal miRNAs have an important role in tumor-endothelial cross-talk occurring in the bone marrow microenvironment, potentially affecting disease progression.

Furthermore, it was demonstrated that some natural compounds can alter gene expression involved in cancer progression⁷⁹. Curcumin, a natural compound present in turmeric, has been recognized as a promising anticancer drug and is being developed as a chemopreventive agent in various cancers. Preclinical studies have shown that Curcumin has antioxidant, anti-inflammatory and antiproliferative activities. Curcumin affects several molecules involved in biochemical and molecular cascades, via direct molecular interactions and epigenetic modulation of gene expression. The modulation of miRNA expression by Curcumin has been shown in several models⁷⁹. The effects of Curcumin on miRNA expression was initially studied in pancreatic cancer cells¹²⁵. Curcumin was reported to downregulate the expression of 18 miRNAs including miR199a* known to target MET proto-oncogene and the downstream extracellular signal-regulated kinase 2¹²⁶. It was also described that Curcumin, in retinoblastoma cells, upregulates the expression of 11 miRNAs including miR-22 that leads to a decreased expression of its downstream genes including the transcription factor SP1, implicated in the growth and metastasis of several cancer types¹²⁷.

In the previous work, we demonstrated that Curcumin caused a decrease of cellular miR-21 in CML cells and an increased miR-21 selective packaging in released exosomes. Furthermore, we showed that addition of Curcumin to CML cells caused a downregulation of Bcr-Abl expression through the cellular increase of miR-196b. Curcumin, therefore, alters mRNA expression that may contribute to its antileukemic effect in CML⁶⁹. MicroRNAs have

been reported to play an important role in several functions of endothelial cells, including migration and angiogenesis^{91,128}. It was demonstrated that miR-21 overexpression affects endothelial cell migration and organization into capillary-like structures. MiR-21 was also found to modify actin cytoskeleton organization, thus affecting cell migration and angiogenesis⁹¹. In this study, we showed that exosomes released by CML cells after Curcumin treatment (Curcu-exosomes) deeply changed their molecular composition, acquiring antiangiogenic properties. Curcu-exosomes, enriched in miR-21 as previously described⁶⁹, are able to shuttle this miRNA in endothelial cells as a biologically active form.

Our data are in agreement with the results of Sabatel et al., demonstrating that miR-21 overexpression reduces the angiogenic capacity of HUVECs⁹¹, targeting directly RhoB, a critical regulator of actin dynamics. RhoB is a Rho GTPase whose expression is inducible by a variety of stimuli including growth factors. Most Rho GTPases act on membranes and affect the movement of cell membranes by changing the membrane-associated cytoskeletal actin. Endothelial Rho proteins are also involved in ICAM1 mediated signaling events¹²⁹. Rho may be activated through cell-surface signals propagated to the cytoskeletal actin¹³⁰.

Curcu-exosomes inhibit the expression of RhoB at protein and mRNA level (Figure 29), via miR-21 transport, thus resulting unable to promote the angiogenic phenotype in endothelial cells. The biological effects of Curcu-exosomes on endothelial barrier stabilization were confirmed with a permeability assay (Figure 35). Several studies have also shown that Curcumin is able to counteract the stimuli-induced production of IL8 through the modulation of NFκB, JNK, ERK1/2, and p38 pathways. Wang et al showed that Curcumin had an inhibitory effect on the expression of IL8 induced by DEHP¹³¹. We observed that CML exosomes added to HUVECs were able to increase IL8 at mRNA and protein level. We also proved that this effect was reverted after treatment of ECs with Curcu-exosomes (Figure 31). The antiangiogenic effect of Curcu-exosomes was reinforced by decreasing the expression of VCAM1 at mRNA and protein level with respect to control exosomes (Figure 32). These antiangiogenic effects were confirmed with *in vitro* and *in vivo* angiogenic assays (Figure 33).

Kalani and colleagues showed that exosomes derived from Curcumin-treated endothelial cells alleviated oxidative stress, affecting tight junctions (ZO-1, claudin-5, occludin) and adherent junction (VE-cadherin) proteins and mitigated the endothelial cell layer permeability induced during EC damage due to high homocysteine levels¹³². It was also

demonstrated that Curcumin had a beneficial effect on blood brain barrier (BBB), under ischemic conditions, protecting the tight junction from a possible dysfunction and ameliorating the BBB permeability¹³³.

We also observed that Curcu-exosomes have protective effects on endothelial barrier, stabilizing tight and adherent junctions. As it has been showed with an immunofluorescence assay, in HUVECs treated with control exosomes, we observed a delocalization of ZO1 and VE-Cadherin with respect to control HUVECs in which ZO1 and VE-Cadherin was localized in plasma membrane. This effect reverted in HUVECs treated with CML Curcu-exosomes.

Interestingly our SWATH analysis of exosomes released by control and Curcumin treated cells evidenced a relevant and significant modulation of several proteins involved in the angiogenic process. In particular, proteomic data highlighted that Curcumin induced the release of exosomes depleted in pro-angiogenic proteins such as: Interferon-induced transmembrane protein 1 (IFITM1), actinin 4, basigin, Guanine nucleotide-binding protein subunit beta-2-like 1 (GNB2L1) and MARCKS¹³⁴, and enriched in proteins, such as Pleckstrin¹³⁵ and Midkine¹³⁶, which present known antiangiogenic abilities (Table 2).

We focused our attention on MARCKS, since it was the most modulated protein, it is described as predictive target of miR-21. MARCKS is a phosphoprotein that belongs to the myristoylated alanine-rich C-kinase substrate (MARCKS) family and possesses actin-binding properties through which it is implicated in control of cell motility¹³⁴; MARCKS dysregulation is closely associated with metastasis in a wide range of cancers and it is also an indicator of poor prognosis. MARCKS expression in Curcu-exosomes was about 11 fold less than control exosomes; moreover in HUVECs treated with Curcu-exosomes, enriched in miR-21, we observed a decrease of MARCKS (Figure 36). The downregulation of this protein was shown to contribute to maintain the vascular integrity by stabilizing the endothelial junctions.

Overall, these data demonstrated that Curcumin is able to induce a modification of CML exosomes composition both at protein and miRNA level. Curcu-exosomes were able to modulate the endothelial barrier organization and attenuated the angiogenic phenotype. Our results indicate that Curcumin could be a potential adjuvant agent for CML treatment with a double effect, on cancer cells and on tumour microenvironment.

CHAPTER 5

Tables and Figures

5.1 Exosomal shuttling of miR-126 in endothelial cells modulates adhesive and migratory abilities of chronic myelogenous leukemia cells

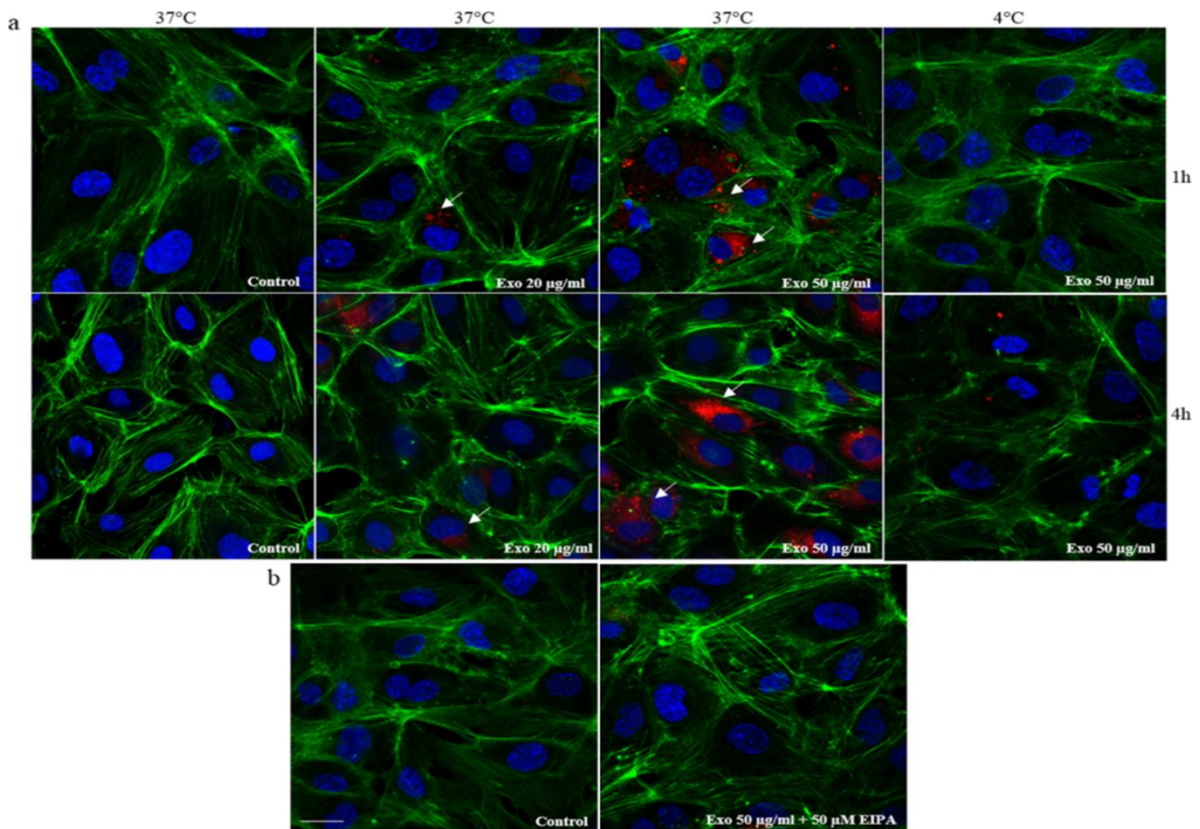


Figure 1: HUVECs internalize LAMA84 exosomes. a: Analysis at confocal microscopy of HUVECs treated, for 1 hour and 4 hours, with 20 µg/ml (Exo 20 µg/ml) and 50 µg/ml (Exo 50 µg/ml) of LAMA84 exosomes, compared with untreated HUVECs (Control). HUVECs were stained with phalloidin Alexa Fluor (green), nuclear counterstaining was performed using Hoescht (blue), exosomes were labelled with PKH26 (red). To evaluate whether exosomes uptake was mediated by endocytosis in an energy-dependent process, HUVECs treated with 20 µg/ml (Exo 20 µg/ml) and 50 µg/ml (Exo 50 µg/ml) of LAMA84 exosomes were incubated at 4°C, for 1 hour and 4 hours and compared with untreated HUVECs. **b:** Analysis at confocal microscopy of HUVECs treated, for 1 hour, with 50 µg/ml of exosomes (Exo 50 µg/ml) and EIPA (50 µM), compared with control cells (Control). Scale bar = 10 µm.

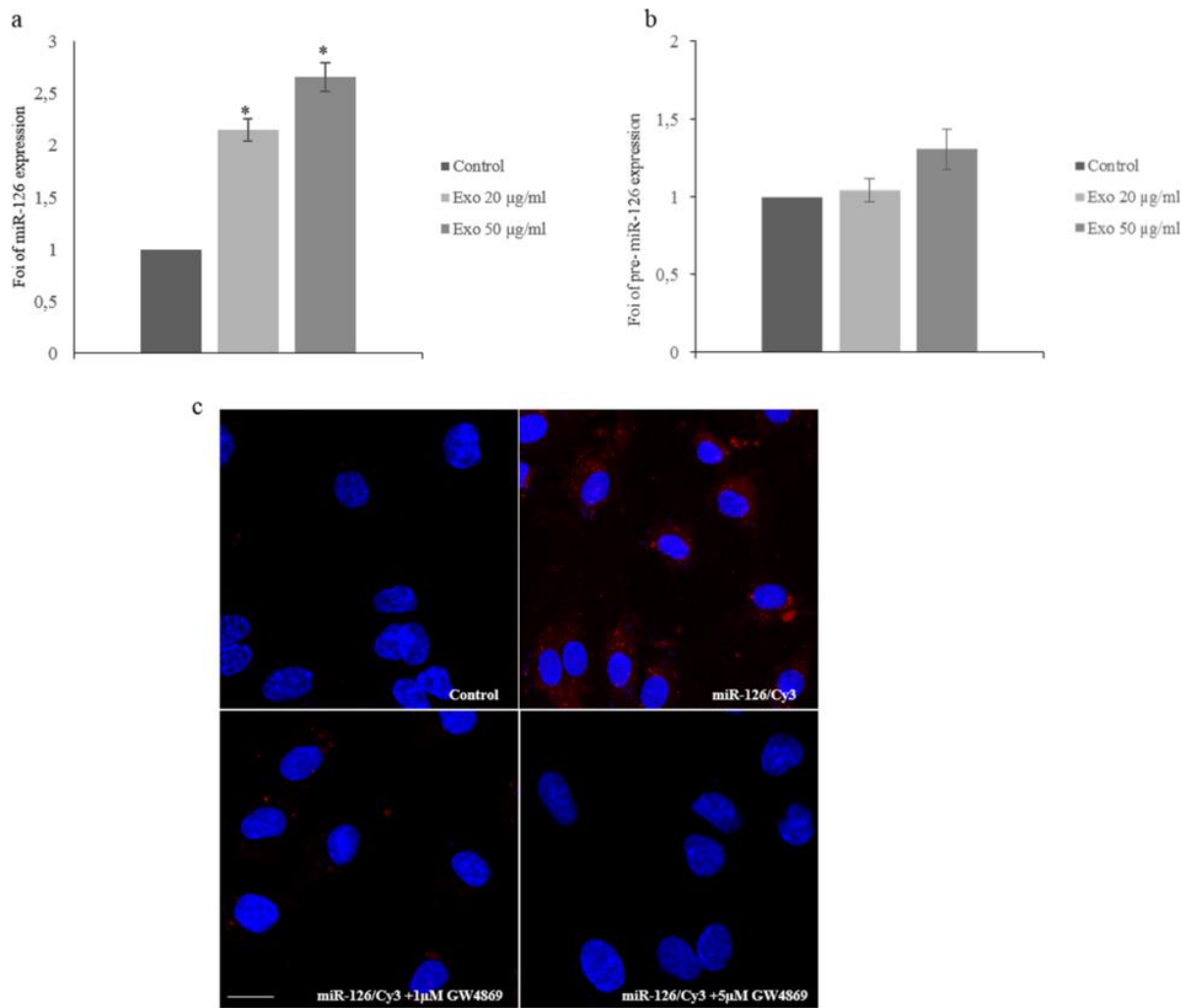


Figure 2: Exosomes shuttle miR-126 in HUVECs. **a:** MiR-126 expression in HUVECs treated with different amounts of LAMA84 exosomes. miR-126 expression levels in HUVECs treated with 20 and 50 µg/ml of LAMA84 exosomes for 24 hours were determined by quantitative Real time PCR analysis. Values are the mean \pm SD of 3 independent experiments * $p \leq 0.05$. **b:** Pre-miR-126 expression in HUVECs treated with different amounts of LAMA84 exosomes. Pre-miR-126 expression levels in HUVECs treated with 20 and 50 µg/ml of LAMA84 exosomes for 24 hours were determined by quantitative Real time PCR analysis. **c:** Localization of exosomal miR-126 into HUVECs. HUVECs were co-cultured with LAMA84/Cy3- miR-126 cells using Transwells. In Red is shown Cy3-miR-126 in the cytoplasm of HUVECs (miR-126/Cy3), nuclear counterstaining was done with Hoescht (blue). As a negative control, HUVECs were co-cultured with untransfected LAMA84 (Control). HUVECs were also cocultured with LAMA84/ Cy3-miR-126 cells treated with 1 µM (miR-126/Cy3 + 1 µM GW4869) and 5 µM (miR-126/Cy3 + 5 µM GW4869) of GW4869.

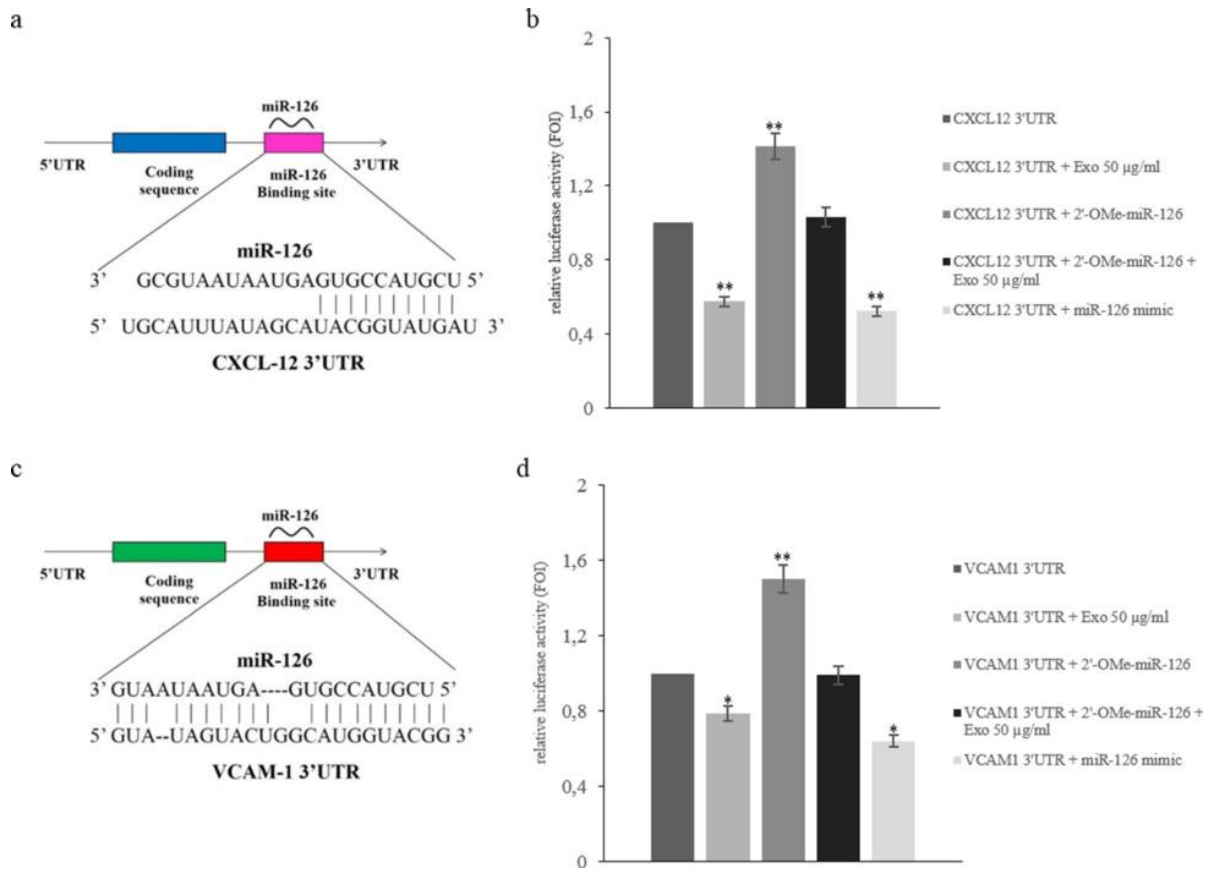


Figure 3: MiR-126 targets CXCL12 and VCAM1. **a:** Schematic representation of matching sequence between CXCL12 3'UTR mRNA and miR-126. **b:** Luciferase activity of HUVECs transfected with reporter plasmid (CXCL12-pEZ), treated with LAMA84 exosomes and/or cotransfected with miR-126 inhibitor or miR-126 mimic. **c:** Schematic representation of matching sequence between VCAM1 3'UTR mRNA and miR-126. **d:** Luciferase activity of HUVECs transfected with reporter plasmid (VCAM1-pEZ), treated with LAMA84 exosomes and/or cotransfected with miR-126 inhibitor or miR-126 mimic. For normalization, Renilla luciferase activity was used. Values are the mean \pm SD of 3 independent experiments *p 0.05; **p 0.01.

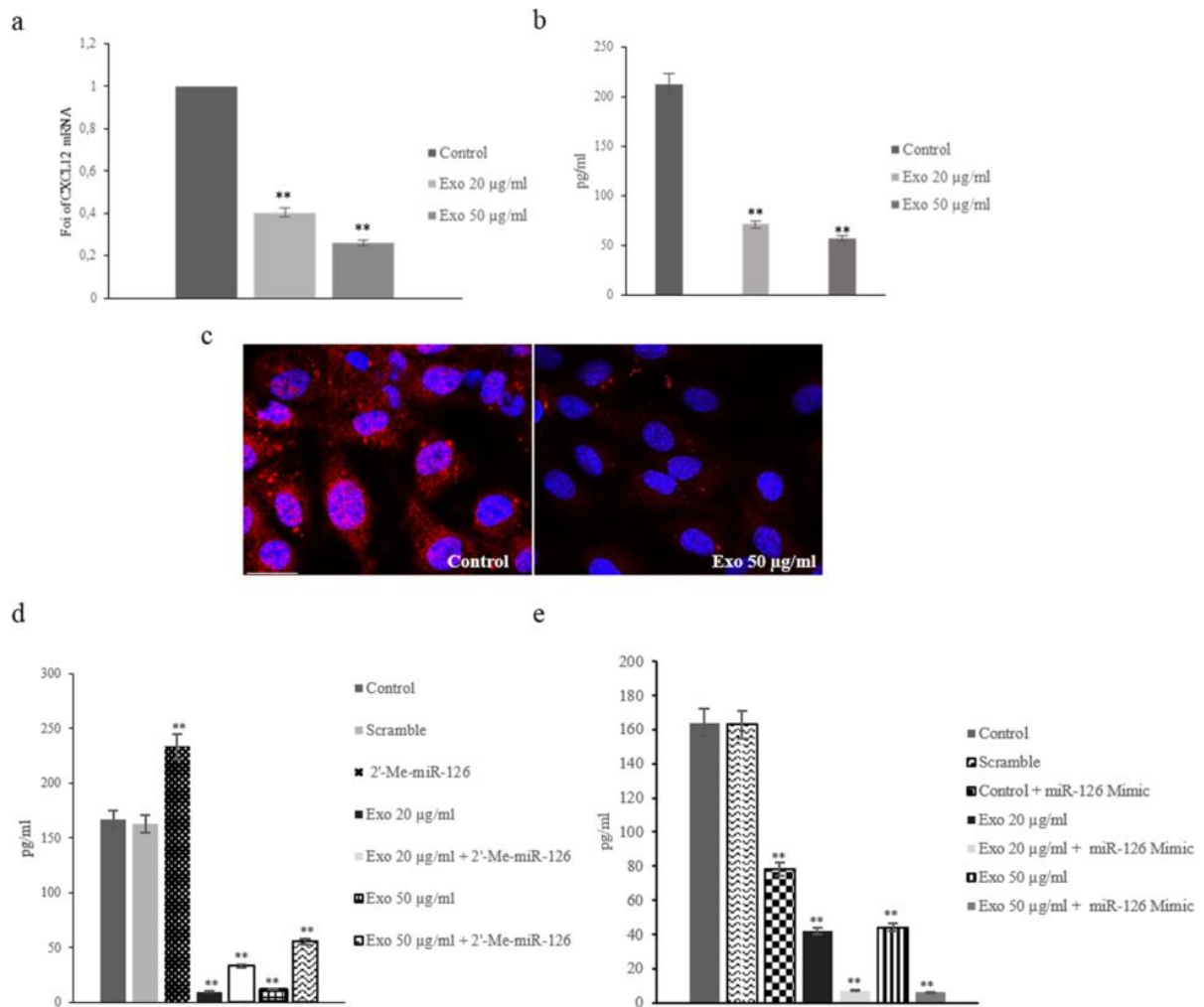


Figure 4: miR-126 shuttled by exosomes modulate CXCL12 expression in HUVECs. **a:** Real time PCR analysis showed that CXCL12 mRNA expression decreased in dose-dependent (20 and 50 µg/ml) manner after addition of exosomes to endothelial cells. Values are the mean ± SD of 3 independent experiments **p ≤ 0.01. **b:** CXCL12 protein levels, assessed by ELISA, in HUVEC-conditioned medium obtained after 24 hours of stimulation with: low serum medium (Control), 20 µg/ml of exosomes (Exo 20 µg/ml) and 50 µg/ml of exosomes (Exo 50 µg/ml). Values are the mean ± SD of 3 independent experiments **p ≤ 0.01. **c:** Confocal microscopy analyses of HUVECs treated with 50 µg/ml of exosomes for 24 h. HUVECs were stained with Texas Red-conjugated anti-CXCL12 antibodies, nuclear counterstaining was performed using Hoescht (blue). Scale bar = 10 µm. **d:** CXCL12 protein levels, assessed by ELISA, in HUVEC-conditioned medium obtained after 24 hours of stimulation with: low serum medium (Control), 20 µg/ml of exosomes (Exo 20 µg/ml) and 50 µg/ml of exosomes (Exo 50 µg/ml). CXCL12 protein levels were also evaluated in HUVECs transfected with miR-126 inhibitor (2-O-Me-miR-126) and treated with: 20 µg/ml of exosomes (Exo 20 µg/ml + 2-Me-miR-126) and 50 µg/ml of exosomes (Exo 50 µg/ml + 2-Me-miR-126). As a negative control, miScript Inhibitor Negative Control (Scramble) was used. **e:** CXCL12 protein levels were also evaluated in HUVECs transfected with miR-126 mimic and treated with: 20 µg/ml of exosomes (Exo 20 µg/ml + miR-126 mimic) and 50 µg/ml of exosomes (Exo 50 µg/ml + miR-126 mimic). As a negative control of transfection, the AllStars Negative Control (Scramble) was used.

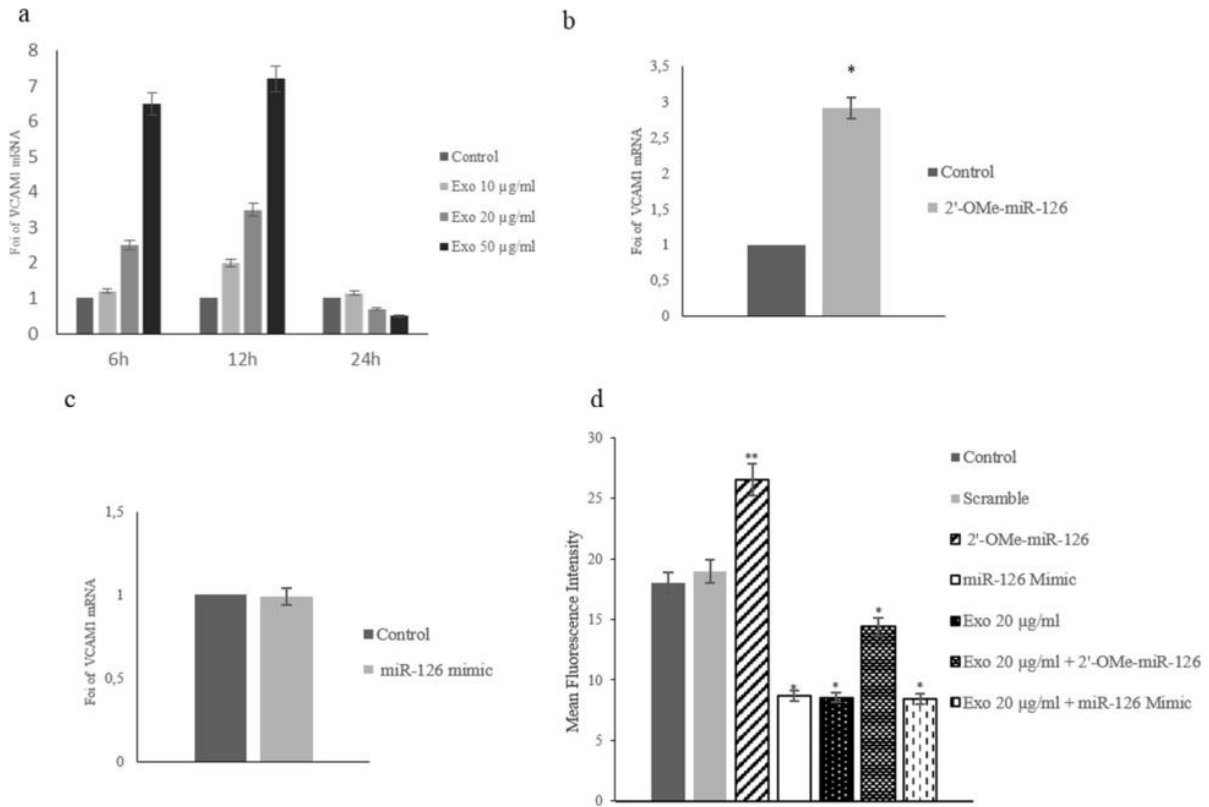


Figure 5: miR-126 shuttled by exosomes modulates VCAM1 expression in HUVECs. **a:** Real Time PCR analysis showed a time dependent modulation of VCAM1 mRNA expression after the addition of 10 (10 µg/ml), 20 (20 µg/ml) and 50 µg/ml (50 µg/ml) exosomes to endothelial cells. **b:** Real Time PCR analysis of VCAM1 mRNA expression levels in HUVECs transfected with miR-126 inhibitor (2-O-Me-miR-126) compared with untransfected HUVECs (Control). **c:** Real Time PCR analysis of VCAM1 expression levels in HUVECs transfected with miR-126 mimic compared with untransfected HUVECs (Control). **d:** Histogram shows the MFI (mean fluorescence intensity) of surface expression of VCAM1 in HUVECs after 24 hours of treatment with: low serum medium (Control), 20 µg/ml of exosomes (Exo 20 µg/ml). Surface expression of VCAM1 was evaluated, with FACS analysis, in HUVECs transfected with miR-126 inhibitor (2-Ome-miR-126) and treated with 20 µg/ml of exosomes (2-Ome-miR-126 + Exo 20 µg/ml). As a negative control, miScript Inhibitor Negative Control (scramble) was used. Surface expression of VCAM1 was also evaluated in HUVECs transfected with miR-126 mimic (miR-126 mimic) and treated with 20 µg/ml of exosomes (miR-126 mimic + Exo 20 µg/ml). Values are the mean ± SD of 3 independent experiments * $p \leq 0.05$ ** $p \leq 0.01$.

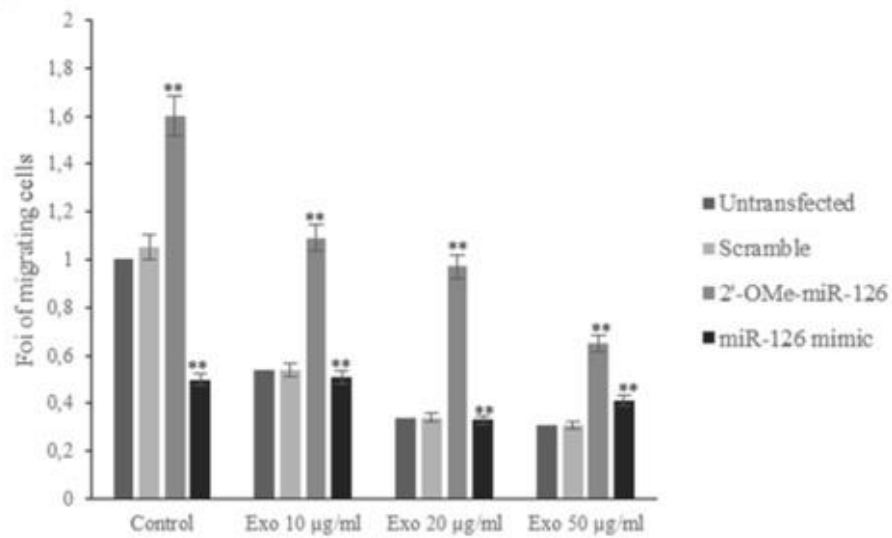


Figure 6: miR-126 delivered by exosomes modulates LAMA84 migration. Effects of conditioned medium (CM) of HUVECs pretreated with 10 µg/ml 20 µg/ml and 50 µg/ml of exosomes on LAMA84 cells motility compared with CM from untreated HUVECs. LAMA84 cells motility was determined towards conditioned medium of HUVECs transfected with miR-126 inhibitor (2'-O-Me-miR-126) and treated with 10 µg/ml (Exo 10µg/ml, 2'-O-Me-miR-126), 20 µg/ml (Exo 20µg/ml, 2'-O-Me-miR-126) and 50 µg/ml (Exo 50 µg/ml, 2'-O-Me-miR-126) of LAMA84 exosomes compared with untransfected cells. MiScript Inhibitor Negative Control (Scramble) was used as a negative control of miR-126 inhibitor transfection. LAMA84 cells motility towards CM of HUVECs transfected with: miR-126 mimic and treated with 10 µg/ml (Exo 10µg/ml, miR-126 mimic), 20 µg/ml (Exo 20 µg/ml, miR-126 mimic) and 50 µg/ml (Exo 50µg/ml, miR-126 mimic) of LAMA84 exosomes compared with untransfected cells. AllStars Negative Control (Scramble) was used as a negative control of miR-126 mimic transfection. Values are expressed as Fold of Increase (FOI). Values are the mean ± SD of 5 fields in 3 independent experiments *p 0.05; **p 0.01.

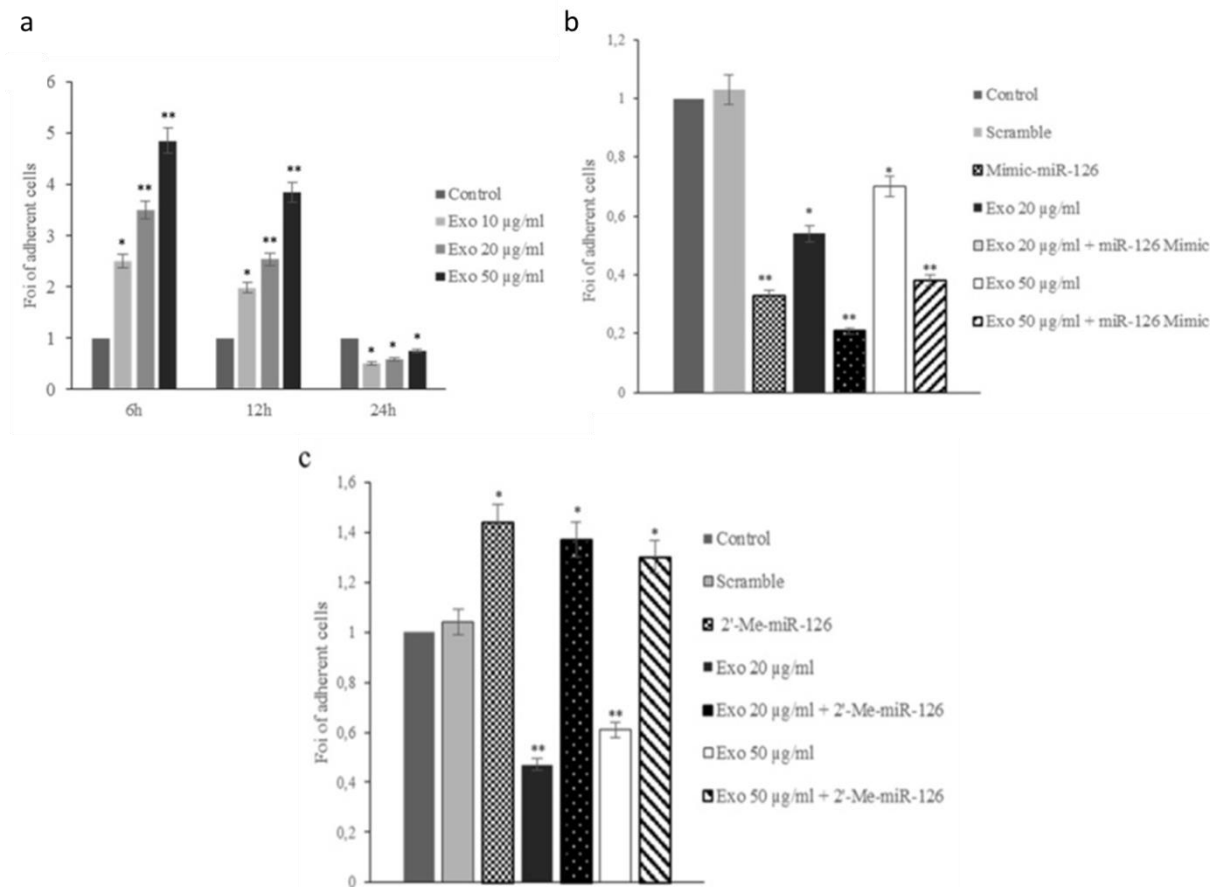


Figure 7: miR-126 delivered by exosomes modulates LAMA84 adhesion. **a.** Adhesion of LAMA84 cells to HUVECs treated, for 6-12-24 hours, with 20 and 50 µg/ml of LAMA84 exosomes compared with control HUVECs. **b:** Adhesion of LAMA84 cells to HUVECs treated with 20 and 50 µg/ml of LAMA84 exosomes compared with control HUVECs. The adhesion of LAMA84 cells was evaluated on HUVECs transfected with miR-126 mimic and then treated with 20 and 50 µg/ml of LAMA84 exosomes. **c:** The adhesion of LAMA84 cells was evaluated in HUVECs transfected with miR-126 inhibitor and then treated with 20 and 50 µg/ml of LAMA84 exosomes. *p 0.05; **p 0.01.

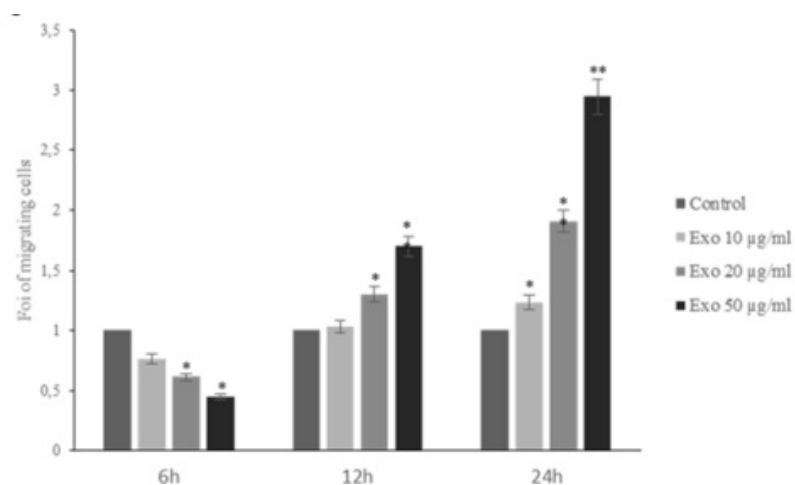


Figure 8: miR-126 delivered by exosomes modulates LAMA84 transendothelial migration. HUVECs were grown as a monolayer and treated with 10, 20, 50 µg/ml of LAMA84 exosomes. After 6-12-24 hours of treatment, we evaluated the transendothelial migration of LAMA84 cells. *p 0.05; **p 0.01.

5.2 Curcumin inhibits *in vitro* and *in vivo* chronic myelogenous leukemia cells growth: a possible role for exosomal disposal of miR-21

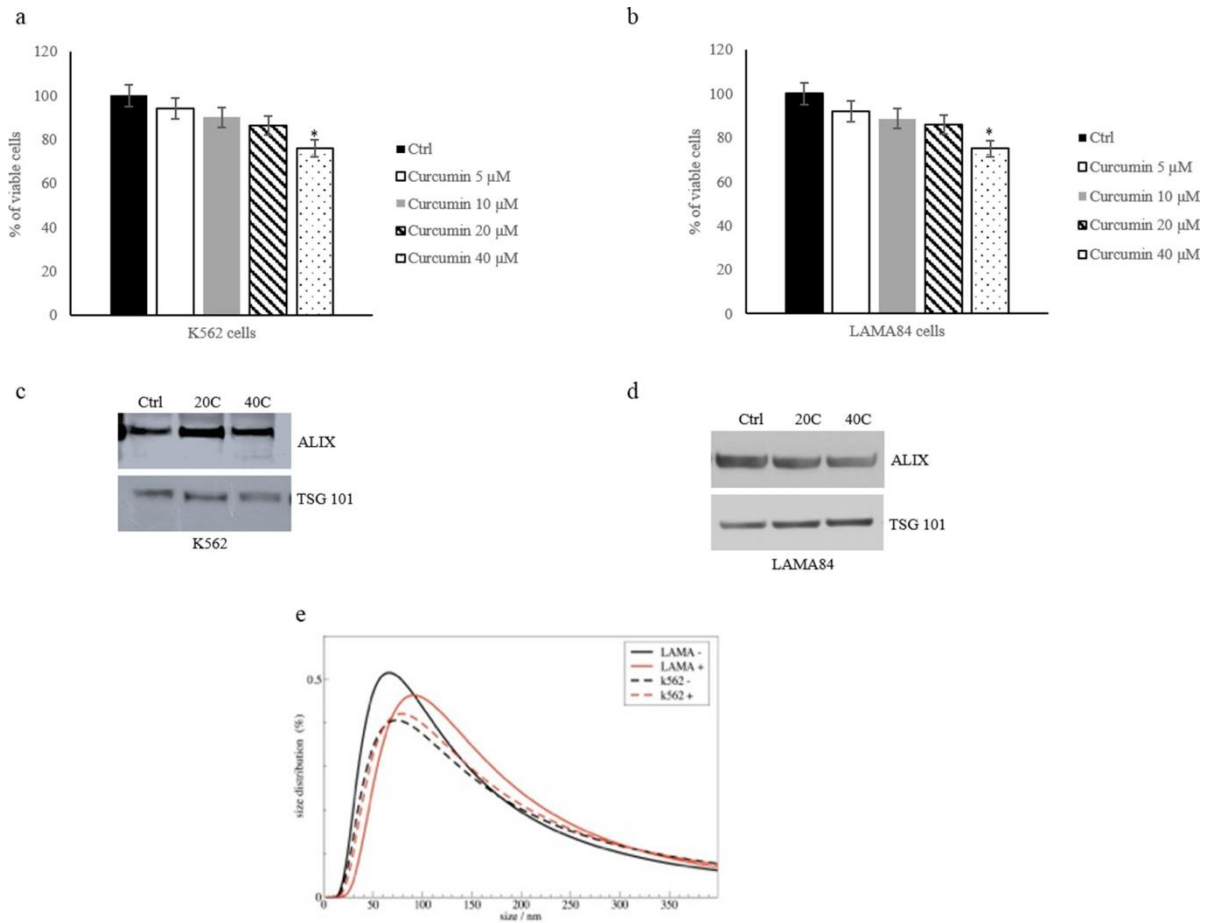


Figure 9: K562 **a.** and LAMA84 **b.** cell viability was measured by MTT assay after 24 h of treatment with Curcumin (5–10–20–40 μM). The values were plotted as a percentage of viable cells. Each point represents the mean ± SD of three independent experiments, * $p \leq 0.05$. Detection of Alix and TSG101 in 30 μg of exosomes purified from conditioned medium of K562 **c.** and LAMA84 **d.** cells treated with 20 (20C) and 40 (40C) μM of Curcumin. **e.** Dynamic light scattering (DLS) analysis of exosomes released by K562 and LAMA84 control (-) and treated with 20 μM of Curcumin (+).

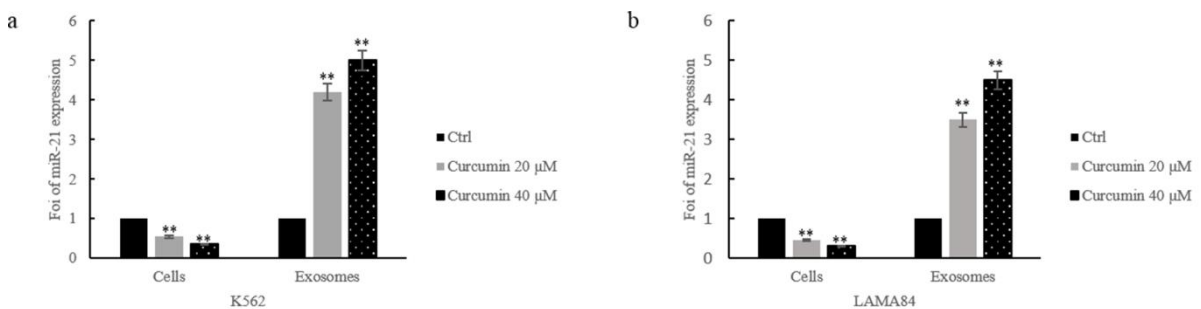


Figure 10: MiR-21 levels in K562 **a.** and LAMA84 **b.** cells and their released exosomes after treatment with 20 and 40 μM of Curcumin, for 24 hours and in their exosomes, were determined by quantitative real time PCR analysis. Values are the mean ± SD of 3 independent experiments ** $p \leq 0.01$.

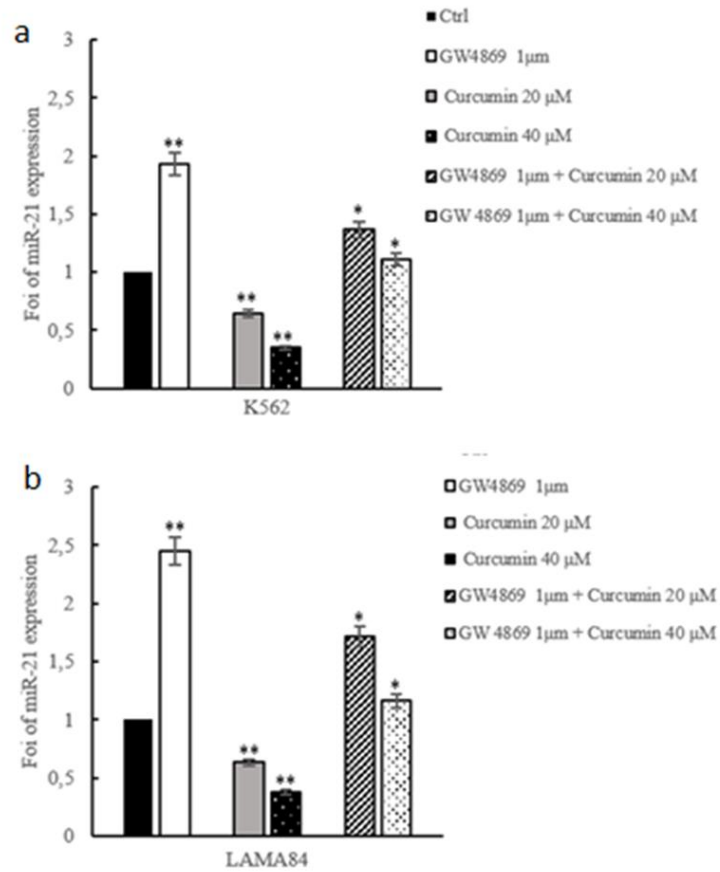


Figure 11: MiR-21 levels in K562 **a.** and LAMA84 **b.** cells treated with 20 and 40 µM of Curcumin and/or GW4869 1 µM, for 24 hours, were determined by quantitative real time PCR analysis. Values are the mean ± SD of 3 independent experiments * $p \leq 0.05$, ** $p \leq 0.01$.

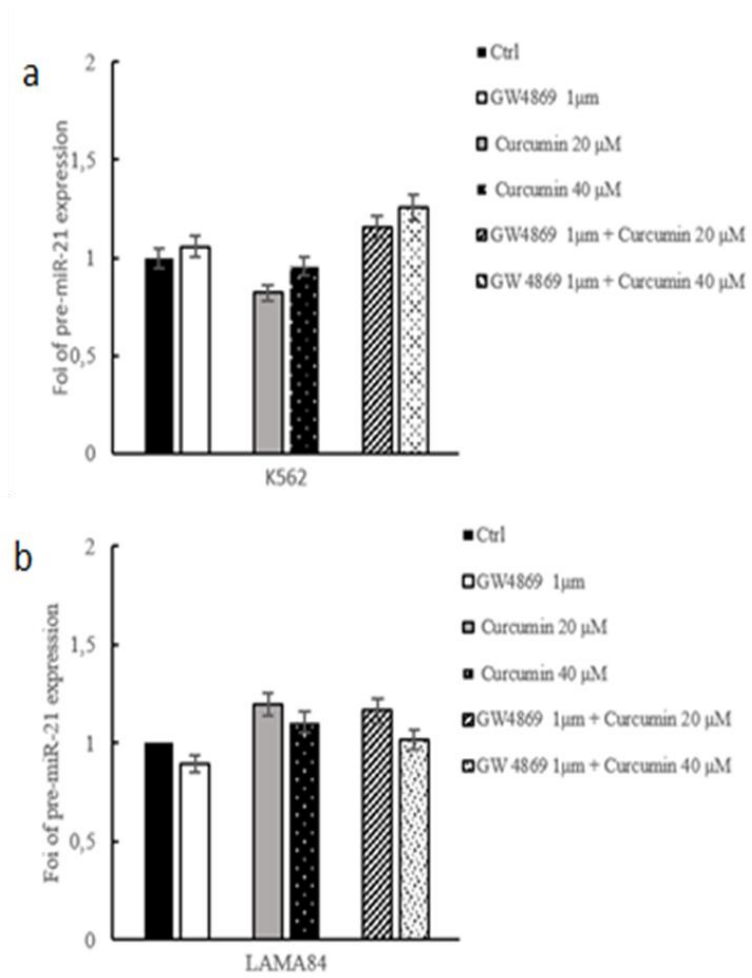


Figure 12: **a.** pre-MiR-21 expression in K562 cells treated with 20 and 40 µM of Curcumin, for 24 hours, was determined by quantitative real time PCR analysis. **b.** pre-MiR-21 expression in exosomes released by LAMA84 cells treated with 20 and 40 µM of Curcumin and/or GW4869 1 µM, for 24 hours, was determined by quantitative real time PCR analysis.

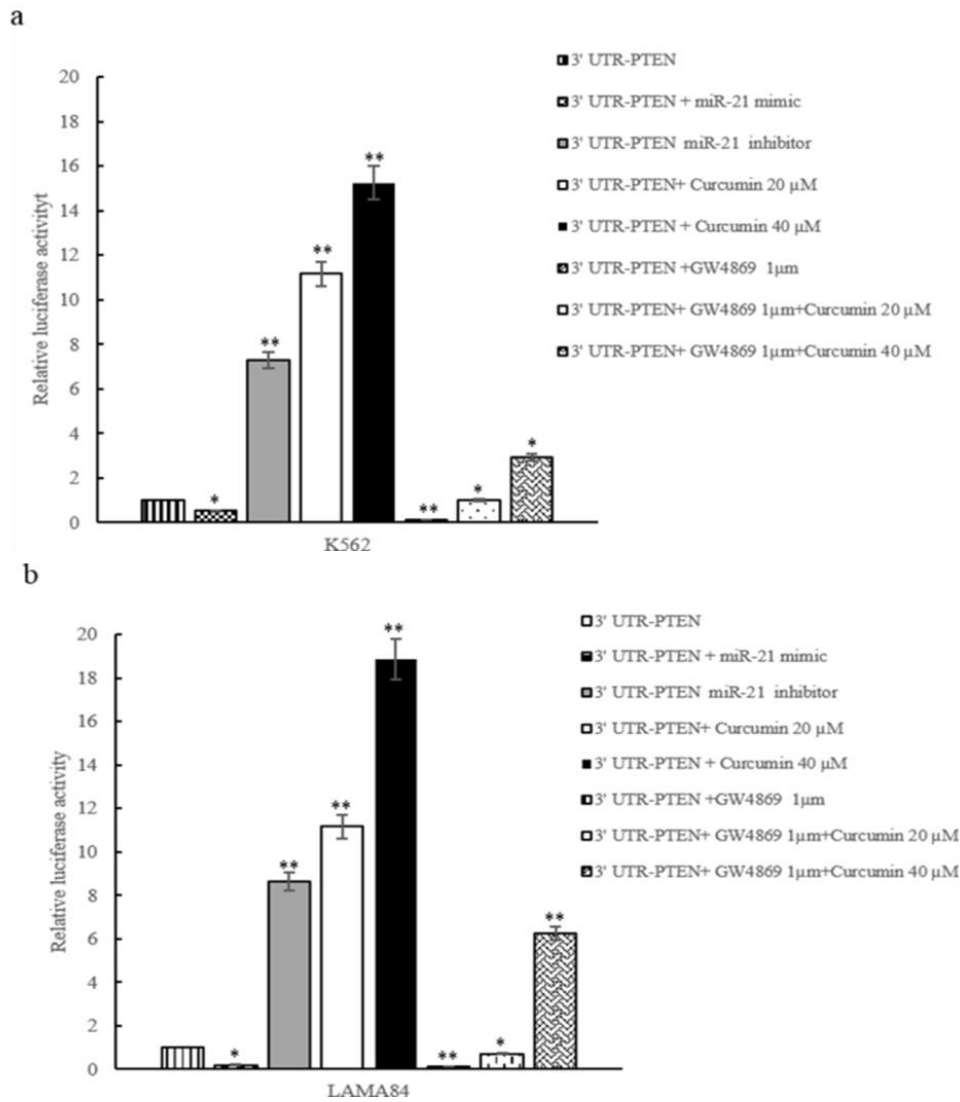


Figure 13: Luciferase activity of K562 **a.** and LAMA84 **b.** cells transfected with reporter plasmid (PTEN-pEZ) and treated with 20 and 40 μM of Curcumin and/or GW4869 1 μM, for 24 hours. K562 (**a**) and LAMA84 (**b**) cells transfected with PTEN-pEZ were also cotransfected with miR-21 inhibitor or miR-21 mimic. Values are the mean ± SD of 2 independent experiments * $p \leq 0.05$, ** $p \leq 0.01$.

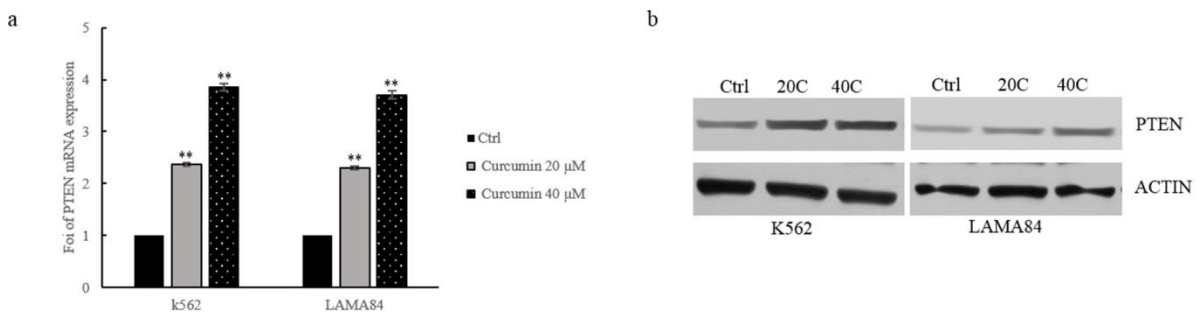


Figure 14: **a.** PTEN expression in K562 and LAMA84 cells treated for 24 hours, with 20 and 40 μM of Curcumin, was determined by quantitative real time PCR analysis. **b.** Western blot analysis of PTEN in K562 and LAMA84 cells treated with 20 (20C) and 40 (40C) μM of Curcumin, for 24 hours. Actin was used as loading control. ** $p < 0.01$.

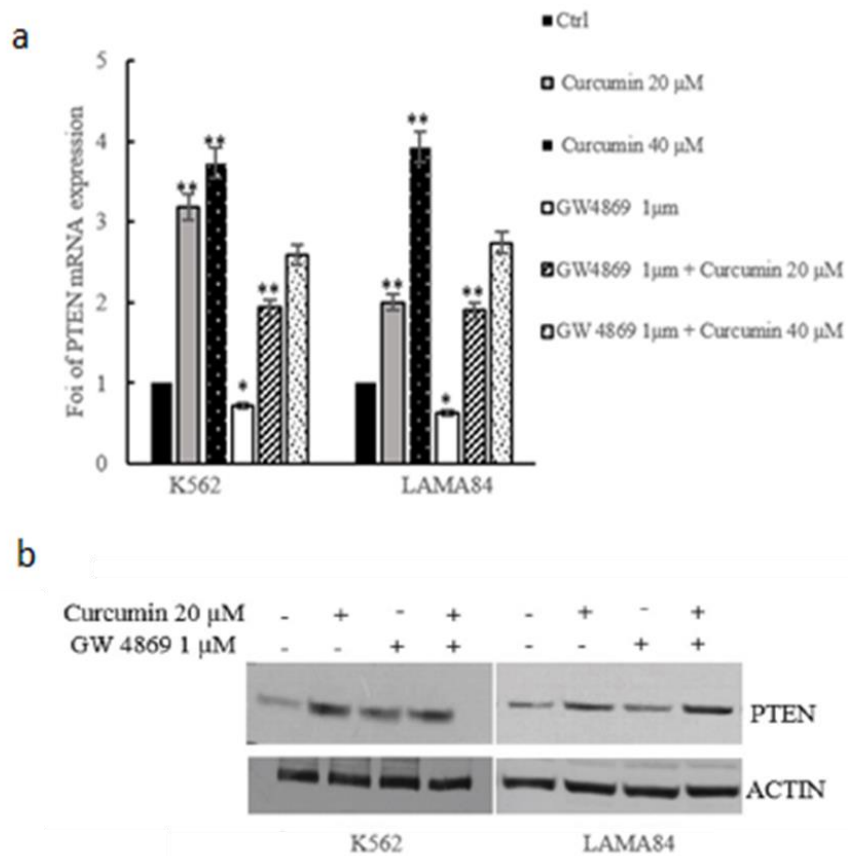


Figure 15: a. PTEN expression in K562 and LAMA84 cells treated with 20 and 40 μ M of Curcumin and/or GW4869 1 μ M, for 24 hours, was determined by quantitative real time PCR analysis. b. Western blot analysis of PTEN in K562 and LAMA84 cells treated with 20 μ M of Curcumin and/or GW4869 1 μ M, for 24 hours. Actin was used as loading control. * p 0.05; ** p 0.01.

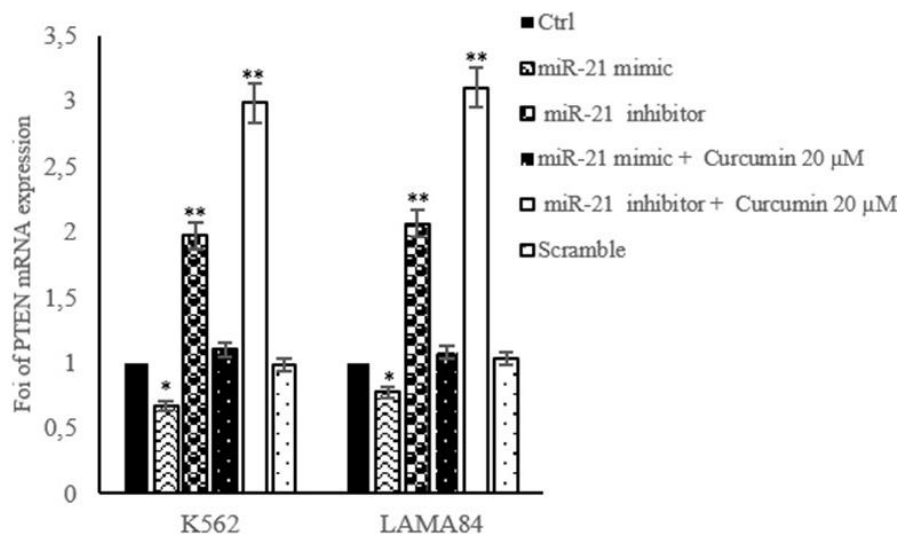


Figure 16: PTEN expression in K562 and LAMA84 cells transfected with miR-21 mimic, miR-21 inhibitor, treated or not with 20 μ M Curcumin, or scramble was determined by quantitative real time PCR analysis. Values are the mean \pm SD of 3 independent experiments * p \leq 0.05, ** p \leq 0.01.

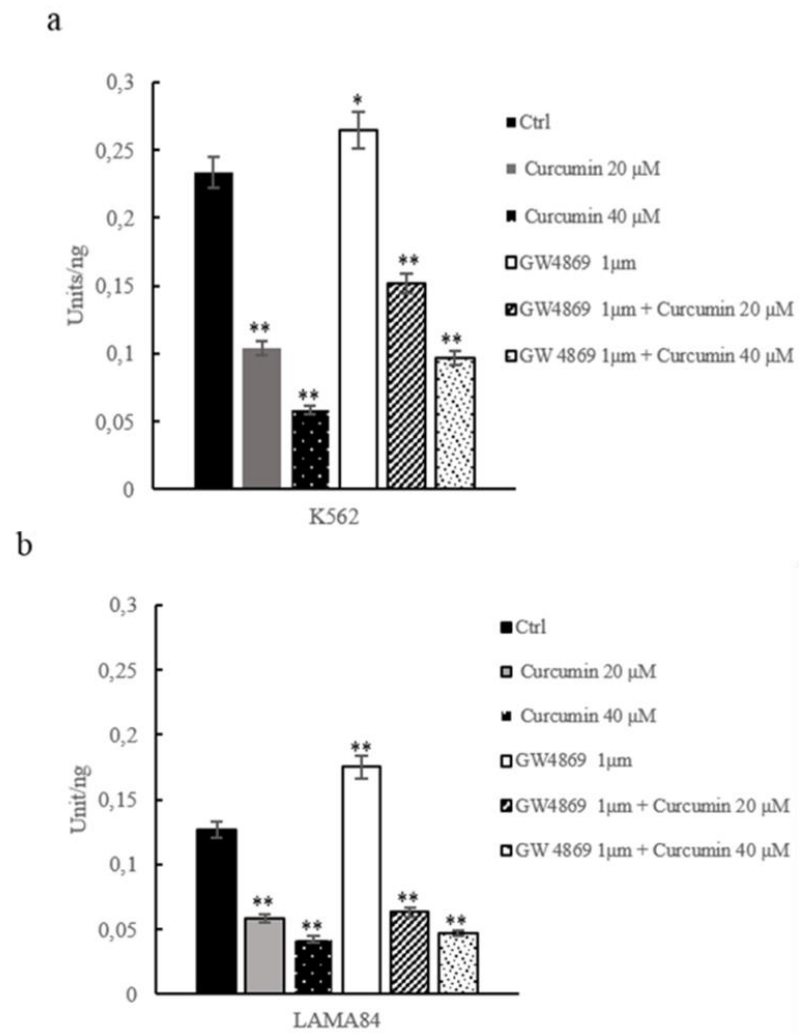


Figure 17: AKT phosphorylation, assessed by ELISA, in K562 a. and LAMA84 b. cells treated with 20 and 40 μ M of Curcumin and/or GW4869, for 24 hours. Values are the mean \pm SD of 2 independent experiments * $p \leq 0.05$, ** $p \leq 0.01$.

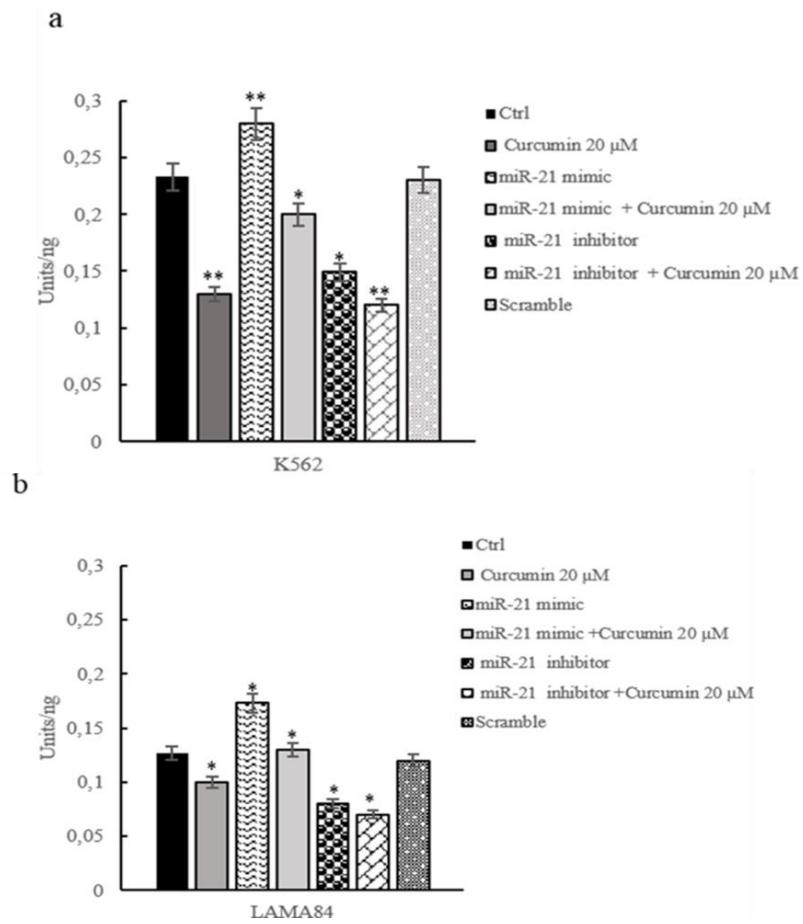


Figure 18: AKT phosphorylation, assessed by ELISA, in K562 a. and LAMA84 b. cells transfected with miR-21 mimic, miR-21 inhibitor or scramble and/or treated with 20 μM of Curcumin. Values are the mean ± SD of 2 independent experiments * $p \leq 0.05$, ** $p \leq 0.01$.

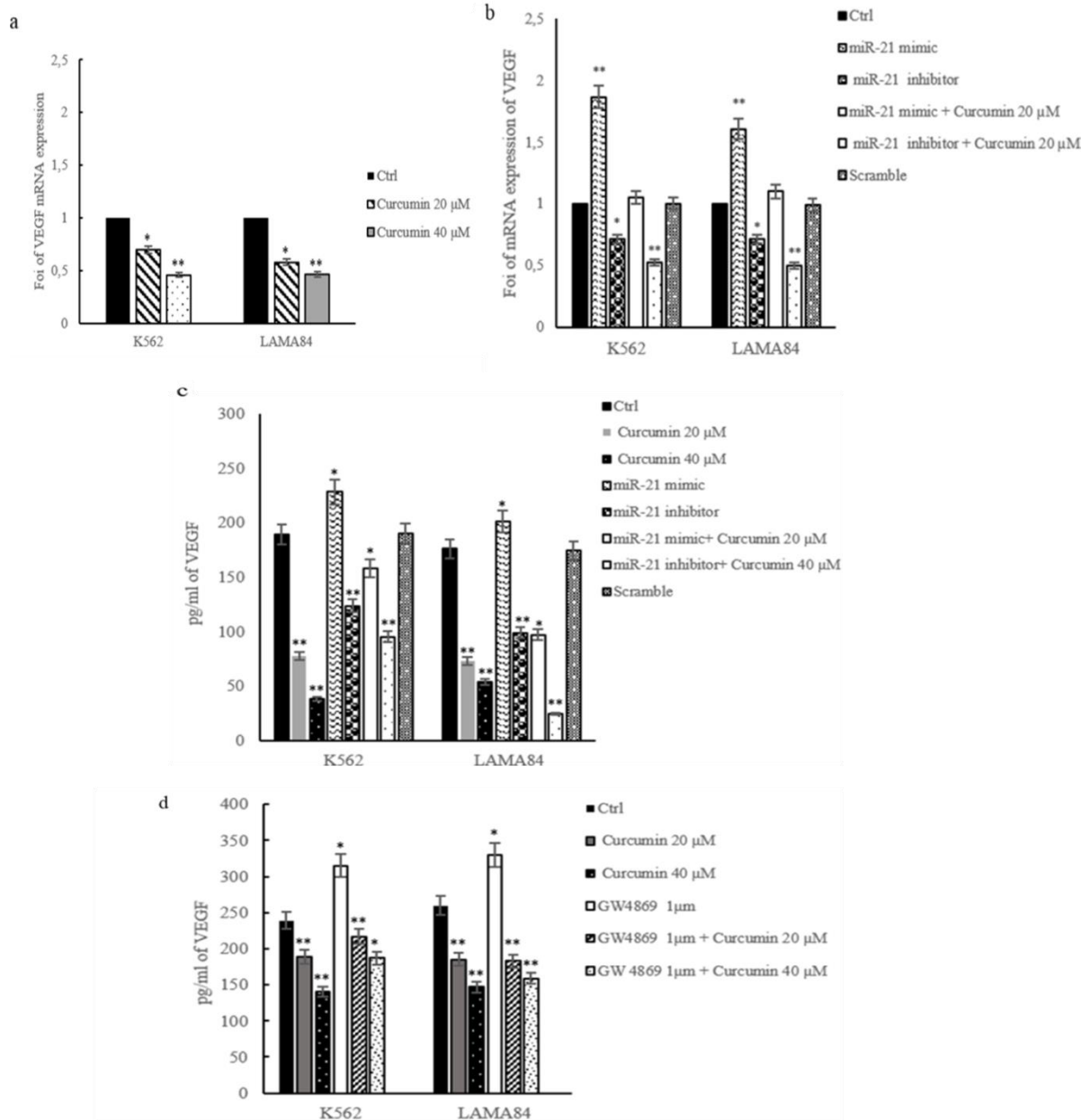


Figure 19: **a.** VEGF expression in K562 and LAMA84 cells treated with 20 and 40 μ M of Curcumin, for 24 hours, was determined by quantitative real time PCR analysis. **b.** VEGF expression in K562 and LAMA84 cells transfected with miR-21 mimic, miR-21 inhibitor or scramble, was determined by quantitative real time PCR analysis. **c.** VEGF protein level, assessed by ELISA, in conditioned medium of K562 and LAMA84 cells transfected with miR-21 mimic, miR-21 inhibitor treated or not with 20 μ M Curcumin, or scramble treated with 20 and 40 μ M of Curcumin, for 24 hours. **d.** VEGF protein level assessed by ELISA, in K562 and LAMA84 cells treated with 20 and 40 μ M of Curcumin and/or GW4869 1 μ M, for 24 hours. Values are the mean \pm SD of 3 independent experiments * $p \leq 0.05$, ** $p \leq 0.01$.

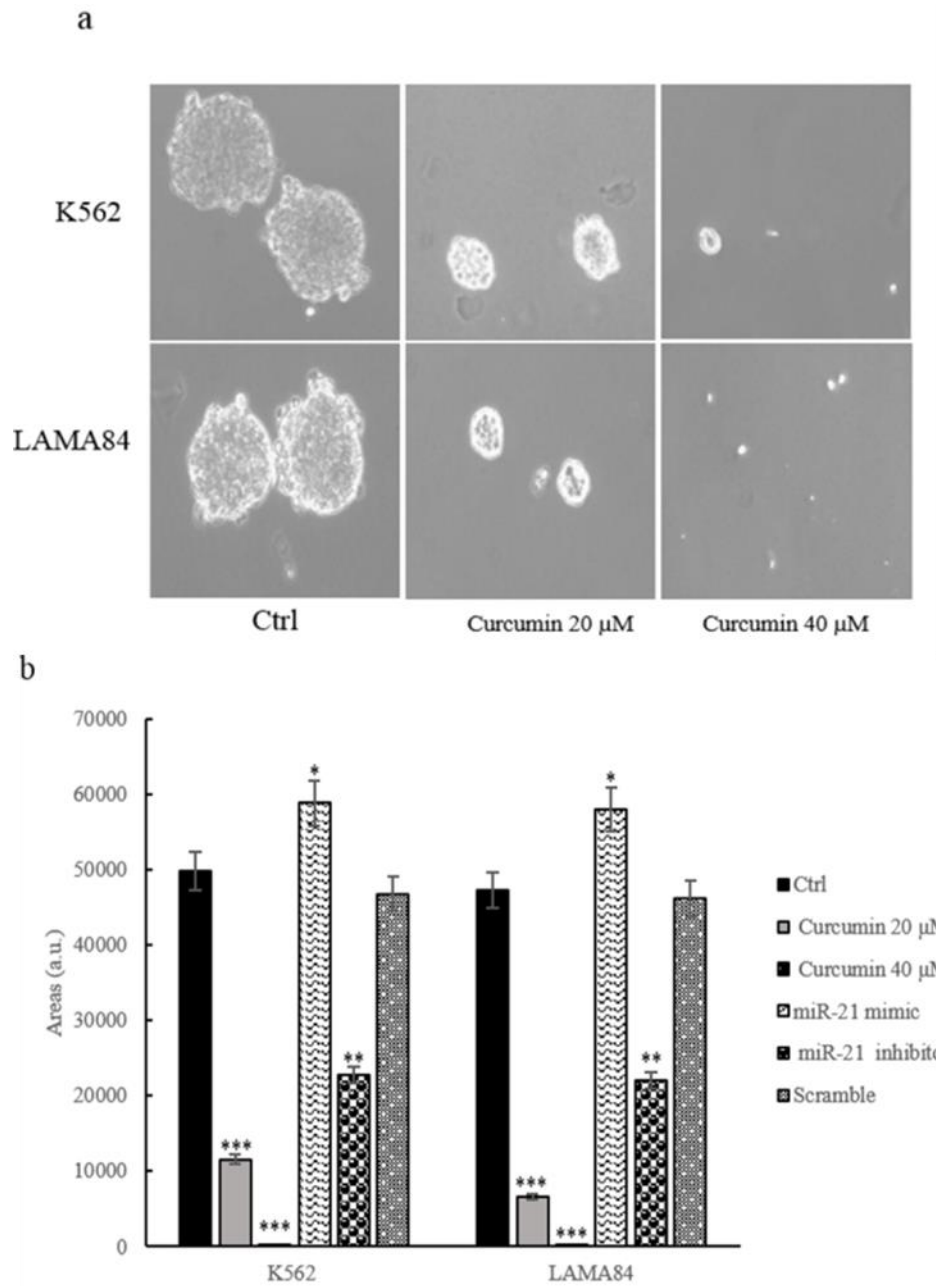


Figure 20: a. Colony formation assay shows that Curcumin treatment caused a decrease of K562 and LAMA84 colonies area with respect to control cells. **b.** Quantitative analysis of colonies area of K562 and LAMA84 cells treated with 20 and 40 μM of Curcumin and/or transfected with miR-21 mimic and miR-21 inhibitor. Values are the mean \pm SD of 3 independent experiments * $p \leq 0.05$, ** $p \leq 0.01$, *** $p \leq 0.001$.

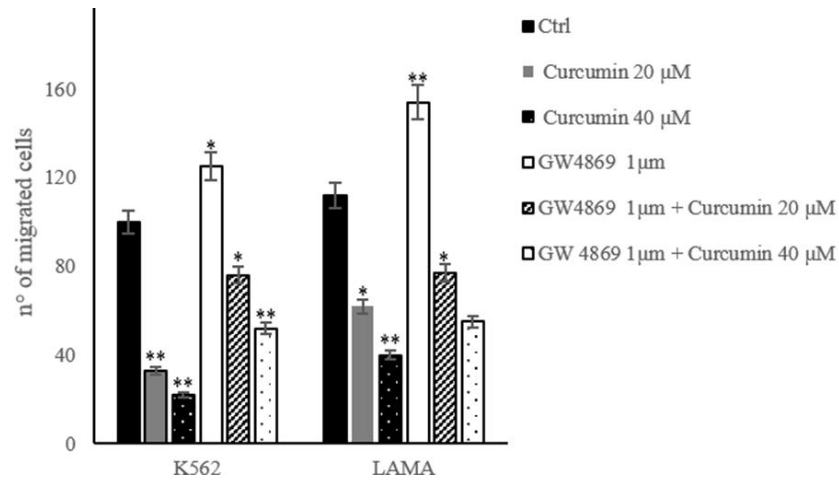


Figure 21: Effect of 20 and 40 μM Curcumin on K562 and LAMA84 cells migration. CML cells were also cotreated with 20 and 40 μM Curcumin and GW4869 1 μM, for 24 hours. Values are the mean ± SD of 3 independent experiments * $p \leq 0.05$, ** $p \leq 0.01$.

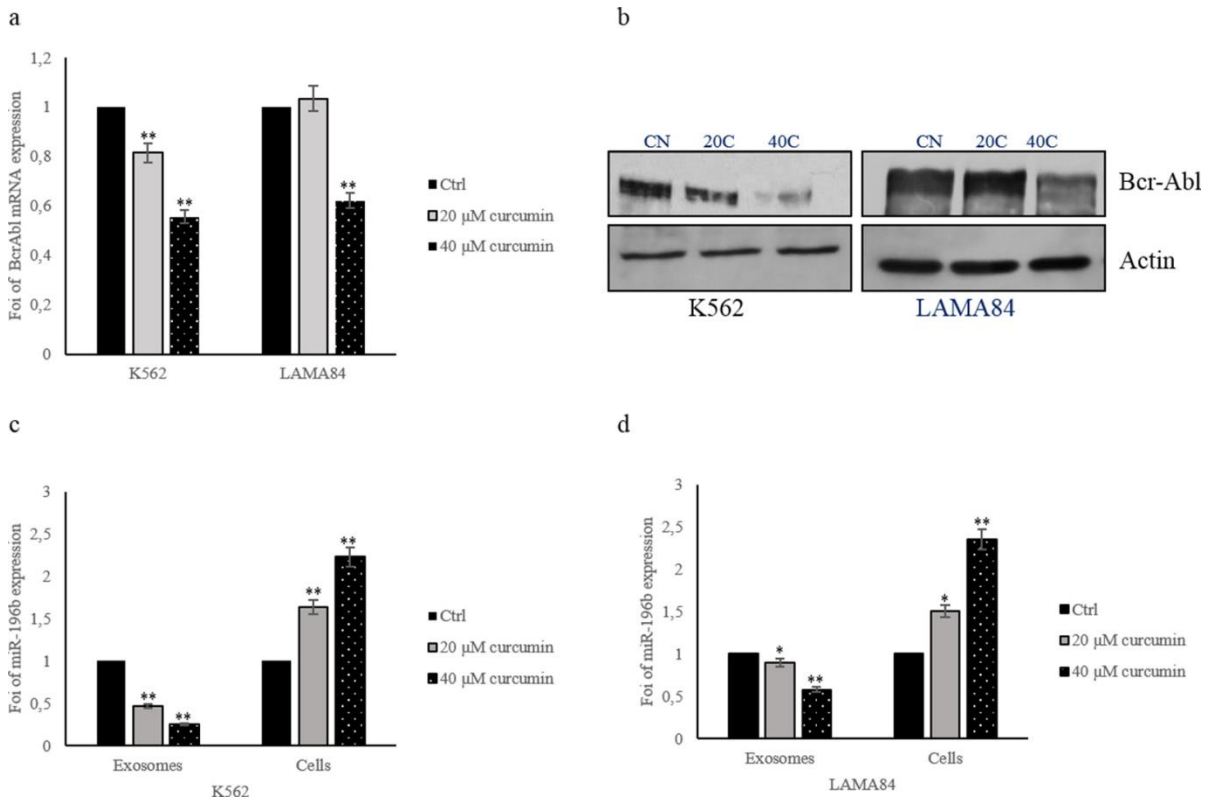


Figure 22: a. Bcr-Abl expression in K562 and LAMA84 cells treated with 20 and 40 μM of Curcumin, for 24 hours, was determined by quantitative real time PCR analysis. **b.** Western blot analysis of Bcr-Abl in K562 and LAMA84 cells treated with 20 (20C) and 40 (40C) μM of Curcumin, for 24 hours. Actin was used as loading control. **c.** miR-196b levels in K562 **c.** and LAMA84 **d.** cells and their released exosomes after treatment with 20 and 40 μM of Curcumin, for 24 hours, were determined by quantitative real time PCR analysis. Values are the mean ± SD of 3 independent experiments * $p \leq 0.05$, ** $p \leq 0.01$.

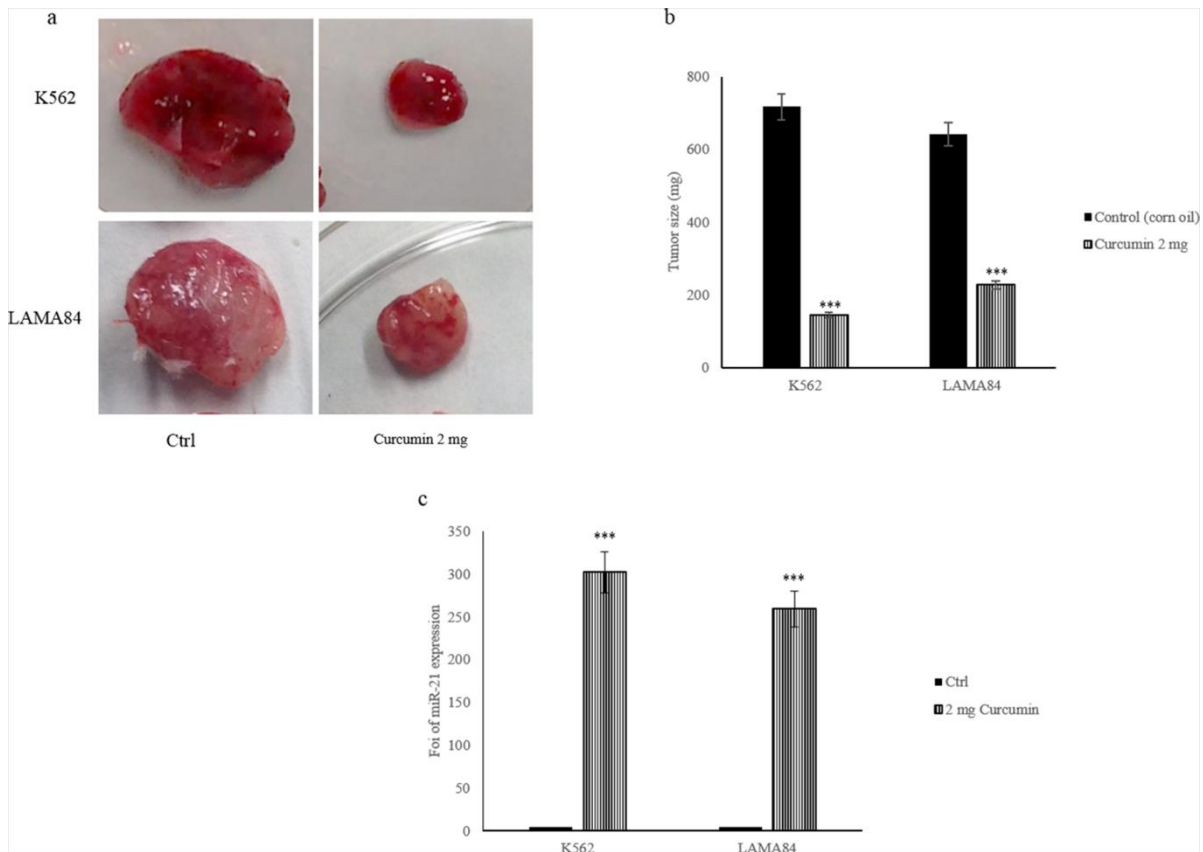


Figure 23: **a.** Representative tumour masses removed from mice treated with corn oil (control) or 2 mg of Curcumin. **b.** Tumour masses size average of mice treated with corn oil (Ctrl) and mice treated with 2 mg of Curcumin. **c.** MiR-21 levels in exosomes collected from serum of control mice and mice treated with 2 mg of Curcumin were determined by quantitative real time PCR analysis. Values are the mean \pm SD of 3 independent experiments * $p \leq 0.05$, ** $p \leq 0.01$ and *** $p \leq 0.005$.

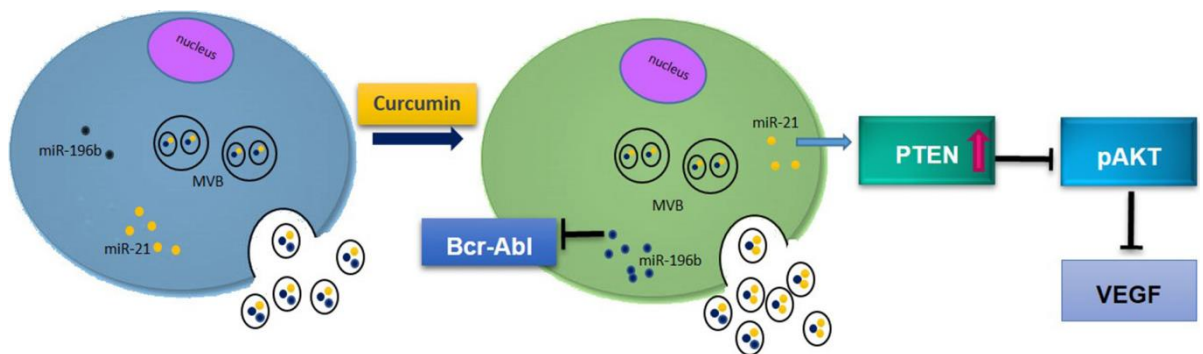


Figure 24: Working hypothesis of the effects of Curcumin on CML cells. Curcumin caused a decrease of cellular levels of miR-21 and a concomitant increase of its amount in exosomes. Reduced levels of miR-21 in CML cells induce PTEN expression and consequently a decrease of AKT phosphorylation and a downregulation of VEGF expression and release. Curcumin also induced the expression of miR-196b and consequently caused a reduction of Bcr-Abl expression.

5.3 Curcumin modulates chronic myelogenous leukemia exosomes composition and affects angiogenic phenotype, *via* exosomal miR-21

Cell lines	Curcumin treatment	Curcumin in exosome (ng/ μ g of exosomes)
K562	10 μ M	0.035 \pm 0.009
	20 μ M	0.175 \pm 0.031
	40 μ M	1.376 \pm 0.206
LAMA84	10 μ M	0.091 \pm 0.018
	20 μ M	0.239 \pm 0.024
	40 μ M	1.083 \pm 0.162

Table 1: Curcumin quantification in exosomes.

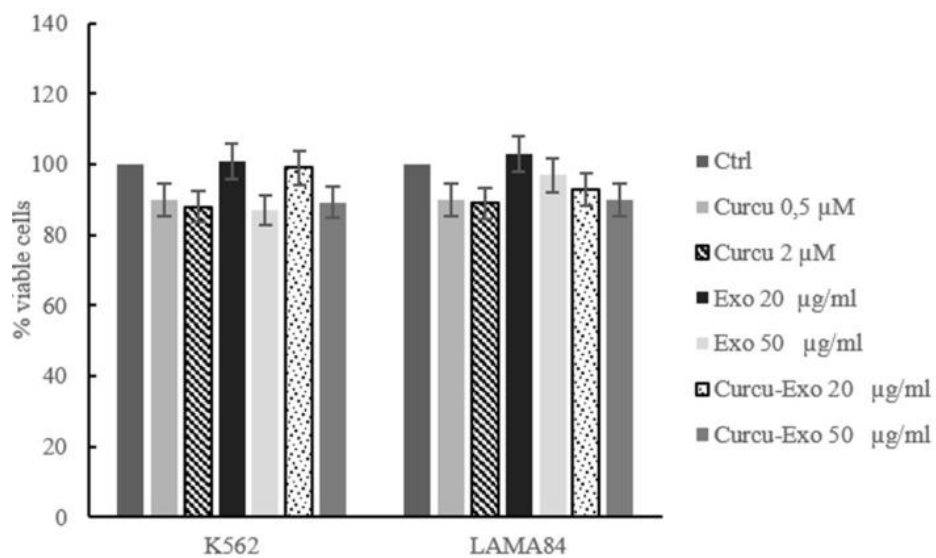


Figure 25: HUVECs cell viability was measured by MTT assay after treatment with Curcu-Exo (20–50 μ g/ml), Curcumin (0.5 and 2 μ M) was used as negative control. The values were plotted as a percentage of viable cells. Each point represents the mean \pm SD of three independent experiments.

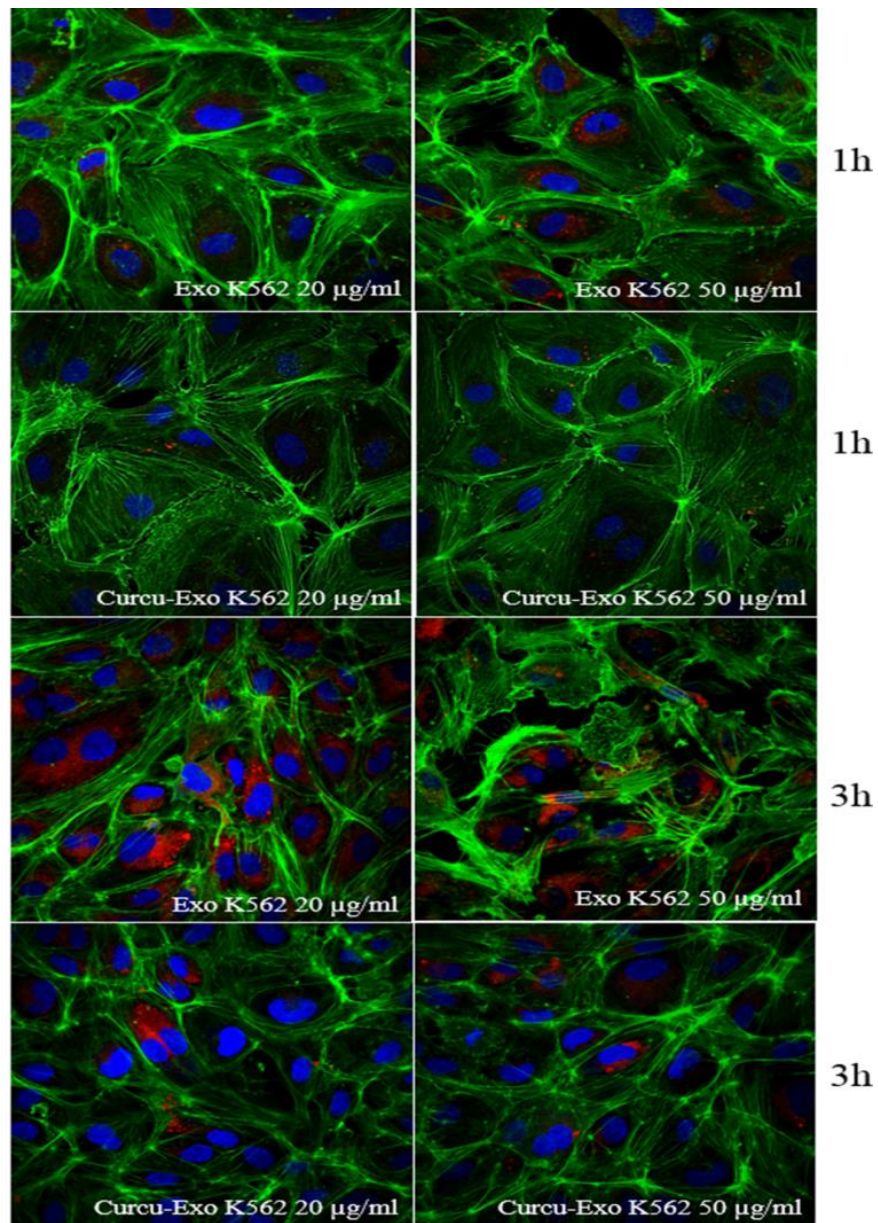


Figure 26: Uptake of Curcu-exosomes by HUVECs. Analysis at confocal microscopy of HUVECs treated, for 1 and 3 hours, with 20 µg/ml (Exo 20 µg/ml) and 50 µg/ml (Exo 50 µg/ml) of K562 exosomes, compared with HUVECs treated, for 1 and 3 hours, with 20 µg/ml (Curcu-Exo 20 µg/ml) and 50 µg/ml (Curcu-Exo 50 µg/ml) of exosomes released from K562 cells treated with 20 µM Curcumin. HUVECs were stained with ActinGreen (green), nuclear counterstaining was performed using Hoescht (blue); exosomes were labelled with PKH26 (red).

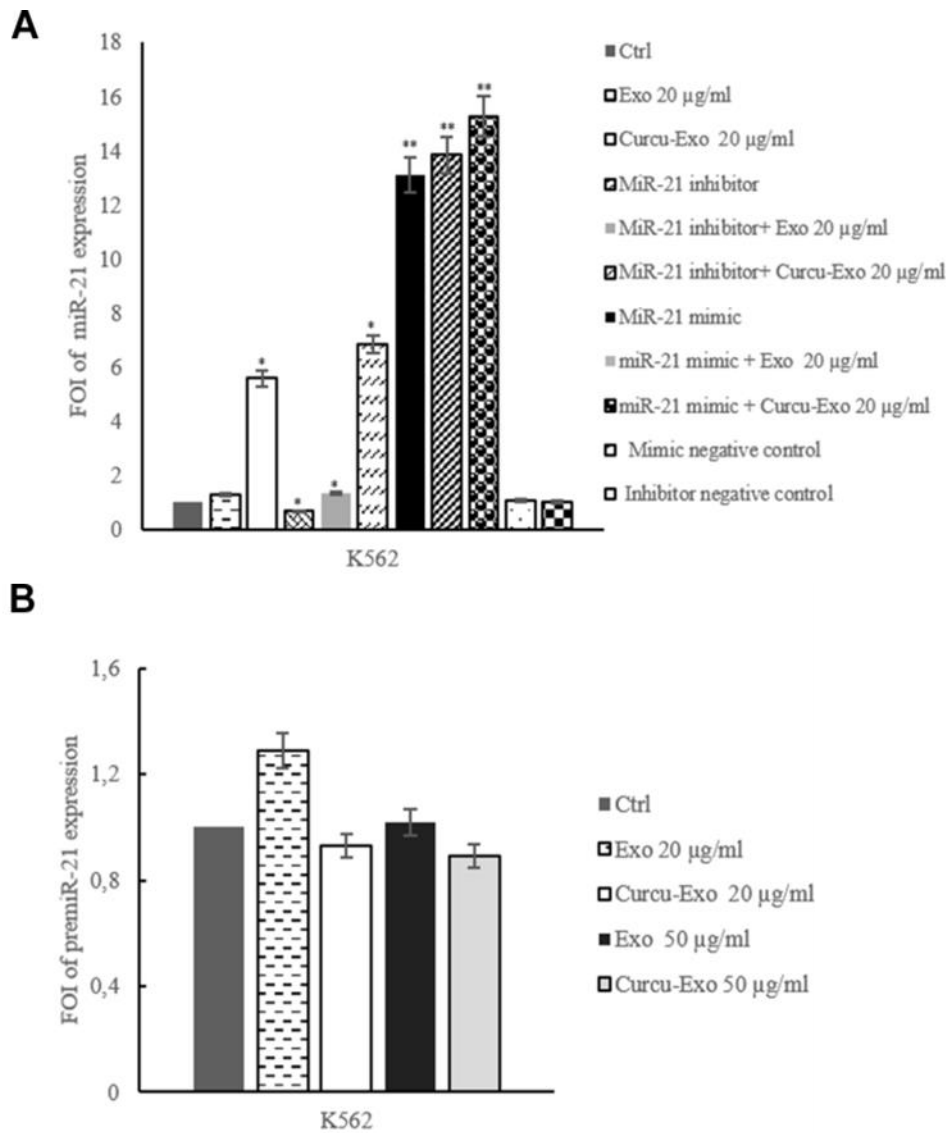


Figure 27: MiR-21 expression in HUVECs treated with exosomes released by K562 treated or not with Curcumin. a: miR-21 expression levels in HUVECs treated with 20 µg/ml of K562 Curcu-exosomes and control exosomes were determined by quantitative Real time PCR analysis. We also analyzed miR-21 expression in HUVECs treated with K562 Curcu-exosomes and control exosomes and/or transfected with miR-21 inhibitor or miR-21 mimic. Values (FOI: fold of induction) are the mean ± SD of 3 independent experiments * $p \leq 0.05$, ** $p \leq 0.01$. b: Pre-miR-21 expression in HUVECs treated with different amounts of K562 exosomes. Pre-miR-21 expression levels in HUVECs treated with 20 and 50 µg/ml of K562 exosomes were determined by quantitative Real time PCR analysis. We also analyzed pre-miR-21 expression in HUVECs treated with K562 Curcu-exosomes and control exosomes and/or transfected with miR-21 inhibitor or miR-21 mimic.

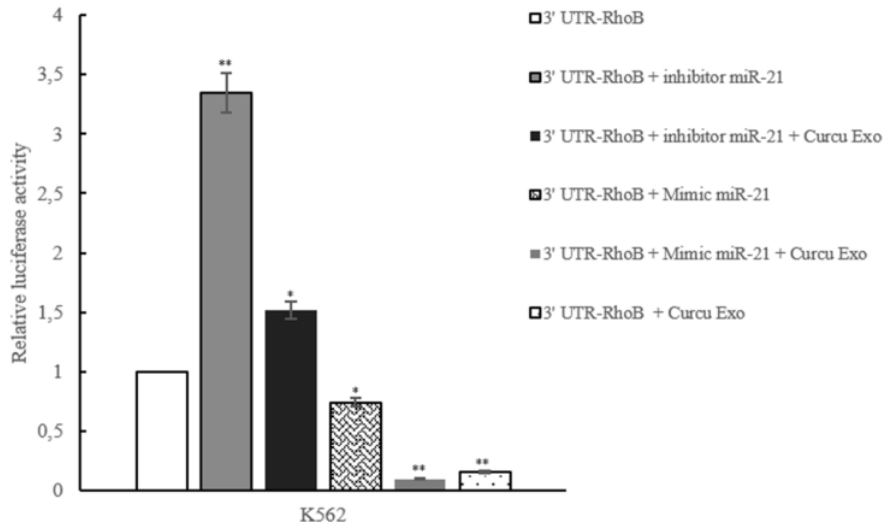


Figure 28: Luciferase activity of HUVECs transfected with reporter plasmid (RhoB-pEZ), treated with K562 Curcu-exosomes and control exosomes and/or cotransfected with miR-21 inhibitor or miR-21 mimic. *p 0.05; **p 0.01.

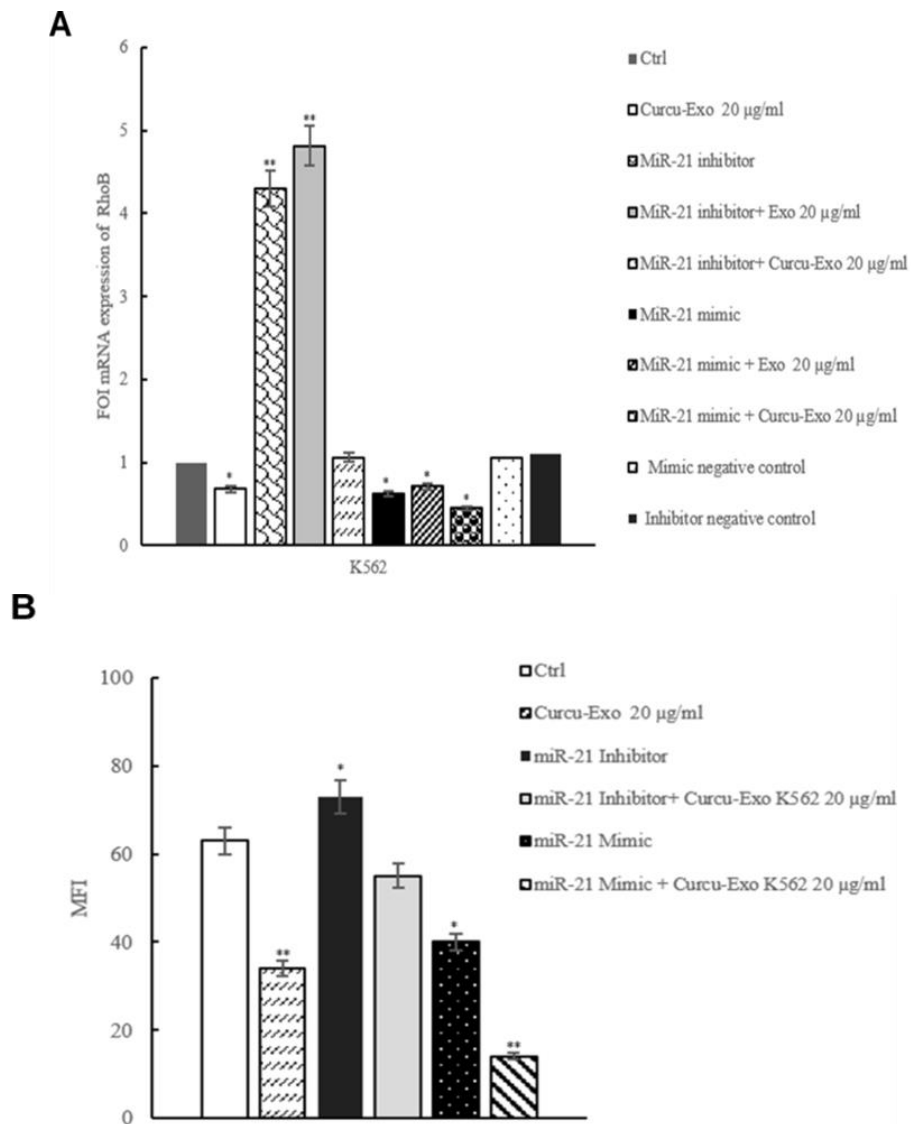


Figure 29: MiR-21, shuttled by exosomes, modulates RhoB expression in HUVECs. a: Real time PCR analysis showed that RhoB mRNA expression decreased in HUVECs treated with Curcu-exosomes compared to control exosomes. Expression of

RhoB was evaluated in HUVECs transfected with 2-Ome-miR-21 (miR-21 inhibitor) treated or not with 20 µg/ml of control exosomes (miR- 21 inhibitor + Exo 20 µg/ml) and Curcu-exosomes (miR-21 inhibitor + Curcu-Exo 20 µg/ml). Expression of RhoB was also evaluated in HUVECs transfected with miR-21 mimic (miR-21 mimic) treated or not with 20 µg/ml of control exosomes (miR-21 mimic + Exo 20 µg/ ml) and Curcu-exosomes (miR-21 mimic + Curcu-Exo 20 µg/ml). Values (FOI: fold of induction) are the mean ± SD of 3 independent experiments * $p \leq 0.05$, ** $p \leq 0.01$. **b:** Histogram shows the MFI (Mean Fluorescence Intensity) relative to the expression of RhoB in HUVECs after treatment with low serum medium (Control), 20 µg/ml of exosomes (Exo 20 µg/ml) and 20 µg/ml of Curcu-exosomes (Curcu-exo 20 µg/ml). Expression of RhoB was evaluated, with FACS analysis, in HUVECs transfected with 2-Ome-miR-21(miR-21 inhibitor) and treated with 20 µg/ml of control exosomes (miR-21 inhibitor + Exo 20 µg/ml) and Curcu-exosomes (miR-21 inhibitor + Curcu-Exo 20 µg/ml). Surface expression of VCAM1 was evaluated in HUVECs transfected with miR-21 mimic (miR-21 mimic) and treated with 20 µg/ml of control exosomes (miR-21 mimic + Exo 20 µg/ml) and 20 µg/ml of Curcu-exosomes (miR-21 mimic + Curcu-Exo 20 µg/ml). Values are the mean ± SD of 3 independent experiments * $p \leq 0.05$ ** $p \leq 0.01$.

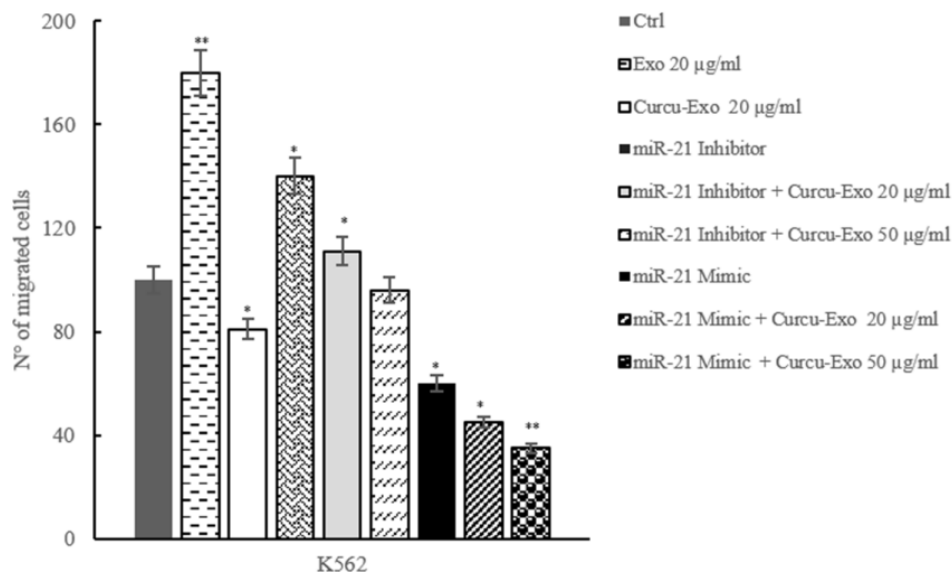


Figure 30: Curcu-exosomes inhibit HUVECs migration. Addition of control exosomes (20, 50 µg/ml) to the upper wells of the chamber induces dose-dependent increase of HUVEC migration, the addition of Curcu-exosomes reverts this effects. Values are the mean ± SD of 3 fields in three independent experiments * $p \leq 0.05$, ** $p \leq 0.01$. The ability of migrating of HUVECs transfected with 2-Ome-miR-21 (miR-21 inhibitor) treated or not with 20 µg/ml of control exosomes (miR-21 inhibitor + Exo 20 µg/ml) and with 20 µg/ml of Curcu-exosomes (miR-21 inhibitor + Curcu-Exo 20 µg/ml), was evaluated. The ability of migration of HUVECs transfected with miR-21 mimic (miR-21 mimic) treated or not with 20 µg/ml of control exosomes (miR-21 mimic + Exo 20 µg/ ml) and with 20 µg/ml of Curcu-exosomes (miR-21 mimic + Curcu-Exo 20 µg/ml) was also measured.

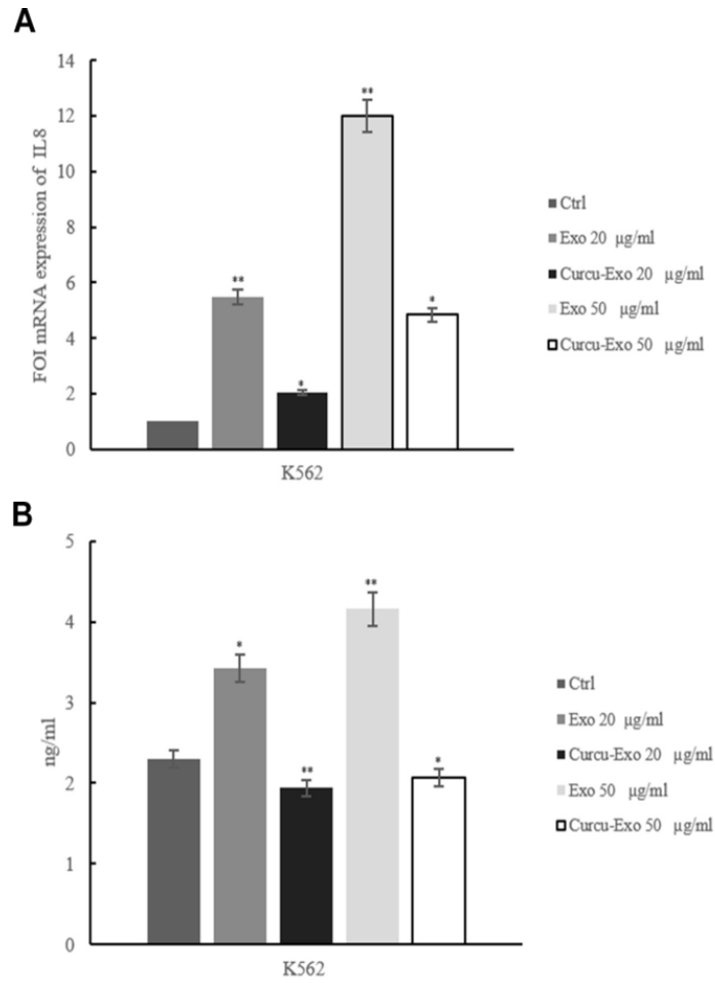


Figure 31: Treatment of HUVECs with Curcu-exosomes modulated IL8 expression. a: Real time PCR analysis showed that IL8 mRNA expression decreased in dose dependent manner in EC treated Curcu-exosomes compared to control exosomes. Values (FOI: fold of induction) are the mean \pm SD of 3 independent experiments * $p \leq 0.05$, ** $p \leq 0.01$. **b:** ELISA assay showed that IL8 protein expression decreased in EC treated with Curcu-exosomes respect to control exosomes, in a dose dependent manner.

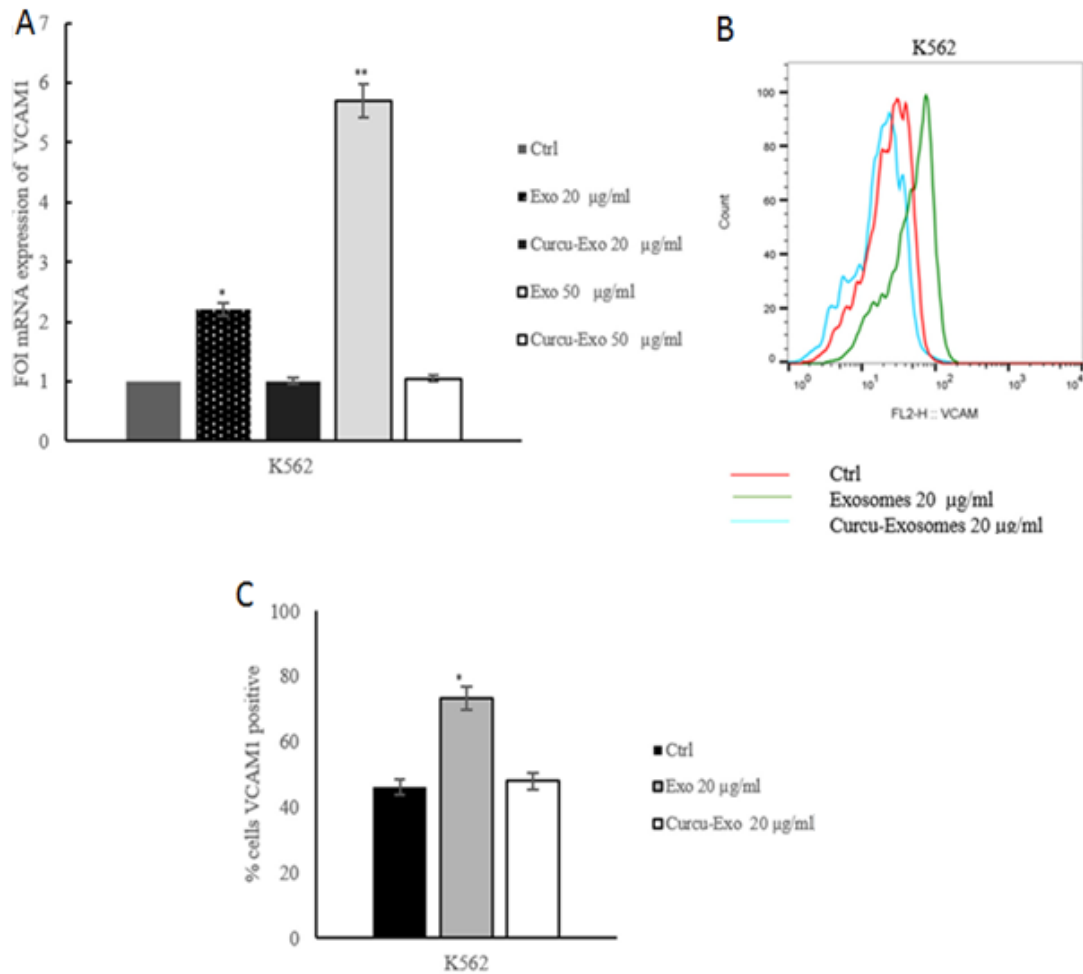


Figure 32: a: Real time PCR analysis showed that VCAM1 mRNA expression decreased in dose dependent manner in HUVECs treated with Curcu-exosomes compared to control exosomes. Values (FOI: fold of induction) are the mean \pm SD of 3 independent experiments $*p \leq 0.05$, $**p \leq 0.01$. b: FACS analysis showed that VCAM1 protein expression decreased in EC treated with Curcu-exosomes respect to control exosomes. c: Histogram shows the percentage of VCAM1 positive HUVECs after 6 hours of treatment with low serum medium (Ctrl), 20 $\mu\text{g/ml}$ of exosomes (Exo 20 $\mu\text{g/ml}$) and 20 $\mu\text{g/ml}$ of Curcu-exosomes (Curcu-exo 20 $\mu\text{g/ml}$). Values are the mean \pm SD of 3 fields in three independent experiments $*p \leq 0.05$, $**p \leq 0.01$.

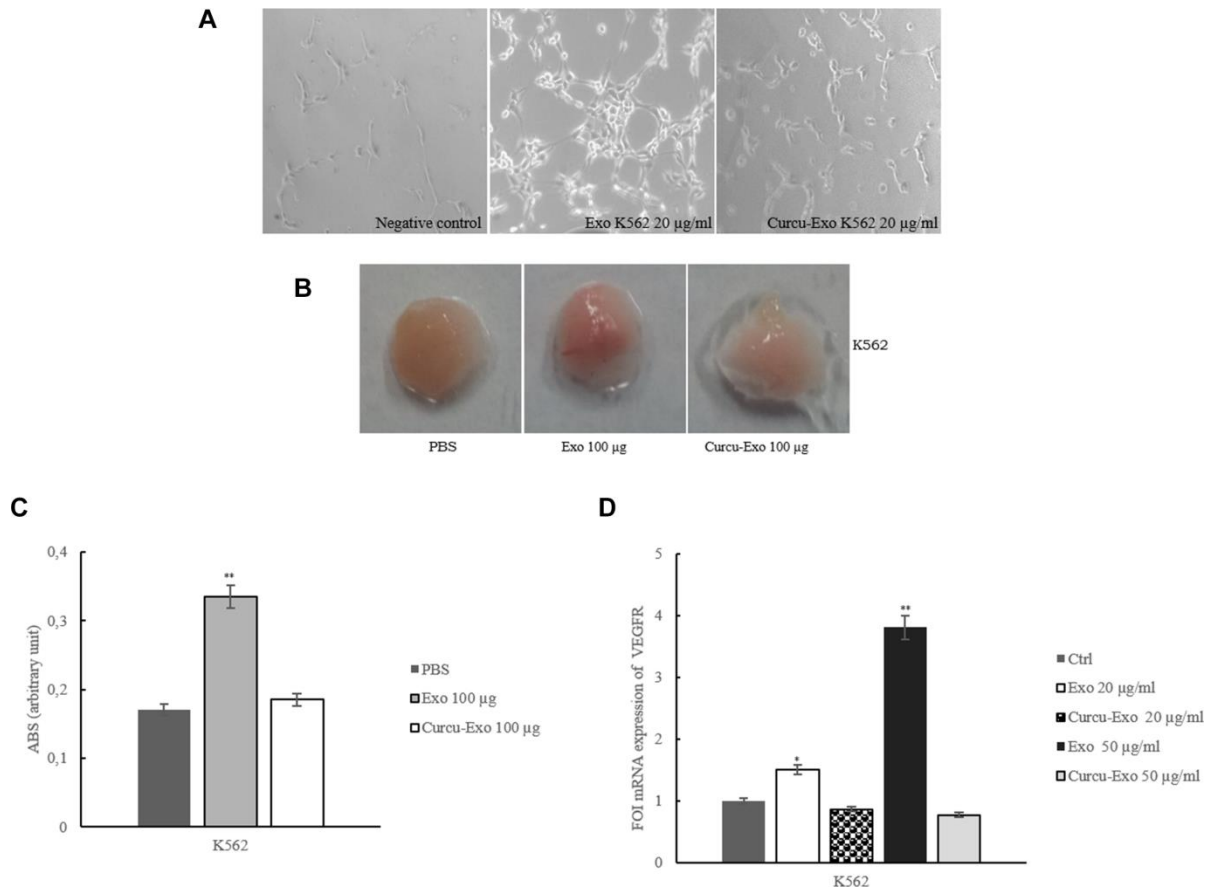


Figure 33: K562 exosomes stimulate *in vitro* and *in vivo* angiogenesis. a: Phase contrast micrographs showing that K562 control exosomes induce an endothelial network formation on Matrigel, K562 Curcu-exosomes revert this effect. No tube formation is observed when HUVECs are plated in low-serum medium (negative control). **b:** Matrigel plug containing K562 exosomes stimulate angiogenesis in mice (Exo 100 µg), this effect revert when K562 Curcu-exosomes (Curcu-Exo 100 µg) are used. PBS was used as a negative control. **c:** Haemoglobin concentration in the exosomes-containing Matrigel was evaluated with Dabkin's assay. **d:** Real time PCR analysis showed that VEGFR mRNA expression decreased in EC treated with Curcu-exosomes compared to control exosomes. Values (FOI: fold of induction) are the mean \pm SD of 3 independent experiments * $p \leq 0.05$, ** $p \leq 0.01$.

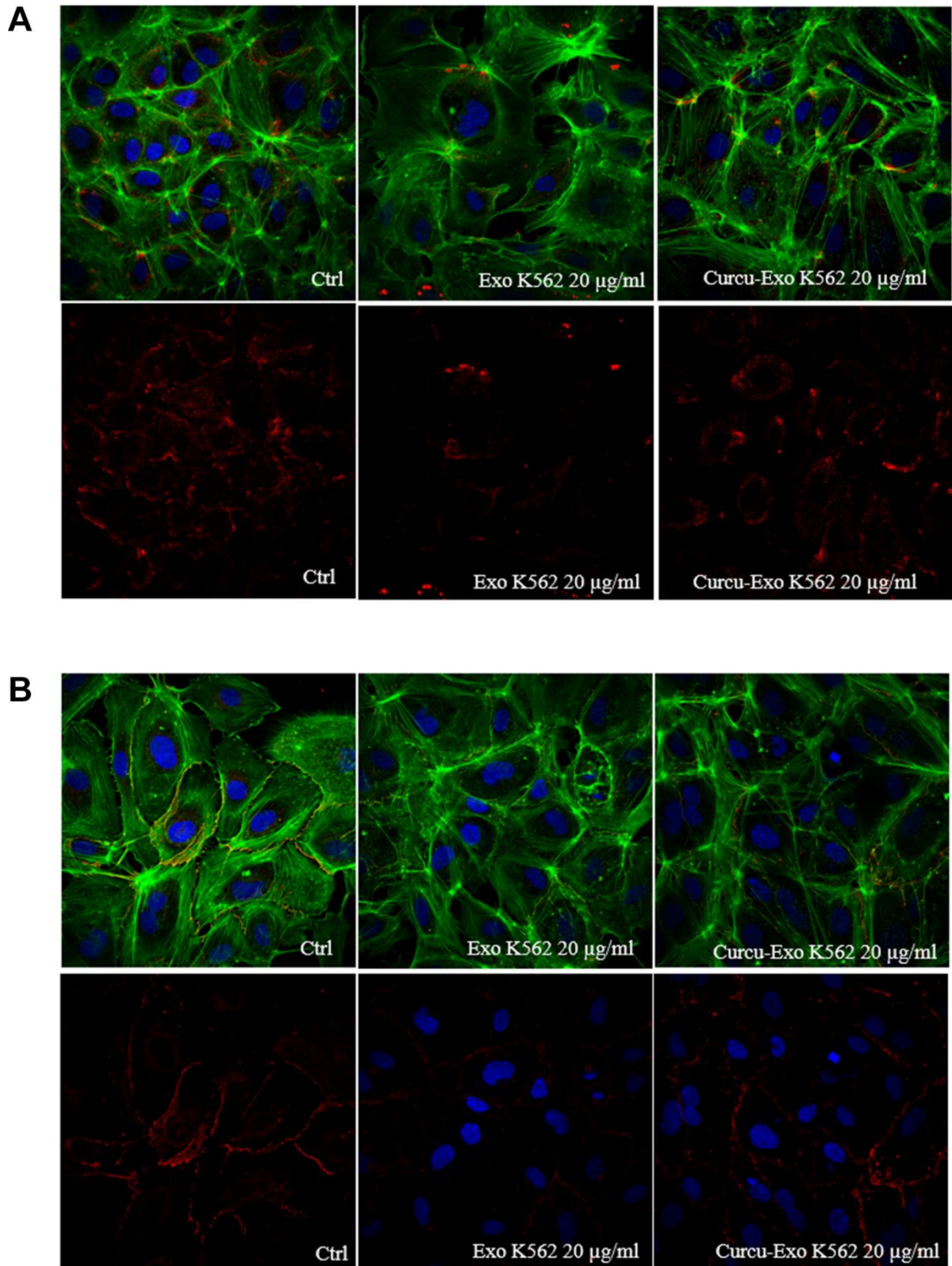


Figure 34: Alteration of HUVEC monolayer after addition of K562 exosomes. a: Analysis at confocal microscopy of ZO-1 localization in HUVECs treated with K562 exosomes (Exo K562 20 µg/ml) revealed a decrease of immunostaining compared to untreated cells (Ctrl). The treatment with K562 Curcu-exosomes (Curcu-Exo K562, 20 µg/ml) reverted this effect. **b:** Analysis at confocal microscopy of VE-Cadherin localization in HUVECs treated with K562 exosomes (Exo K562 20 µg/ml) revealed a decrease of immunostaining compared to untreated cells (Ctrl). The treatment with K562 Curcu-exosomes reverted this effect (Curcu-Exo K562 20 µg/ml).

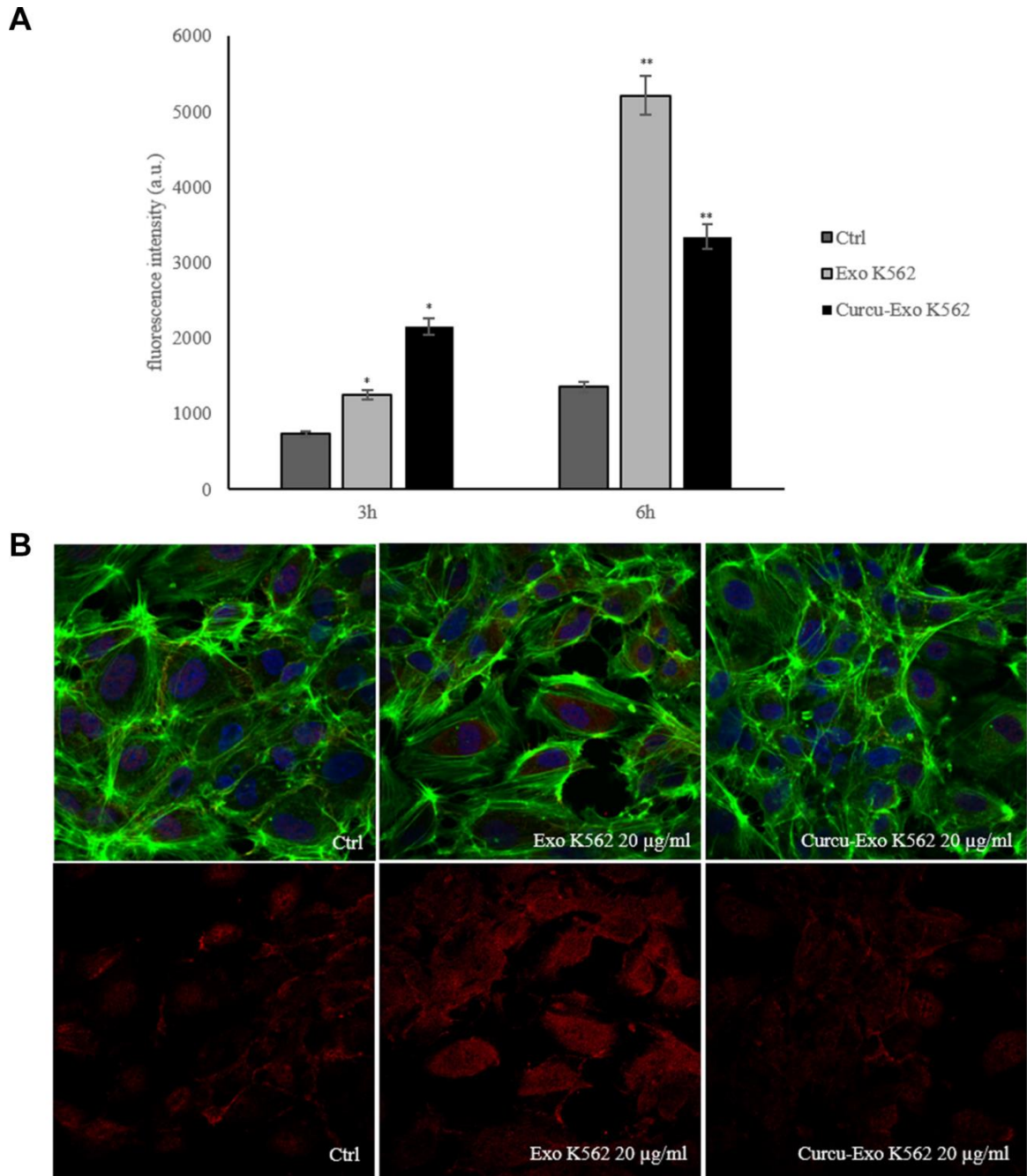


Figure 35: Vascular permeability is modulated by K562 control and Curcu-exosomes. **a:** The permeability of HUVEC monolayer increased after treatment, for 3 and 6 hours, with K562 control exosomes (Exo K562) compared to untreated HUVEC monolayer (Ctrl), the treatment with Curcu-exosomes (Curcu-Exo K562), protected the endothelial monolayer. **b:** Upper panel: Analysis at confocal microscopy of endothelial monolayer. The integrity of the monolayer was altered, after treatment with K562 control exosomes (Exo K562 20 µg/ml); the treatment of Curcu-exosomes alleviated the alteration of the EC monolayer (Exo K562 20 µg/ml). Lower panel: Analysis at confocal microscopy of RhoB expression in HUVECs treated with K562 Curcu-exosomes and control exosomes. K562 control exosomes (Exo K562 20 µg/ml) induce an increase of immunostaining for RhoB compared to untreated cells (Ctrl). The treatment with K562 Curcu-exosomes (Curcu-Exo K562, 20 µg/ml) reverted this effect.

Table 2 - Angiogenesis- and migration-related proteins

AC ^a	Protein name (Gene name)	Curcu-Exo vs Control Exo ^b		Description	References
		Fold Change	p-Value		
P49006	MARCKS-related protein (MARCKSL1)	-10.6	0.000590	Regulates of actin assembly dynamics during migration in multiple types of cells. Regulation of migration in multiple cell types; its dysregulation is associated with metastasis and is an indicator of poor prognosis. Increase of cell motility in many cell types (fibroblasts, glial cells, macrophages, neutrophils, skeletal myoblasts, endothelial cells and VSMCs) through several molecular mechanisms: protein kinase B pathway, direct binding to actin, control of PIP2 availability at the plasma membrane and regulation of the small GTPases, Rac1 and Cdc42. Key mediator of the H ₂ O ₂ -induced permeability change in bovine aortic endothelial cells.	137–139
P13164	Interferon-induced transmembrane protein 1 (IFITM1)	-7.2	0.000022	Promotion of cancer progression by enhancing cell migration and invasion in gastric cancer and head and neck cancer. Its knockdown inhibits migration and invasion by decreasing expression and activity of MMP9, in glioma cells. Key Role in the formation of functional blood vessels; stabilization of EC-EC interactions during endothelial lumen formation by regulating tight junction assembly.	140–143
O43707	Alpha-actinin-4 (ACTN4)	-3.2	0.004910	Enhancement of cancer cell motility, invasion, and metastasis; concentration at the leading edge of migrating cells.	137
H0YDJ9	Tetraspanin (CD81)	-3.1	0.012240	Components of the endothelial lateral junctions implicated in the regulation of cell motility. Involvement in cell migration of tumor and immune cells. Its association with the small GTPase Rac limits the GTPase activation within the plasma membrane so contributing to regulation of Rac activity turnover.	144,145
J3KPF3	4F2 cell-surface antigen heavy chain (SLC3A2)	-2.9	0.032730	Regulation of tumour cell migration, proliferation, spreading and survival in vitro. Transport of L-arginine, required for NO synthesis in HUVECs, in association with SLC7A6 or SLC7A7.	146,147
P35613	Basigin (BSG)	-2.6	0.000042	Regulation of expression of vascular endothelial growth factor (VEGF) and MMPs in stromal cells; stimulation of the production of MMPs in human umbilical vein endothelial cells (HUVECs) and of VEGF expression in tumor compartment. Involvement in angiogenesis through different ways such as the modulation of VEGF isoforms secretion.	148–150
P63244	Guanine nucleotide- binding protein subunit beta-2-like 1 (GNB2L1)	-2.5	0.006900	Massive up-regulation in vascular endothelial cells during angiogenesis <i>in vitro</i> and <i>in vivo</i> and in human carcinoma cells. Involvement in Gbg-mediated adherens junction assembly in endothelial cells. Regulation of VEGF-Flt1-dependent cell migration of endothelial cells and macrophages through direct interaction with Flt1 and activation of PI3K/Ak-Rac1.	151–155
P02792	Ferritin light chain (FTL)	-2.1	0.020850	Binding to a 22-aa subdomain of Hka, so antagonizing antiangiogenic effects of this last and enhancing the migration, assembly and survival of Hka-treated endothelial cells.	156
P08238	Heat shock protein HSP 90-beta (HSP90AB1)	-1.7	0.036260	Exposure of endothelial cells to VEGF triggers the association of HSP90 with VEGFR2, that drives the phosphorylation of FAK on Tyr407 in a RhoA-ROCK-dependent manner, and recruitment of paxillin and vinculin to FAK so leading to the assembly of focal adhesions and endothelial cell migration.	157
O00299	Chloride intracellular channel protein 1 (CLIC1)	-1.6	0.006680	Strong expression in endothelial cells; important in multiple steps of <i>in vitro</i> angiogenesis and in regulation of cell surface expression of various integrins acting in angiogenesis. Mediation of endothelial cell growth, branching morphogenesis and migration, possibly via regulation of integrin expression.	158
P08567	Pleckstrin (PLEK)	4.2	0.044860	Its overexpression in COS-1 cells leads to a reorganization of the actin cytoskeleton partially dependent on Rac1 but independent of PI3K and Cdc42. Stabilization of apical junctional adhesion complexes (AJCs), that were composed of adherens junctions and tight junctions and are involved in cell-to-cell adhesion, by bridging transmembrane cadherins to the intracellular microtubule network of proteins.	135,159
E9PPJ5	Midkine (MDK)	3.5	0.000280	Abrogation of the VEGF-A-induced proliferation of human microvascular endothelial cells <i>in vitro</i> through the downregulation of proangiogenic cytokines and through the upregulation of antiangiogenic factors. Downregulation of VEGF-A-induced neovascularization and vascular permeability <i>in vivo</i> .	136

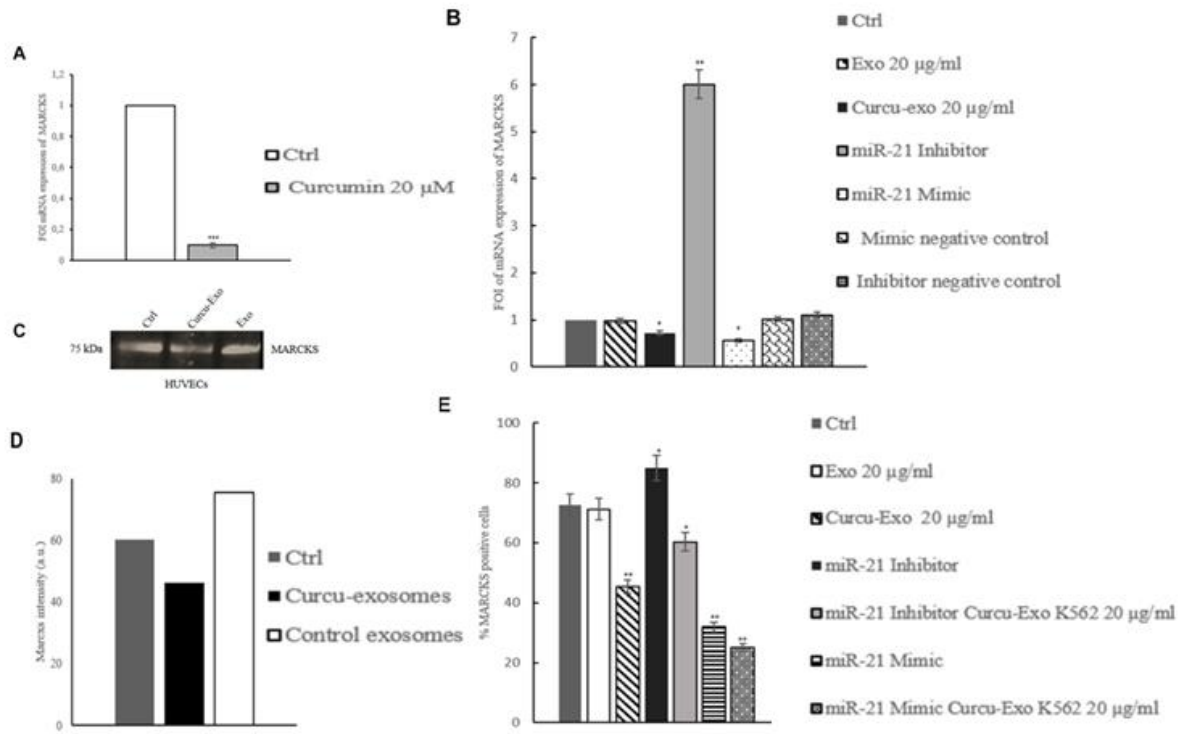


Figure 36: Curcumin modulates MARCKS expression in K562 cells and HUVECs. **a:** Real time PCR analysis showed that in K562 cells MARCKS mRNA expression decreases after treatment with Curcumin respect to untreated cells. Real time PCR analysis showed that MARCKS mRNA expression decreased in HUVECs treated with Curcu-exosomes respect to control exosomes. **b:** Expression of MARCKS was evaluated in HUVECs transfected with 2-Ome-miR-21 (miR-21 inhibitor) treated or not with 20 $\mu\text{g/ml}$ of control (miR- 21 inhibitor + Exo 20 $\mu\text{g/ml}$) and Curcu-exosomes (miR-21 inhibitor + Curcu-Exo 20 $\mu\text{g/ml}$). Expression of MARCKS was also evaluated in HUVECs transfected with miR-21 mimic (miR-21 mimic) treated or not with 20 $\mu\text{g/ml}$ of control exosomes (miR-21 mimic + Exo 20 $\mu\text{g/ml}$) and Curcu-exosomes (miR-21 mimic + Curcu-Exo 20 $\mu\text{g/ml}$). Values (FOI: fold of induction) are the mean \pm SD of 3 independent experiments * $p \leq 0.05$, ** $p \leq 0.01$. **c:** Western blotting analyses of MARCKS in HUVECs treated with Curcu-exosomes and control exosomes. **d:** Densitometric analysis of Western blotting against MARCKS. **e:** Facs analysis of MARCKS expression.

Bibliography:

1. ROWLEY, J. D. A New Consistent Chromosomal Abnormality in Chronic Myelogenous Leukaemia identified by Quinacrine Fluorescence and Giemsa Staining. *Nature* **243**, 290–293 (1973).
2. Tabarestani, S. & Movafagh, A. New developments in chronic myeloid leukemia: Implications for therapy. *Iranian Journal of Cancer Prevention* **9**, 1–8 (2016).
3. Advani, A. S. & Pendergast, A. M. Bcr-Abl variants: Biological and clinical aspects. *Leukemia Research* **26**, 713–720 (2002).
4. Skorski, T. *et al.* Transformation of hematopoietic cells by BCR/ABL requires activation of a PI-3k/Akt-dependent pathway. *EMBO J.* **16**, 6151–6161 (1997).
5. Massimino, M. *et al.* IRF5 is a target of BCR-ABL kinase activity and reduces CML cell proliferation. *Carcinogenesis* **35**, 1132–1143 (2014).
6. Ahmed, W. & Van Etten, R. A. Alternative approaches to eradicating the malignant clone in chronic myeloid leukemia: tyrosine-kinase inhibitor combinations and beyond. *Hematology / the Education Program of the American Society of Hematology. American Society of Hematology. Education Program* **2013**, 189–200 (2013).
7. Steelman, L. S. *et al.* JAK/STAT, Raf/MEK/ERK, PI3K/Akt and BCR-ABL in cell cycle progression and leukemogenesis. *Leukemia* **18**, 189–218 (2004).
8. Oyekunle, A. *et al.* Challenges for allogeneic hematopoietic stem cell transplantation in chronic myeloid Leukemia in the era of tyrosine kinase inhibitors. *Acta Haematologica* **126**, 30–39 (2011).
9. Mahon, F. X. *et al.* Selection and characterization of BCR-ABL positive cell lines with differential sensitivity to the tyrosine kinase inhibitor STI571: diverse mechanisms of resistance. *Blood* **96**, 1070–9 (2000).
10. Ernst, T. & Hochhaus, A. Chronic myeloid leukemia: clinical impact of BCR-ABL1 mutations and other lesions associated with disease progression. *Semin Oncol* **39**, 58–66 (2012).
11. Tiribelli, M. *et al.* Impact of BCR-ABL mutations on response to dasatinib after imatinib failure in elderly patients with chronic-phase chronic myeloid leukemia. *Ann. Hematol.* **92**, 179–183 (2013).
12. Clark, B. R. & Keating, A. Biology of bone marrow stroma. in *Annals of the New York Academy of Sciences* **770**, 70–78 (1995).
13. Marastoni, S., Ligresti, G., Lorenzon, E., Colombatti, A. & Mongiat, M. Extracellular matrix: a matter of life and death. *Connect. Tissue Res.* **49**, 203–206 (2008).
14. Al-Khaldi, a *et al.* Postnatal bone marrow stromal cells elicit a potent VEGF-dependent neoangiogenic response in vivo. *Gene Ther.* **10**, 621–629 (2003).
15. Reyes, M. *et al.* Purification and ex vivo expansion of postnatal human marrow

mesodermal progenitor cells. *Blood* **98**, 2615–2625 (2001).

16. Hu, M. & Polyak, K. Molecular characterisation of the tumour microenvironment in breast cancer. *Eur. J. Cancer* **44**, 2760–2765 (2008).
17. Sharma, M., Afrin, F., Satija, N., Tripathi, R. P. & Gangenahalli, G. U. Stromal-derived factor-1/CXCR4 signaling: indispensable role in homing and engraftment of hematopoietic stem cells in bone marrow. *Stem Cells Dev.* **20**, 933–46 (2011).
18. Jin, L. *et al.* CXCR4 up-regulation by imatinib induces chronic myelogenous leukemia (CML) cell migration to bone marrow stroma and promotes survival of quiescent CML cells. *Mol. Cancer Ther.* **7**, 48–58 (2008).
19. Geay, J. F. *et al.* p210BCR-ABL inhibits SDF-1 chemotactic response via alteration of CXCR4 signaling and down-regulation of CXCR4 expression. *Cancer Res.* **65**, 2676–2683 (2005).
20. Waugh, D. J. J. & Wilson, C. The interleukin-8 pathway in cancer. *Clinical Cancer Research* **14**, 6735–6741 (2008).
21. Singh, R. K., Gutman, M., Radinsky, R., Bucana, C. D. & Fidler, I. J. Expression of interleukin 8 correlates with the metastatic potential of human melanoma cells in nude mice. *Cancer Res* **54**, 3242–3247 (1994).
22. Nyberg, P., Salo, T. & Kalluri, R. Tumor microenvironment and angiogenesis. *Front. Biosci.* **13**, 6537–6553 (2008).
23. Mazo, I. B. *et al.* Hematopoietic progenitor cell rolling in bone marrow microvessels: parallel contributions by endothelial selectins and vascular cell adhesion molecule 1. *J. Exp. Med.* **188**, 465–74 (1998).
24. Hwang, I. Cell-cell communication via extracellular membrane vesicles and its role in the immune response. *Molecules and Cells* **36**, 105–111 (2013).
25. Corrado, C. *et al.* Exosomes as intercellular signaling organelles involved in health and disease: Basic science and clinical applications. *International Journal of Molecular Sciences* **14**, 5338–5366 (2013).
26. They, C. *et al.* Proteomic analysis of dendritic cell-derived exosomes: A secreted subcellular compartment distinct from apoptotic vesicles. *J. Immunol.* **166**, 7309–7318 (2001).
27. Subra, C. *et al.* Exosomes account for vesicle-mediated transcellular transport of activatable phospholipases and prostaglandins. *J. Lipid Res.* **51**, 2105–20 (2010).
28. Headland, S. E., Jones, H. R., D'Sa, A. S. V, Perretti, M. & Norling, L. V. Cutting-edge analysis of extracellular microparticles using ImageStream(X) imaging flow cytometry. *Sci. Rep.* **4**, 5237 (2014).
29. Mueller, M. M. & Fusenig, N. E. Friends or foes - bipolar effects of the tumour stroma in cancer. *Nat. Rev. Cancer* **4**, 839–49 (2004).
30. Peinado, H. *et al.* Melanoma exosomes educate bone marrow progenitor cells toward

- a pro-metastatic phenotype through MET. *Nat. Med.* **18**, 883–891 (2013).
31. Costa-Silva, B. *et al.* Pancreatic cancer exosomes initiate pre-metastatic niche formation in the liver. *Nat Cell Biol* **17**, 816–826 (2015).
 32. Lin, J. *et al.* Exosomes: Novel Biomarkers for Clinical Diagnosis. *Sci. World J.* **2015**, 1–8 (2015).
 33. Cocucci, E. & Meldolesi, J. Ectosomes and exosomes: Shedding the confusion between extracellular vesicles. *Trends in Cell Biology* **25**, 364–372 (2015).
 34. Urbanelli, L. *et al.* Signaling pathways in exosomes biogenesis, secretion and fate. *Genes* **4**, 152–170 (2013).
 35. Kowal, J., Tkach, M. & Théry, C. Biogenesis and secretion of exosomes. *Curr. Opin. Cell Biol.* **29**, 116–125 (2014).
 36. Henne, W. M., Buchkovich, N. J. & Emr, S. D. The ESCRT Pathway. *Developmental Cell* **21**, 77–91 (2011).
 37. Trajkovic, K. *et al.* Ceramide triggers budding of exosome vesicles into multivesicular endosomes. *Science* **319**, 1244–1247 (2008).
 38. Mathivanan, S., Fahner, C. J., Reid, G. E. & Simpson, R. J. ExoCarta 2012: database of exosomal proteins, RNA and lipids. *Nucleic Acids Res.* **40**, D1241-4 (2012).
 39. Kalra, H. *et al.* Vesiclepedia: A Compendium for Extracellular Vesicles with Continuous Community Annotation. *PLoS Biol.* **10**, (2012).
 40. Gajos-Michniewicz, A., Duechler, M. & Czyz, M. MiRNA in melanoma-derived exosomes. *Cancer Letters* **347**, 29–37 (2014).
 41. Huang, X. *et al.* Exosomal miR-1290 and miR-375 as prognostic markers in castration-resistant prostate cancer. *Eur. Urol.* **67**, 33–41 (2015).
 42. Kole, R., Krainer, A. R. & Altman, S. RNA therapeutics: beyond RNA interference and antisense oligonucleotides. *Nat. Rev. Drug Discov.* **11**, 125–140 (2012).
 43. Record, M., Carayon, K., Poirot, M. & Silvente-Poirot, S. Exosomes as new vesicular lipid transporters involved in cell-cell communication and various pathophysiologicals. *Biochimica et Biophysica Acta - Molecular and Cell Biology of Lipids* **1841**, 108–120 (2014).
 44. Rolfo, C. *et al.* Liquid biopsies in lung cancer: the new ambrosia of researchers. *Biochim. Biophys. Acta* **1846**, 539–46 (2014).
 45. Feng, D. *et al.* Cellular internalization of exosomes occurs through phagocytosis. *Traffic* **11**, 675–687 (2010).
 46. Krebs, M. G. *et al.* Evaluation and prognostic significance of circulating tumor cells in patients with non-small-cell lung cancer. *J. Clin. Oncol.* **29**, 1556–63 (2011).
 47. Verstovsek, S. *et al.* Prognostic significance of cellular vascular endothelial growth

- factor expression in chronic phase chronic myeloid leukemia. *Blood* **99**, 2265–2267 (2002).
48. Fontana, S., Saieva, L., Taverna, S. & Alessandro, R. Contribution of proteomics to understanding the role of tumor-derived exosomes in cancer progression: State of the art and new perspectives. *Proteomics* **13**, 1581–1594 (2013).
 49. Valadi, H. *et al.* Exosome-mediated transfer of mRNAs and microRNAs is a novel mechanism of genetic exchange between cells. *Nat. Cell Biol.* **9**, 654–659 (2007).
 50. Eldh, M. *et al.* Exosomes Communicate Protective Messages during Oxidative Stress; Possible Role of Exosomal Shuttle RNA. *PLoS One* **5**, 1–8 (2010).
 51. Zocco, D., Ferruzzi, P., Cappello, F., Kuo, W. P. & Fais, S. Extracellular vesicles as shuttles of tumor biomarkers and anti-tumor drugs. *Front. Oncol.* **4**, 267 (2014).
 52. Santonocito, M. *et al.* Molecular characterization of exosomes and their microRNA cargo in human follicular fluid: Bioinformatic analysis reveals that exosomal microRNAs control pathways involved in follicular maturation. *Fertil. Steril.* **102**, 1751–1761 (2014).
 53. Zhang, J. *et al.* Exosome and exosomal microRNA: Trafficking, sorting, and function. *Genomics, Proteomics and Bioinformatics* **13**, 17–24 (2015).
 54. Corrado, C. *et al.* Exosome-mediated crosstalk between chronic myelogenous leukemia cells and human bone marrow stromal cells triggers an Interleukin 8-dependent survival of leukemia cells. *Cancer Lett.* **348**, 71–76 (2014).
 55. Safaei, R. *et al.* Abnormal lysosomal trafficking and enhanced exosomal export of cisplatin in drug-resistant human ovarian carcinoma cells. *Mol. Cancer Ther.* **4**, 1595–1604 (2005).
 56. Fujita, Y., Kuwano, K., Ochiya, T. & Takeshita, F. The Impact of Extracellular Vesicle-Encapsulated Circulating MicroRNAs in Lung Cancer Research. *BioMed Research International* **2014**, (2014).
 57. Ramakrishna, R. & Rostomily, R. Seed, soil, and beyond: The basic biology of brain metastasis. *Surg. Neurol. Int.* **4**, S256-64 (2013).
 58. Kahlert, C. & Kalluri, R. Exosomes in tumor microenvironment influence cancer progression and metastasis. *Journal of Molecular Medicine* **91**, 431–437 (2013).
 59. Azmi, A. S., Bao, B. & Sarkar, F. H. Exosomes in cancer development, metastasis, and drug resistance: A comprehensive review. *Cancer and Metastasis Reviews* **32**, 623–642 (2013).
 60. Vader, P., Breakefield, X. O. & Wood, M. J. A. Extracellular vesicles: Emerging targets for cancer therapy. *Trends in Molecular Medicine* **20**, 385–393 (2014).
 61. Ravindran, J., Prasad, S. & Aggarwal, B. B. Curcumin and cancer cells: how many ways can curry kill tumor cells selectively? *AAPS J.* **11**, 495–510 (2009).
 62. Anand, P., Sundaram, C., Jhurani, S., Kunnumakkara, A. B. & Aggarwal, B. B. Curcumin

- and cancer: An 'old-age' disease with an 'age-old' solution. *Cancer Lett.* **267**, 133–164 (2008).
63. Aggarwal, B. B., Sethi, G., Baladandayuthapani, V., Krishnan, S. & Shishodia, S. Targeting cell signaling pathways for drug discovery: An old lock needs a new key. *Journal of Cellular Biochemistry* **102**, 580–592 (2007).
 64. Yang, C. L. *et al.* Curcumin blocks small cell lung cancer cells migration, invasion, angiogenesis, cell cycle and neoplasia through janus kinase-STAT3 signalling pathway. *PLoS One* **7**, (2012).
 65. Howell, J. C. *et al.* Global microRNA expression profiling: curcumin (diferuloylmethane) alters oxidative stress-responsive microRNAs in human ARPE-19 cells. *Mol. Vis.* **19**, 544–60 (2013).
 66. Mudduluru, G. *et al.* Curcumin regulates miR-21 expression and inhibits invasion and metastasis in colorectal cancer. *Biosci. Rep.* **31**, 185–197 (2011).
 67. Roy, S., Yu, Y., Padhye, S. B., Sarkar, F. H. & Majumdar, A. P. N. Difluorinated-Curcumin (CDF) Restores PTEN Expression in Colon Cancer Cells by Down-Regulating miR-21. *PLoS One* **8**, (2013).
 68. Taverna, S. *et al.* Exosomal shuttling of miR-126 in endothelial cells modulates adhesive and migratory abilities of chronic myelogenous leukemia cells. *Mol. Cancer* **13**, 169 (2014).
 69. Taverna, S. *et al.* Curcumin inhibits in vitro and in vivo chronic myelogenous leukemia cells growth: a possible role for exosomal disposal of miR-21. *Oncotarget* **26**, 21918-33. (2015).
 70. Taverna, S. *et al.* Curcumin modulates chronic myelogenous leukemia exosomes composition and affects angiogenic phenotype, via exosomal miR-21. *Oncotarget* **21**, 30420-39. (2016).
 71. Corrado, C. *et al.* Carboxyamidotriazole-ototate inhibits the growth of imatinib-resistant chronic myeloid leukaemia cells and modulates exosomes-stimulated angiogenesis. *PLoS One* **7**, (2012).
 72. Taverna, S. *et al.* Role of exosomes released by chronic myelogenous leukemia cells in angiogenesis. *Int. J. Cancer* **130**, 2033–2043 (2012).
 73. Umezu, T., Ohyashiki, K., Kuroda, M. & Ohyashiki, J. Leukemia cell to endothelial cell communication via exosomal miRNAs. *Oncogene* **32**, 2747–2755 (2012).
 74. Tadokoro, H., Umezu, T., Ohyashiki, K., Hirano, T. & Ohyashiki, J. H. Exosomes derived from hypoxic leukemia cells enhance tube formation in endothelial cells. *J. Biol. Chem.* **288**, 34343–34351 (2013).
 75. Fish, J. E. *et al.* miR-126 Regulates Angiogenic Signaling and Vascular Integrity. *Dev. Cell* **15**, 272–284 (2008).
 76. Harris, T. A., Yamakuchi, M., Ferlito, M., Mendell, J. T. & Lowenstein, C. J. MicroRNA-

- 126 regulates endothelial expression of vascular cell adhesion molecule 1. *Proc. Natl. Acad. Sci. U. S. A.* **105**, 1516–21 (2008).
77. Sanz-Rodríguez, F., Hidalgo, A. & Teixidó, J. Chemokine stromal cell-derived factor-1 α modulates VLA-4 integrin-mediated multiple myeloma cell adhesion to CS-1/fibronectin and VCAM-1. *Blood* **97**, 346–351 (2001).
 78. Gao, S. *et al.* Pure curcumin decreases the expression of WT1 by upregulation of miR-15a and miR-16-1 in leukemic cells. *J. Exp. Clin. Cancer Res.* **31**, 27 (2012).
 79. Teiten, M. H., Dicato, M. & Diederich, M. Curcumin as a regulator of epigenetic events. *Molecular Nutrition and Food Research* **57**, 1619–1629 (2013).
 80. Vallianou, N. G., Evangelopoulos, A., Schizas, N. & Kazazis, C. Potential anticancer properties and mechanisms of action of curcumin. *Anticancer Research* **35**, 645–651 (2015).
 81. Gandhi, S. U., Kim, K., Larsen, L., Rosengren, R. J. & Safe, S. Curcumin and synthetic analogs induce reactive oxygen species and decreases specificity protein (Sp) transcription factors by targeting microRNAs. *BMC Cancer* **12**, 564 (2012).
 82. Meng, F. *et al.* MicroRNA-21 Regulates Expression of the PTEN Tumor Suppressor Gene in Human Hepatocellular Cancer. *Gastroenterology* **133**, 647–658 (2007).
 83. Song, M. S., Salmena, L. & Pandolfi, P. P. The functions and regulation of the PTEN tumour suppressor. *Nat Rev Mol Cell Biol* **13**, 283–296 (2012).
 84. Shafee, N., Kaluz, S., Ru, N. & Stanbridge, E. J. PI3K/Akt activity has variable cell-specific effects on expression of HIF target genes, CA9 and VEGF, in human cancer cell lines. *Cancer Lett.* **282**, 109–115 (2009).
 85. Zhiyong, C., Wentong, L., Xiaoyang, Y. & Ling, P. PTEN's regulation of VEGF and VEGFR1 expression and its clinical significance in myeloid leukemia. *Med. Oncol.* **29**, 1084–1092 (2012).
 86. Peng, C. *et al.* PTEN is a tumor suppressor in CML stem cells and BCR-ABL-induced leukemias in mice. *Blood* **115**, 626–635 (2010).
 87. Bhatia, S., Kaul, D. & Varma, N. Potential tumor suppressive function of miR-196b in B-cell lineage acute lymphoblastic leukemia. *Mol. Cell. Biochem.* **340**, 97–106 (2010).
 88. Liu, Y., Zheng, W., Song, Y., Ma, W. & Yin, H. Low Expression of miR-196b Enhances the Expression of BCR-ABL1 and HOXA9 Oncogenes in Chronic Myeloid Leukemogenesis. *PLoS One* **8**, (2013).
 89. Wu, L. *et al.* Curcumin derivative C817 inhibits proliferation of imatinib-resistant chronic myeloid leukemia cells with wild-type or mutant Bcr-Abl in vitro. *Acta Pharmacol. Sin.* **35**, 401–9 (2014).
 90. Meehan, K. & Vella, L. J. The contribution of tumour-derived exosomes to the hallmarks of cancer. *Crit. Rev. Clin. Lab. Sci.* **8363**, 1–11 (2015).
 91. Sabatel, C. *et al.* MicroRNA-21 exhibits antiangiogenic function by targeting RhoB

expression in endothelial cells. *PLoS One* **6**, (2011).

92. Mokady, D. & Meiri, D. RhoGTPases - A novel link between cytoskeleton organization and cisplatin resistance. *Drug Resist. Updat.* **19**, 22–32 (2015).
93. Timmerman, I. *et al.* A local VE-cadherin/Trio-based signaling complex stabilizes endothelial junctions through Rac1. *J. Cell Sci.* **128**, 3041–3054 (2015).
94. Escrevente, C., Keller, S., Altevogt, P. & Costa, J. Interaction and uptake of exosomes by ovarian cancer cells. *BMC Cancer* **11**, 108 (2011).
95. Chairoungdua, A., Smith, D. L., Pochard, P., Hull, M. & Caplan, M. J. Exosome release of beta-catenin: A novel mechanism that antagonizes Wnt signaling. *J. Cell Biol.* **190**, 1079–1091 (2010).
96. Zhang, W., Bai, W. & Zhang, W. MiR-21 suppresses the anticancer activities of curcumin by targeting PTEN gene in human non-small cell lung cancer A549 cells. *Clin. Transl. Oncol.* **16**, 708–713 (2014).
97. Alessandro, R. *et al.* Effects of carboxyamidotriazole on in vitro models of imatinib-resistant chronic myeloid leukemia. *J. Cell. Physiol.* **215**, 111–121 (2008).
98. Mineo, M. *et al.* Exosomes released by K562 chronic myeloid leukemia cells promote angiogenesis in a src-dependent fashion. *Angiogenesis* **15**, 33–45 (2012).
99. Takahashi, S. & Mendelsohn, M. E. Calmodulin-dependent and -independent activation of endothelial nitric-oxide synthase by heat shock protein 90. *J. Biol. Chem.* **278**, 9339–44 (2003).
100. Finlayson, A. E. & Freeman, K. W. A cell motility screen reveals role for MARCKS-related protein in adherens junction formation and tumorigenesis. *PLoS One* **4**, (2009).
101. Zhang, B. *et al.* Altered Microenvironmental Regulation of Leukemic and Normal Stem Cells in Chronic Myelogenous Leukemia. *Cancer Cell* **21**, 577–592 (2012).
102. Castells, M., Thibault, B., Delord, J.-P. & Couderc, B. Implication of tumor microenvironment in chemoresistance: tumor-associated stromal cells protect tumor cells from cell death. *Int. J. Mol. Sci.* **13**, 9545–71 (2012).
103. Mittelbrunn, M. *et al.* Unidirectional transfer of microRNA-loaded exosomes from T cells to antigen-presenting cells. *Nat. Commun.* **2**, 282 (2011).
104. Wang, S. *et al.* The Endothelial-Specific MicroRNA miR-126 Governs Vascular Integrity and Angiogenesis. *Dev. Cell* **15**, 261–271 (2008).
105. Ebrahimi, F., Gopalan, V., Smith, R. A. & Lam, A. K. Y. MiR-126 in human cancers: Clinical roles and current perspectives. *Experimental and Molecular Pathology* **96**, 98–107 (2014).
106. Shen, W.-F., Hu, Y.-L., Uttarwar, L., Passegue, E. & Largman, C. MicroRNA-126 regulates HOXA9 by binding to the homeobox. *Mol. Cell. Biol.* **28**, 4609–19 (2008).
107. Cammarata, G. *et al.* Differential expression of specific microRNA and their targets in

- acute myeloid leukemia. *Am J Hematol* **85**, 331–339 (2010).
108. Burger, J. A., Burger, M. & Kipps, T. J. Chronic Lymphocytic Leukemia B Cells Express Functional CXCR4 Chemokine Receptors that Mediate Spontaneous Migration Beneath Bone Marrow Stromal Cells. *Blood* **94**, 3658–3667 (1999).
 109. Zepeda-Moreno, A. *et al.* Modeling SDF-1-induced mobilization in leukemia cell lines. *Exp. Hematol.* **40**, 666–674 (2012).
 110. Sipkins, D. a *et al.* In vivo imaging of specialized bone marrow endothelial microdomains for tumour engraftment. *Nature* **435**, 969–73 (2005).
 111. Salvucci, O. *et al.* MicroRNA126 contributes to granulocyte colony-stimulating factor-induced hematopoietic progenitor cell mobilization by reducing the expression of vascular cell adhesion molecule 1. *Haematologica* **97**, 818–826 (2012).
 112. Quintás-Cardama, A. *et al.* Dasatinib early intervention after cytogenetic or hematologic resistance to imatinib in patients with chronic myeloid leukemia. *Cancer* **115**, 2912–2921 (2009).
 113. Aggarwal, B. B. & Sung, B. Pharmacological basis for the role of curcumin in chronic diseases: an age-old spice with modern targets. *Trends in Pharmacological Sciences* **30**, 85–94 (2009).
 114. Feng, D. Q. *et al.* Selective miRNA expression profile in chronic myeloid leukemia K562 cell-derived exosomes. *Asian Pacific J. Cancer Prev.* **14**, 7501–7508 (2013).
 115. Ostefeld, M. S. *et al.* Cellular disposal of miR23b by RAB27-dependent exosome release is linked to acquisition of metastatic properties. *Cancer Res.* **74**, 5758–5771 (2014).
 116. de Candia, P. *et al.* Intracellular Modulation, Extracellular Disposal and Serum Increase of MiR-150 Mark Lymphocyte Activation. *PLoS One* **8**, (2013).
 117. Yang, C. H. *et al.* The oncogenic microRNA-21 inhibits the tumor suppressive activity of FBXO11 to promote tumorigenesis. *J. Biol. Chem.* **290**, 6037–6046 (2015).
 118. Yan, S. *et al.* Inhibition of NADPH oxidase protects against metastasis of human lung cancer by decreasing microRNA-21. *Anticancer. Drugs* **26**, 388–398 (2015).
 119. Yang, Y. *et al.* Downregulation of microRNA-21 expression restrains non-small cell lung cancer cell proliferation and migration through upregulation of programmed cell death 4. *Cancer Gene Ther.* **22**, 23–29 (2015).
 120. Li, Y. *et al.* Anti-miR-21 oligonucleotide sensitizes leukemic K562 cells to arsenic trioxide by inducing apoptosis. *Cancer Sci.* **101**, 948–954 (2010).
 121. Hu, H. *et al.* Antisense oligonucleotide against miR-21 inhibits migration and induces apoptosis in leukemic K562 cells. *Leuk. Lymphoma* **51**, 694–701 (2010).
 122. Morotti, a *et al.* BCR-ABL disrupts PTEN nuclear-cytoplasmic shuttling through phosphorylation-dependent activation of HAUSP. *Leukemia* **28**, 1–8 (2013).

123. Medinger, M. & Passweg, J. Role of tumour angiogenesis in haematological malignancies. *Swiss medical weekly* **144**, w14050 (2014).
124. Masuelli, L. *et al.* Resveratrol potentiates the in vitro and in vivo anti-tumoral effects of curcumin in head and neck carcinomas. *Oncotarget* **5**, 10745–62 (2014).
125. Sun, M. *et al.* Curcumin (diferuloylmethane) alters the expression profiles of microRNAs in human pancreatic cancer cells. *Mol Cancer Ther* **7**, 464–473 (2008).
126. Kim, S. *et al.* MicroRNA miR-199a * regulates the MET proto-oncogene and the downstream extracellular signal-regulated kinase 2 (ERK2). *J. Biol. Chem.* **283**, 18158–18166 (2008).
127. Sreenivasan, S., Thirumalai, K., Danda, R. & Krishnakumar, S. Effect of Curcumin on miRNA Expression in Human Y79 Retinoblastoma Cells. *Curr. Eye Res.* **37**, 421–428 (2012).
128. Wang, S. & Olson, E. N. AngiomiRs-Key regulators of angiogenesis. *Current Opinion in Genetics and Development* **19**, 205–211 (2009).
129. Adamson, P., Etienne, S., Couraud, P. O., Calder, V. & Greenwood, J. Lymphocyte migration through brain endothelial cell monolayers involves signaling through endothelial ICAM-1 via a rho-dependent pathway. *J. Immunol.* **162**, 2964–73 (1999).
130. Nobes, C. D. & Hall, A. Rho, Rac, and Cdc42 GTPases Regulate the Assembly of Multimolecular Focal Complexes Associated with Actin Stress Fibers, Lamellipodia, and Filopodia. *Cell* **81**, 53–62 (1995).
131. Wang, J. & Dong, S. ICAM-1 and IL-8 are expressed by DEHP and suppressed by curcumin through ERK and p38 MAPK in human umbilical vein endothelial cells. *Inflammation* **35**, 859–870 (2012).
132. Kalani, A., Kamat, P. K., Chaturvedi, P., Tyagi, S. C. & Tyagi, N. Curcumin-primed exosomes mitigate endothelial cell dysfunction during hyperhomocysteinemia. *Life Sci.* **107**, 1–7 (2014).
133. Wang, Y. F., Gu, Y. T., Qin, G. H., Zhong, L. & Meng, Y. N. Curcumin ameliorates the permeability of the blood-brain barrier during hypoxia by upregulating heme oxygenase-1 expression in brain microvascular endothelial cells. *J. Mol. Neurosci.* **51**, 344–351 (2013).
134. Sheetz, M. P., Sable, J. E. & Döbereiner, H.-G. Continuous Membrane-Cytoskeleton Adhesion Requires Continuous Accommodation To Lipid and Cytoskeleton Dynamics. *Annu. Rev. Biophys. Biomol. Struct.* **35**, 417–434 (2006).
135. Ma, A. D. & Abrams, C. S. Pleckstrin induces cytoskeletal reorganization via a Rac-dependent pathway. *J. Biol. Chem.* **274**, 28730–28735 (1999).
136. van der Horst, E. H. *et al.* The growth factor Midkine antagonizes VEGF signaling in vitro and in vivo. *Neoplasia* **10**, 340–347 (2008).
137. Honda, K. *et al.* Actinin-4, a novel actin-bundling protein associated with cell motility

- and cancer invasion. *J. Cell Biol.* **140**, 1383–1393 (1998).
138. Micallef, J. *et al.* Epidermal growth factor receptor variant III-induced glioma invasion is mediated through myristoylated alanine-rich protein kinase C substrate overexpression. *Cancer Res.* **69**, 7548–7556 (2009).
 139. Techasen, A. *et al.* Myristoylated alanine-rich C kinase substrate phosphorylation promotes cholangiocarcinoma cell migration and metastasis via the protein kinase C-dependent pathway. *Cancer Sci.* **101**, 658–665 (2010).
 140. Popson, S. A. *et al.* Interferon-induced transmembrane protein 1 regulates endothelial lumen formation during angiogenesis. *Arterioscler. Thromb. Vasc. Biol.* **34**, 1011–1019 (2014).
 141. Yang, Y. *et al.* The interferon-inducible 9-27 gene modulates the susceptibility to natural killer cells and the invasiveness of gastric cancer cells. *Cancer Lett.* **221**, 191–200 (2005).
 142. Hatano, H. *et al.* IFN-induced transmembrane protein 1 promotes invasion at early stage of head and neck cancer progression. *Clin. Cancer Res.* **14**, 6097–105 (2008).
 143. Yu, F. *et al.* Knockdown of interferon-induced transmembrane protein 1 (IFITM1) inhibits proliferation, migration, and invasion of glioma cells. *J. Neurooncol.* **103**, 187–195 (2011).
 144. Yáñez-Mó, M. *et al.* Regulation of endothelial cell motility by complexes of retraspan molecules CD81/TAPA-1 and CD151/PETA-3 with $\alpha 3 \beta 1$ integrin localized at endothelial lateral junctions. *J. Cell Biol.* **141**, 791–804 (1998).
 145. Tejera, E. *et al.* CD81 regulates cell migration through its association with Rac GTPase. *Mol. Biol. Cell* **24**, 261–73 (2013).
 146. Poettler, M. *et al.* CD98hc (SLC3A2) drives integrin-dependent renal cancer cell behavior. *Mol. Cancer* **12**, 1–12 (2013).
 147. Arancibia-Garavilla, Y., Toledo, F., Casanello, P. & Sobrevia, L. Nitric oxide synthesis requires activity of the cationic and neutral amino acid transport system y+L in human umbilical vein endothelium. *Exp. Physiol.* **88**, 699–710 (2003).
 148. Chen, Y. *et al.* Upregulation of HAb18G/CD147 in activated human umbilical vein endothelial cells enhances the angiogenesis. *Cancer Lett.* **278**, 113–121 (2009).
 149. Liao, C.-G. *et al.* The human tumor cell-derived collagenase stimulatory factor (renamed EMMPRIN) is a member of the immunoglobulin superfamily. *J. Biol. Chem.* **55**, 3154–3158 (2011).
 150. Tang, Y., Kesavan, P., Nakada, M. T. & Yan, L. Tumor-stroma interaction: positive feedback regulation of extracellular matrix metalloproteinase inducer (EMMPRIN) expression and matrix metalloproteinase-dependent generation of soluble EMMPRIN. *Mol. Cancer Res.* **2**, 73–80 (2004).
 151. Berns, H., Humar, R., Hengerer, B., Kiefer, F. N. & Battegay, E. J. RACK1 is up-regulated

- in angiogenesis and human carcinomas. *FASEB J.* **14**, 2549–2558 (2000).
152. Boratko, A., Gergely, P. & Csontos, C. RACK1 is involved in endothelial barrier regulation via its two novel interacting partners. *Cell Commun.Signal.* **11**, 2 (2013).
 153. Dalby, M. J., Hart, A. & Yarwood, S. J. The effect of the RACK1 signalling protein on the regulation of cell adhesion and cell contact guidance on nanometric grooves. *Biomaterials* **29**, 282–289 (2008).
 154. Knezevic, N., Tauseef, M., Thennes, T. & Mehta, D. The G protein betagamma subunit mediates reannealing of adherens junctions to reverse endothelial permeability increase by thrombin. *J. Exp. Med.* **206**, 2761–77 (2009).
 155. Wang, F. *et al.* RACK1 regulates VEGF/Flt1-mediated cell migration via activation of a PI3K/Akt pathway. *J. Biol. Chem.* **286**, 9097–9106 (2011).
 156. Coffman, L. G., Parsonage, D., D'Agostino, R., Torti, F. M. & Torti, S. V. Regulatory effects of ferritin on angiogenesis. *Proc. Natl. Acad. Sci. U. S. A.* **106**, 570–5 (2009).
 157. Le Boeuf, F., Houle, F. & Huot, J. Regulation of vascular endothelial growth factor receptor 2-mediated phosphorylation of focal adhesion kinase by heat shock protein 90 and Src kinase activities. *J. Biol. Chem.* **279**, 39175–39185 (2004).
 158. Tung, J. J. & Kitajewski, J. Chloride intracellular channel 1 functions in endothelial cell growth and migration. *J. Angiogenes. Res.* **2**, 23 (2010).
 159. Pulimeno, P., Paschoud, S. & Citi, S. A role for ZO-1 and PLEKHA7 in recruiting paracingulin to tight and adherens junctions of epithelial cells. *J. Biol. Chem.* **286**, 16743–16750 (2011).

Scientific Products: publications, book chapters and acts in congresses

Publications:

- Discussed in this thesis:

- 1. Exosomal shuttling of miR-126 in endothelial cells modulates adhesive and migratory abilities of chronic myelogenous leukemia cells.** Taverna et al. *Molecular Cancer*. 2014; 13:169. doi:10.1186/1476-4598-13-169. (IF 4.257) ⁶⁸
M.G. worked in the confocal studies and in the migration assays.
- 2. Curcumin inhibits in vitro and in vivo chronic myelogenous leukemia cells growth: a possible role for exosomal disposal of miR-21.** Taverna S, Giallombardo M. et al. *Oncotarget*. 2015; 6:21918–21933. doi: 10.18632/oncotarget.4204. (IF 5.008) ⁶⁹
M.G. participated in the design of the study and in cell cultures, exosomes isolation, qPCR analysis, western blotting analysis, bioinformatic analysis and in *in vivo* studies.
- 3. Curcumin modulates chronic myelogenous leukemia exosomes composition and affects angiogenic phenotype via exosomal miR-21.** Taverna, et al. *Oncotarget*. 2016; 7(21), 30420-30439. doi: 10.18632/oncotarget.8483. (IF 5.008) ⁷⁰
M.G. worked on cell cultures, exosomes isolation, qPCR analysis, western blotting analysis and in bioinformatics analysis.

- Not included in this thesis:

- 4. Exosome-mediated drug resistance in cancer: the near future is here.** Marco Giallombardo, Simona Taverna, Riccardo Alessandro, David Hong and Christian Rolfo. *Therapeutic Advances in Medical Oncology*. 2015, In press (I.F. 2.827)
- 5. Exosomal miRNA analysis in non-small cell lung cancer (NSCLC) patients' plasma through qPCR: a feasible liquid biopsy tool.** Giallombardo M. et al. 2015. Jove article. 2016 In press (I.F. 1.325)
- 6. Exosomes isolation and characterization in serum is feasible in Non-Small Cell Lung Cancer patients: critical analysis of evidence and potential role in clinical practice.** Taverna S* & Giallombardo M.* , Gil-Bazo I, Carreca AP, Castiglia M, Chacártegui J, Araujo A, Alessandro R, Pauwels P, Peeters M, Rolfo C. *Oncotarget*. 2016 Feb 23. doi: 10.18632/oncotarget.7638. (IF 5.008)

- 7. Looking in the garden of the hesperides: new drugs in hepato-cellular carcinoma.** Castañón Alvarez E, **Giallombardo M**, Gil-Bazo I, Papadimitriou K, Pauwels P, Peeters M, Rolfo C. *Minerva Chir.* 2015 Apr;70(2):119-29. Epub 2015 Jan 23. Review. (IF 0.707)
- 8. Nintedanib in Non-Small Cell Lung Cancer (NSCLC): from the preclinical to the approval** C.Caglevic, M. Grassi , L. Raez, A. Listi, **M. Giallombardo** , E.Bustamante, I. Gil-Bazo, C. Rolfo. *Ther Adv Respir Dis.* 2015 Aug;9(4):164-72. doi: 10.1177/1753465815579608. Epub 2015 Apr 7. Review. (I.F. 1.949)
- 9. Reduction of mdx mouse muscle degeneration by low-intensity endurance exercise: a proteomic analysis in quadriceps muscle of exercised versus sedentary mdx mice.** Fontana S, Schillaci O, Frinchi M, **Giallombardo M**, Morici G, Di Liberto V, Alessandro R, De Leo G, Perciavalle V, Belluardo N, Mudo' G. *Biosci Rep.* 2015 May 12;35(3). pii: e00213. doi: 10.1042/BSR20150013. (I.F. 2.637)
- 10. Entrectinib, a potent new TRK, ROS1, and ALK inhibitor: new therapeutic opportunity not only for Non-Small Cell Lung Cancer.** Rolfo C, Ruiz R, Giovannetti E, Gil-Bazo I, Russo A, Passiglia F, **Giallombardo M**, Peeters M, Raez L. *Expert Opin Investig Drugs.* 2015;24(11):1493-500. doi: 10.1517/13543784.2015.1096344. Epub 2015 Oct 12. (I.F. 5.528)
- 11. The potential of neurotrophic tyrosine kinase (NTRK) inhibitors for treating lung cancer.** Passiglia F, Caparica R, Giovannetti E, **Giallombardo M**, Listi A, Diana P, Cirrincione G, Caglevic C, Raez LE, Russo A, Rolfo C. *Expert Opin Investig Drugs.* 2016 Apr;25(4):385-92. doi: 10.1517/13543784.2016.1152261. Epub 2016 Feb 24. (I.F. 5.528)
- 12. BRAF mutations in non-small cell lung cancer: is finally Janus opened the door?.** Rafael Caparica, Gilberto de Castro Jr., Ignacio Gil-Bazo, Christian Caglevic, Raffaele Calogero, **Marco Giallombardo**, Edgardo S. Santos, Luis E. Raez & Christian Rolfo. *Crit Rev Oncol Hematol.* 2016 May;101:32-9. doi: 10.1016/j.critrevonc.2016.02.012. Epub 2016 Feb 27. Review. (I.F. 4.027)
- 13. In silico pathway analysis in cervical carcinoma reveals potential new targets for treatment.** van Dam PA, van Dam PJ, Rolfo C, **Giallombardo M**, van Berckelaer C, Trinh XB, Altintas S, Huizing M, Papadimitriou K, Tjalma WA, van Laere S. *Oncotarget.* 2016 Jan 19;7(3):2780-95. doi: 10.18632/oncotarget.6667. (IF 5.008)
- 14. Exosomes in lung cancer liquid biopsies: two sides of the same coin?.** Christian Rolfo, **Marco Giallombardo**, et al. *Lung Cancer.* 2016 Nov 18. pii: S0169-5002(16)30530-X. doi: 10.1016/j.lungcan.2016.11.014. (I.F. 3.767)

15. Exosomes genetic cargo in lung cancer: a truly Pandora's box. Pablo Reclusa, Rafael Sirera, Antonio Araujo, **Marco Giallombardo**, Anna Valentino, Laure Sorber, Ignacio Gil Bazo, Patrick Pauwels, Christian Rolfo. *Translational Lung Cancer Research*. 2016. Oct;5(5):483-491

Acts in congresses:

- 1. Can curcumin induces selective packaging of miRNAs in exosomes? A pilot study in chronic myelogenous leukemia cells.** Christian Diego Rolfo, Simona Taverna, **Marco Giallombardo** , Mariano Provencio, Jorge Chacartegui, Marc Peeters, Patrick Pauwels, Riccardo Alessandro *J Clin Oncol* 33, 2015 (suppl; abstr e13563) ASCO meeting 2015, Chicago. (I.F. 20.98)
- 2. Exosomes isolation and characterization in non-small cell lung carcinoma patients: Proof of concept study.** Christian D. Rolfo, **Marco Giallombardo** , Marta Castiglia, Jorge Jorge Chacartegui, Mariano Provencio, Riccardo Alessandro, Anna Paola Carreca, Pilar Roca, Jordi Oliver, Isabel Bover, Jan P. Van Meerbeeck, Antonio Russo, Marc Peeters, Patrick Pauwels. *J Clin Oncol* 33, 2015 (suppl; abstr 11101) , ASCO meeting 2015, Chicago. (I.F. 20.98)
- 3. Exosomes analysis in Non-Small Cell Lung Cancer (NSCLC): looking for clinical application.** Christian Rolfo, Marta Castiglia, **Marco Giallombardo** et al. AACR 106th Annual Meeting 2015; April 18-22, 2015; Philadelphia, PA. doi: 10.1158/1538-7445.AM2015-3382 *Cancer Res* August 1, 2015 75; 3382.
- 4. Exosomal miRNA analysis in Non-Small Cell Lung Cancer: new liquid biopsy biomarker?** Marta Castiglia, Anna P. Carreca, Marco Giallombardo, Jorge Chacartegui Borrás, Nele Van Der Steen, Inge Mertens, Marc Peeters, Antonio Russo, Patrick Pauwels & Christian Rolfo. AACR 106th Annual Meeting 2015. April 18-22, 2015; Philadelphia.
- 5. Exosomal MiRNA Analysis of Non-Small Cell Lung Cancer (NSCLC) Liquid Biopsies. Mirror of the Disease Status?: Proof of Concept Study.** **M. Giallombardo** , J. Chacartegui, L. Sober, J.P. Van Meerbeeck, S. Goethals, R. Alessandro, P. Pauwels, C. Rolfo P2.04-094 Abstract – WCLC IASLC Sept. 2015- Denver (CO). USA
- 6. Follow up analysis by exosomal miRNAs in EGFR Mutated non-small cell lung cancer (NSCLC) patients during Osimertinib (AZD9291) treatment: a potential prognostic biomarker tool.** **Marco Giallombardo***, Jorge Chacartegui Borrás*, Pablo Reclusa, Jan P. Van Meerbeeck, Riccardo Alessandro, Marc Peeters, Patrick Pauwels & Christian Rolfo. ASCO Meeting 2016. Under review.

7. **Erlotinib Induce miRNA Alterations in T790M EGFR Mutated NSCLC: Preclinical Study.** J. Chacartegui, **M. Giallombardo** , N. Van Der Steen, P. Pauwels, C. Rolfo P2.04-027 Abstract – WCLC IASLC Sept. 2015- Denver (CO). USA
8. **Curcumin induces selective packaging of miR-21 in exosomes released by chronic myelogenous leukemia cells.** Simona Taverna, **Marco Giallombardo**, Anna Flugy, Christian Rolfo, Marzia Pucci, Giacomo De Leo and Riccardo Alessandro. XII-EVs in Cancer – ISEV 2015. Abstract and Poster.
9. **Quadriceps muscle proteomic profiling of exercised versus sedentary mdx mice.** Frinchi, M., Fontana, S., **Giallombardo, M.**, Schillaci, O., Morici, G., Di Liberto, V., et al. (2014). Abstract - 65th SIF National Congress.
10. **Comparison of exosome and exosomal RNA isolation methods in NSCLC liquid biopsies. Assessment of hsa-miR-1228-3p as normalizer for exosomal microRNA analysis.** **Marco Giallombardo** , Jorge Chacartegui Borrás, Nele Van Der Steen, Simona Taverna, Nathalie Claes, Frederik Leroux, Sara Bals, Riccardo Alessandro, Marc Peeters, Patrick Pauwels & Christian Rolfo. Abstract, Poster and oral presentation – EORTC/PAMM Int. Congress, Antwerp, 2016.
11. **Exosomes isolated in plasma of non-small cell lung cancer patients contain microRNA related to the EGFR pathway: Proof of concept** C. Rolfo, J. Chacartegui, **M. Giallombardo** , R. Alessandro, M. Peeters. ELCC Meeting 2016. Under review.
12. **Exosomes in pathological conditions: new insights for biomarker development and therapeutic applications.** Pucci M., Taverna S., Corrado C., Giallombardo M., Rolfo C., Alessandro R. AICC, Roma 2016. Best Poster.
13. **Effetti degli esosomi rilasciati dalle cellule di carcinoma polmonare non a piccole cellule sul differenziamento degli osteoclasti.** Taverna S. et al. Abstract and Oral Presentation. AIBG Congress, Cagliari 2016.
14. **Curcumin modulates chronic myelogenous leukemia exosomes composition and affects angiogenic phenotype, via exosomal Mir-21.** Taverna S. et al. Abstract and poster. ITPA XI Annual congress of the Italian Proteomics Association. Perugia 2016.
15. **Effects of exosomes released by NSCLC cells on osteoclasts differentiation.** Pucci M., Taverna S., Corrado C., **Giallombardo M.**, Rolfo C. and Alessandro R. Abstract e Poster – EORTC/PAMM Int. Congress, Antwerp, 2015.

Book chapters:

1. **The liquid biopsies: A new level of complexity in cancer regulation and a promising source of biomarkers.** Book: Molecular Targets and Strategies in Cancer Prevention. Christian Rolfo; Jorge Chacártegui Borrás; **Marco Giallombardo**. Springer EDITOR – 2016
2. **Technical aspects for the evaluation of Exosome and their content.** Book: Liquid Biopsy in Cancer Patients. Simona Fontana; **Marco Giallombardo**; Riccardo Alessandro. Springer EDITOR – 2016 Submitted.

Oral presentations:

1. **Comparison of exosome and exosomal RNA isolation methods in NSCLC liquid biopsies. Assessment of hsa-miR-1228-3p as normalizer for exosomal microRNA analysis.** EORTC/PAMM International Congress, Antwerp, 2016.
2. **Esosomi e microRNA circolanti: piccole molecole e microvescicole con un grande ruolo?** Congresso Congiunto delle Società Scientifiche Italiane di Chirurgia, Roma, 25-29/09/2016.

10. Acknowledgements

I would like to thank all those who have accompanied me during the training process:

- A special thanks is addressed to my tutor and mentor, **Prof Riccardo Alessandro**, for believing in me and for giving me this special opportunity to work on cancer research, I will never forget all his teachings useful in order to do great scientific research.

- I would like to thanks also **Drs. Simona Taverna**, with which we have always collaborated, for all technical and scientific teaching and advices.

- A thanks also to all the **Biology Section** of the Biopathology and Medical Biotechnology Department (**DIBIMED**) at the University of Palermo, consisting of an exceptional team, both from scientific and personal points of view, with whom I shared this splendid research experience.

- A special thanks is addressed also to **Prof. Christian Rolfo** which, together with **Prof. Marc Peeters** and **Prof. Patrick Pauwels**, has given me the opportunity to performe a memorable and productive research period abroad in Belgium, learning a lot in order to do translational research and to believe in myself. I also thank my colleague Nele Van Der Steen for his generous support during the whole research period abroad.

Finally, I thank all my **family** for believed in me and supported me during all my PhD training experience.